

SHRP-C-363

**Mechanical Behavior of  
High Performance Concretes, Volume 3  
Very Early Strength Concrete**

Paul Zia  
Shuaib H. Ahmad  
Michael L. Leming  
North Carolina State University  
Raleigh, North Carolina

John J. Schemmel  
Robert P. Elliott  
University of Arkansas  
Fayetteville, Arkansas



**Strategic Highway Research Program**  
National Research Council  
Washington, DC 1993

SHRP-C-363  
ISBN 0-309-05623-3  
Contract C-205  
Product No. 2014, 2023, 2024

Program Manager: *Don M. Harriott*  
Project Manager: *Inam Jawed*  
Production Editor: *Cara J. Tate*  
Program Area Secretary: *Carina S. Hreib*

November 1993

key words:  
admixture  
aggregate  
blended cement  
concrete mixture  
durability  
fly ash  
high performance concrete  
mixture proportioning  
portland cement concrete  
    early strength  
    high strength  
silica fume

Strategic Highway Research Program  
National Academy of Sciences  
2101 Constitution Avenue N.W.  
Washington, DC 20418

(202) 334-3774

The publication of this report does not necessarily indicate approval or endorsement of the findings, opinions, conclusions, or recommendations either inferred or specifically expressed herein by the National Academy of Sciences, the United States Government, or the American Association of State Highway and Transportation Officials or its member states.

© 1993 National Academy of Sciences

## Acknowledgments

The research described herein was supported by the Strategic Highway Research Program (SHRP). SHRP is a unit of the National Research Council that was authorized by section 128 of the Surface Transportation and Uniform Relocation Assistance Act of 1987.

The research was conducted by a consortium among researchers at North Carolina State University (prime contractor), the University of Arkansas, and the University of Michigan. The team included Paul Zia, Shuaib H. Ahmad, and Michael L. Leming at North Carolina State University; John J. Schemmel and Robert P. Elliott at the University of Arkansas; and A. E. Naaman at the University of Michigan.

The late Robert E. Philleo served as a project consultant during the initial stage of the project. He helped in defining the criteria for high performance concrete and in setting the direction of the research. The research team benefited greatly from his guidance and many stimulating discussions.

The research team also received valuable support, counsel, and guidance from the Expert Task Group (see cover 3 for a listing of ETG members). The support and encouragement provided by Inam Jawed, SHRP program manager, are deeply appreciated.

Special recognition is given to the New York Department of Transportation, the North Carolina Department of Transportation, the Illinois Department of Transportation, the Arkansas State Highway and Transportation Department, and the Nebraska Department of Roads. The cooperation and assistance of the staff of these five state transportation agencies were critical to the field installations of pavements to demonstrate the use of high performance concrete.

A group of materials producers and suppliers donated the necessary materials used for the laboratory studies of high performance concrete. These industrial partners included Blue Circle Cement, Inc., Pyrament/Lone Star Industries, Inc., Martin Marietta Company, Memphis Stone and Gravel Co., McClinton-Anchor, Arkhola Sand and Gravel, Monex Resources, Inc., Fly Ash Products, Elkem Chemicals, Cormix, Dow Chemical, and W. R. Grace. Their generous support of this research program is deeply appreciated.

The authors of this report would also like to acknowledge the contributions of many collaborators who participated in the various phases of this research program. At North Carolina State University, they included former and present graduate research assistants William K. Chi,

Wayne L. Ellenberger, M. R. Hansen, Aykut Cetin, Kristina M. Hanes, Johnny D. Waycaster, Randy Maccaferri, and Dena Firebaugh, and former undergraduate laboratory assistants Randall A. Boyd, Joseph B. Taylor, Wesley N. Denton, and Harold D. Ingram. The collaborators at the University of Arkansas included former and present graduate research assistants James R. Powell, Vikas Arora, and Mike Callahan, and former undergraduate laboratory assistant Memory Rodgers.

Opinions expressed in this report reflect the views of the authors, who should be held accountable for any errors and omissions.

# Contents

<b>Acknowledgments .....</b>	<b>iii</b>
<b>List of Figures.....</b>	<b>vii</b>
<b>List of Tables .....</b>	<b>ix</b>
<b>Preface.....</b>	<b>xi</b>
<b>Abstract.....</b>	<b>1</b>
<b>Executive Summary .....</b>	<b>3</b>
<b>1 Introduction .....</b>	<b>7</b>
1.1 Definition of Very Early Strength Concrete	8
1.2 Potential Applications of Very Early Strength Concrete	9
<b>2 Objective and Scope.....</b>	<b>11</b>
<b>3 Characterizations of Constituent Materials .....</b>	<b>13</b>
3.1 Cements	13
3.2 Coarse Aggregates	16
3.3 Fine Aggregates	16
3.4 Chemical Admixtures	17
3.5 Mineral Admixtures	17
<b>4 Mixture Proportions.....</b>	<b>19</b>

<b>5</b>	<b>Mixing and Curing Procedures</b>	21
5.1	Mixing Procedures	21
5.2	Curing Procedures	22
<b>6</b>	<b>Laboratory Experiments</b>	27
6.1	Compression Tests	27
6.2	Tension Tests	43
6.3	Freezing-Thawing Tests	52
6.4	Shrinkage Tests	67
6.5	Rapid Chloride Permeability Tests	72
6.6	AC Impedance Tests	76
6.7	Concrete-to-Concrete Bond Tests	78
<b>7</b>	<b>Conclusions</b>	89
	<b>References</b>	93
	<b>Appendix</b>	95

## List of Figures

Figure 5.1a	Styrofoam insulation block used for curing concrete cylinders at NCSU .....	23
Figure 5.1b	Styrofoam insulation block used for curing concrete cylinders at the University of Arkansas.....	24
Figure 5.2	Insulated curing box for concrete specimens at NCSU .....	26
Figure 6.1a	Stress-strain relationship of VES (A) concrete at design age of 6 hrs .....	32
Figure 6.1b	Stress-strain relationship of VES (B) concrete at design age of 4 hrs .....	32
Figure 6.2a	Effect of coarse aggregate on VES (A) stress-strain relationship at 28 days .....	34
Figure 6.2b	Effect of coarse aggregate on VES (B) stress-strain relationship at 28 days .....	34
Figure 6.3a	Effect of age on stress-strain relationship of VES (A) MM (6hrs, 3d, 7d, 28d).....	35
Figure 6.3b	Effect of age on stress-strain relationship of VES (B) MM (4hrs, 3d, 7d, 28d).....	35
Figure 6.4a	Variation of compressive strength with time for VES (A) .....	38
Figure 6.4b	Variation of compressive strength with time for VES (B).....	38
Figure 6.5a	Variation of modulus of elasticity with time for VES (A).....	40
Figure 6.5b	Variation of modulus of elasticity with time for VES (B).....	40
Figure 6.6a	Comparison of observed versus predicted modulus of elasticity of VES concrete considering all test ages.....	41
Figure 6.6b	Average size effect of VES concrete at design age.....	41
Figure 6.7	Comparison of observed versus predicted split cylinder strength of VES concrete at design age .....	45
Figure 6.8	Comparison of observed versus predicted modulus of rupture of VES concrete at design age.....	45
Figure 6.9a	Variation of modulus of rupture with time for VES (A) concrete .....	49
Figure 6.9b	Variation of modulus of rupture with time for VES (B) concrete .....	49
Figure 6.10a	Load-midspan deflection of VES (A) at design age of 6 hrs .....	50
Figure 6.10b	Load-midspan deflection of VES (B) at design age of 4 hrs .....	50
Figure 6.11a	Load-midspan deflection of VES (A) CG (6hrs, 7d, 28d).....	51
Figure 6.11b	Load-midspan deflection of VES (B) CG (4hrs, 7d, 28d) .....	51
Figure 6.12a	Load-tensile strain of VES (A) at design age of 6 hrs .....	53
Figure 6.12b	Load-tensile strain of VES (B) at design age of 4 hrs.....	53

Figure 6.13a	Load-tensile strain of VES (A) CG at 6hrs, 7d, 28d .....	54
Figure 6.13b	Load-tensile strain of VES (B) CG at 4hrs, 7d, 28d .....	54
Figure 6.14	Relative dynamic modulus vs number of freezing-thawing cycles for C/VE(C)/3 .....	58
Figure 6.15	Relative dynamic modulus vs number of freezing-thawing cycles for C/VE(C)/.34 .....	59
Figure 6.16	Relative dynamic modulus vs number of freezing-thawing cycles for C/VE(C)/3R6.....	60
Figure 6.17	Relative dynamic modulus vs number of freezing-thawing cycles for C/VE(PYR)/3 .....	61
Figure 6.18a	Variation of shrinkage strain with time for VES (A) concrete .....	70
Figure 6.18b	Variation of shrinkage strain with time for VES (B) concrete.....	70
Figure 6.19a	Comparison of AC impedance with initial current.....	80
Figure 6.19b	Comparison of AC impedance with total charge .....	81
Figure 6.19c	Comparison of inverse AC impedance with initial current.....	82
Figure 6.19d	Comparison of inverse AC impedance with total charge.....	83
Figure 6.20	Load vs interfacial deformation for C-C bond of VES concrete.....	86



## List of Tables

Table 2.1	Types of coarse and fine aggregates .....	11
Table 3.1	Results of physical and chemical analyses of Type III cement compared with ASTM C 150 .....	14
Table 3.2	Results of physical and chemical analyses of PBC-XT cement compared with ASTM C 595 .....	15
Table 3.3	Properties of coarse aggregates.....	17
Table 3.4	Properties of fine aggregates.....	18
Table 3.5	Chemical admixtures used in the test program .....	18
Table 4.1	Mixture proportions of VES (A) concrete with four different aggregate types...	20
Table 4.2	Mixture proportions of VES (B) concrete with four different aggregate types...	20
Table 6.1	Test program for compressive strength and modulus of elasticity — Group 1 .....	28
Table 6.2	Test program for modulus of rupture, tensile strain capacity, and split tensile strength — Group 2 .....	28
Table 6.3	Test program for frost durability, shrinkage, and chloride permeability — Group 3 .....	29
Table 6.4	Test program for bond strength — Group 5 .....	29
Table 6.5a	Summary of test results for compressive strength (psi) and modulus of elasticity ( $10^6$ psi) at different test ages for VES (A) concrete.....	36
Table 6.5b	Summary of test results for compressive strength (psi) and modulus of elasticity ( $10^6$ psi) at different test ages for VES (B) concrete.....	37
Table 6.6a	Summary of test results for 4 x 8-in. cylinder strength (psi) and 6 x 12-in. cylinder strength (psi) for VES (A) concrete .....	42
Table 6.6b	Summary of test results for 4 x 8-in. cylinder strength (psi) and 6 x 12-in. cylinder strength (psi) for VES (B) concrete .....	42
Table 6.7a	Summary of test results for modulus of rupture, tensile strain capacity, and split cylinder tensile strength for VES (A) concrete .....	46
Table 6.7b	Summary of test results for modulus of rupture, tensile strain capacity, and split cylinder tensile strength for VES (B) concrete.....	47
Table 6.8a	Mixture proportions, strength, and plastic properties of VES concrete used for freezing-thawing test specimens .....	62
Table 6.8b	Mixture proportions, strength, and plastic properties of VES concrete used for freezing-thawing test specimens .....	63

Table 6.8c	Mixture proportions, strength, and plastic properties of VES concrete used for freezing-thawing test specimens .....	64
Table 6.8d	Mixture proportions, strength, and plastic properties of VES concrete used for freezing-thawing test specimens .....	65
Table 6.9	Results of freezing-thawing test of VES concrete .....	66
Table 6.10a	Summary of shrinkage test results for VES(A) concrete .....	68
Table 6.10b	Summary of shrinkage test results for VES (B) concrete .....	69
Table 6.11a	Results of rapid chloride permeability test of VES concrete .....	74
Table 6.11b	Results of rapid chloride permeability test of VES concrete .....	75
Table 6.12	Results of AC impedance test of VES concrete.....	79
Table 6.13	Summary of test results for concrete-to-concrete bond tests of VES concrete.....	85

## Preface

The strategic Highway Research Program (SHRP) is a 5-year, nationally coordinated research effort initiated in 1987 at a cost of \$150 million. This highly focused and mission oriented program originated from a thorough and probing study\* to address the serious problems of deterioration of the nation's highway and bridge infrastructure. The study documented the need for a concerted research effort to produce major innovations for increasing the productivity and safety of the nation's highway system. Further, it recommended that the research effort be focused on six critical areas in which the nation spends most of the \$50 billion used for roads annually and thus technical innovations could lead to substantial payoffs. The six critical research areas were as follows:

- Asphalt Characteristics
- Long-Term Pavement Performance
- Maintenance Cost-Effectiveness
- Concrete Bridge Component Protection
- Cement and Concrete
- Snow and Ice Control

When SHRP was initiated, the two research areas of Concrete Bridge Component Protection and Cement and Concrete were combined under a single program directorate of Concrete and Structures. Likewise, the two research areas of Maintenance Cost-Effectiveness and Snow and Ice Control were also combined under another program directorate of Highway Operations.

---

\* *America's Highways: Accelerating the Search for Innovation*. Special Report 202, Transportation Research Board, National Research Council, Washington, D. C. 1984.

## Abstract

This report details the laboratory investigation of the mechanical behavior and field trials of high performance concrete for highway applications. High performance concrete (HPC) is defined as concrete with much higher early strength and greatly enhanced durability against freezing and thawing in comparison to conventional concrete. Very early strength (VES) concrete is one of the three categories of HPC investigated in this program. The objective is to obtain information on the mechanical behavior of VES concrete.

The laboratory investigation consisted of tests for both the fresh or plastic concrete and the hardened concrete. Tests for the plastic concrete included slump, air content, unit weight, and concrete temperature, and the results of these tests are presented in volume 2 of this report series, *Production of High Performance Concrete*. The laboratory tests for the hardened concrete include compression tests for strength and modulus of elasticity; tension tests for tensile strength, flexural strength, and tensile strain capacity; freezing-thawing tests for durability factor; shrinkage tests; rapid chloride permeability tests; tests for AC impedance; and tests for concrete-to-concrete bond.

The results of the laboratory work indicated that VES concretes with enhanced frost resistance can be successfully produced in the laboratory and utilized in the field for highway pavements.

## Executive Summary

This report documents the laboratory investigations of the mechanical behavior and field installations of high performance concrete for highway applications. High performance concrete (HPC) is defined as concrete with much higher early strength and greatly enhanced durability against freezing and thawing in comparison to conventional concrete. Very early strength (VES) concrete is one of the three categories of HPC investigated in this program. The objective is to obtain information on the mechanical behavior of VES concrete.

For the purpose of this program, HPC is defined in terms of certain *target* strength and durability requirements as shown below:

Category of High Performance Concrete	Minimum Compressive Strength	Maximum Water/Cement Ratio	Minimum Frost Durability Factor
Very early strength (VES)			
Option A (with Type III cement)	2,000 psi (14 MPa) in 6 hours	0.40	80%
Option B (with Pyrament PBC-XT cement)	2,500 psi (17.5 MPa) in 4 hours	0.29	80%
High early strength (HES) (with Type III cement)	5,000 psi (35 MPa) in 24 hours	0.35	80%
Very high strength (VHS) (with Type I cement)	10,000 psi (70 MPa) in 28 days	0.35	80%

In the above definition, the target minimum strength should be achieved in the specified time after water is added to the concrete mixture. The compressive strength is determined from 4 x 8-in. (100 x 200-mm) cylinder tested with neoprene caps. The water/cement ratio is based on all cementitious materials. The minimum durability factor of 80% should be achieved after 300 cycles of freezing and thawing according to ASTM C 666, procedure A. This is in contrast to a durability factor of 60% for conventional concrete.

In order for the research results to be applicable in different geographical regions, four different types of coarse aggregates were selected for producing VES concrete. They included crushed granite and marine marl from North Carolina, dense crushed limestone from Arkansas, and washed rounded gravel from Tennessee. These aggregates were used with local sand from the three states. The characteristics of all constituent materials used for producing VES concrete are described in detail in terms of their physical, chemical, and mineral properties. The normal laboratory mixing and batching procedures (ASTM C 192) were modified slightly to approximate typical concrete dry-batch plant operations.

The laboratory investigation consisted of tests for both the fresh or plastic concrete and the hardened concrete. Tests for the plastic concrete included slump, air content, unit weight, and concrete temperature, and the results of these tests are presented in volume 2 of this report series, *Production of High Performance Concrete*. The laboratory tests for the hardened concrete included compression tests for strength and modulus of elasticity; tension tests for tensile strength, flexural strength, and tensile strain capacity; freezing-thawing tests for durability factor; shrinkage tests; rapid chloride permeability tests; AC impedance tests; and concrete-to-concrete bond tests.

Based on the experience of the laboratory investigations, the following conclusions were drawn:

1. Using conventional materials and equipment, but with more care than needed for conventional concrete, two options of VES concrete can be produced. VES (A) will achieve a minimum compressive strength of 2,000 psi (14 MPa) in 6 hours and VES (B) will achieve a minimum compressive strength of 2,500 psi (17.5 MPa) in 4 hours. Such concretes can be produced with a variety of aggregates including crushed granite, marine marl, dense crushed limestone, and washed rounded gravel.
2. Insulation must be used to entrap the heat of hydration in order to accelerate the early strength development of the VES concretes.
3. Use of a larger amount of Type III cement or Pyrament XT cement in the VES concrete mixtures, along with a low W/C, leads to a more rapid strength development of these concretes in the first 3 days than predicted by the current ACI recommendation based on conventional concrete.
4. Since the VES concretes are kept moist only for the first 6 or 4 hours, followed by air curing in the laboratory, the strength development of the small laboratory samples is very rapid during the first 3 days, and the subsequent rate of strength gain is greatly reduced. The same is true with the modulus of elasticity.
5. Since the design strength of both options of the VES concrete is within the range of conventional concrete, the mechanical behavior of the VES concrete, such as the modulus of elasticity and the compressive and tensile strain capacities, is similar to that of conventional concrete. The modulus of elasticity, the flexural modulus, and the splitting tensile strength can all be predicted reasonably well by the ACI Code

equations. At the early design ages (6 or 4 hours), the compressive strain capacity ranges between approximately 1,000 and 2,000 microstrains, and the tensile strain capacity varies between 100 and 180 microstrains. These strain values would increase somewhat as the concrete ages.

6. The stress-strain relationship of the VES concretes is more nonlinear at 6 or 4 hours than at later ages, and the modulus of elasticity is lower for concrete with softer aggregate, such as marine marl.
7. For VES (B) concrete with Pyrament XT cement, the flexural modulus may decrease after the first 7 days because of the drying of the test specimen, possibly due to self-desiccation resulting from the very low W/C of the concrete.
8. Even with a very low W/C, the VES concretes should have an adequate amount of air entrainment to enhance their freeze-thawing resistance because the concretes are subject to moist curing for only a few hours. The test results indicate that if the VES concrete contains at least 5% entrained air, it will meet the stringent requirement of a durability factor of 80% after 300 cycles of freezing and thawing according to the ASTM C 666, procedure A. This is in contrast to the durability factor of 60% commonly expected of quality conventional concrete.
9. The VES concretes produced with washed rounded gravel from Memphis, Tennessee, failed the freeze-thawing test according to ASTM C 666, procedure A, because the aggregate had an absorption of about 5% and pore sizes of about 0.10 microns (as observed in SEM micrographs), the worst possible conditions for freeze-thawing deterioration.
10. Shrinkage of the VES (A) concrete follows the general trend of conventional concrete. The average shrinkage strain of the concretes at 90 days ranges from 59 to 321 microstrains, depending on the type of coarse aggregate used. These values represent 10 to 55% of the ultimate shrinkage strain recommended by ACI Committee 209 for conventional concrete. On the other hand, the 90-day shrinkage strain of the VES (B) concrete with crushed granite was only 52 microstrains; and the VES (B) concrete with marine marl or rounded gravel exhibited an expansion of approximately 140 microstrains, rather than shrinkage for the entire period of 90 days. The expansion is attributed to the lack of evaporable water in the concrete because of its very low W/C (0.17 for marine marl, and 0.22 for rounded gravel).
11. The normal procedure of the rapid chloride permeability test (RCPT) is to measure the total electrical charge in terms of coulombs flowing through a vacuum saturated concrete specimen in 6 hours. This measurement indicates the chloride ion permeability of the concrete. The VES concrete may exhibit high permeability according to the RCPT, since many additional ions introduced in the concrete by the various admixtures will cause the concrete to be more conductive electrically and make it appear more permeable than it really is.

12. The initial current in amperes flowing through the concrete specimen in a RCPT correlates consistently with the total charge measured in 6 hours. Therefore, the initial current, which is an indirect measure of the concrete conductance, can be used as an alternate measurement for the RCPT, thus shortening the total testing time by 6 hours.
13. The AC impedance test measures the total resistance of a concrete specimen in ohms. This test method is simpler and faster than the RCPT, and has the potential of substituting for the RCPT. The best correlation between the two test methods is expressed as the inverse impedance (reciprocal of impedance) in terms of the initial current measured in the RCPT.
14. Concrete-to-concrete bond strength can be determined by a direct shear test. The VES (A) concrete with crushed granite developed a nominal bond strength at 6 hours ranging from 120 psi (0.8 MPa) to 150 psi (1.0 MPa) with the normal NCDOT pavement concrete. The VES (B) concrete with crushed granite developed a 4-hour nominal bond strength of 225 psi (1.6 MPa) with the same NCDOT pavement concrete. These values are much lower than the corresponding value of 330 psi (2.3 MPa) obtained from the control test using NCDOT concrete. However, the control test was performed at the age of 7 days. Since the compressive strength of the VES concretes increases rapidly in the first 3 days, it is expected that its concrete-to-concrete bond strength will also increase substantially as the concrete ages. This should be verified in future tests.



# 1

## Introduction

SHRP's research on the mechanical behavior of high performance concretes had three general objectives:

1. To obtain needed information to fill gaps in the present knowledge;
2. To develop new, significantly improved engineering criteria for the mechanical properties and behavior of high performance concretes; and
3. To provide recommendations and guidelines for using these concretes in highway applications according to the intended use, required properties, environment, and service.

Both plain and fiber-reinforced concretes were included in the study. The research findings are presented in a series of six project reports:

*Volume 1    Summary Report*

*Volume 2    Production of High Performance Concrete*

*Volume 3    Very Early Strength (VES) Concrete*

*Volume 4    High Early Strength (HES) Concrete*

*Volume 5    Very High Strength (VHS) Concrete*

*Volume 6    High Early Strength Fiber-Reinforced Concrete (HESFRC)*

This volume is the third of these reports. The readers will notice a certain uniformity in format and similarity in many general statements in these reports. This feature is adopted intentionally so that each volume of the reports can be read independently without the need to cross-reference to other reports in the series.

## 1.1 Definition of Very Early Strength Concrete

Very early strength (VES) concrete is one of the three categories of high performance concrete (HPC) investigated in this research program. Two options (A and B) of VES concrete were considered. In volume 2 of this report series, *Production of High Performance Concrete*, the strength and durability criteria were defined for each of the three categories of HPC.

For VES (A) concrete, a minimum compressive strength of 2,000 psi (14 MPa) is required 6 hours after water is added to the concrete mixture using portland cement with a maximum W/C of 0.40. For VES (B) concrete, a minimum compressive strength of 2,500 psi (17.5 MPa) is required 4 hours after water is added to the concrete mixture using Pyrament PBC-XT cement, with a maximum W/C of 0.29. Both types of concrete must also achieve a minimum durability factor of 80% at 300 cycles of freezing and thawing according to ASTM C 666, procedure A.

These criteria were adopted after considering several factors pertinent to the construction and design of highway pavements and structures. The rationale for the selection of the various limits is discussed below.

The use of a time constraint of 4 to 6 hours for VES concrete is intended for projects with very tight construction schedules involving full-depth pavement replacements in urban or heavily traveled areas. The strength requirement of 2,000 to 2,500 psi (14 to 17.5 MPa) is selected to provide a class of concrete that would meet the need for rapid replacement and construction of pavements.

Since VES concrete is intended for pavement applications where exposure to frost must be expected, it is essential that the concrete must be frost resistant. Thus, it is appropriate to select a maximum W/C of 0.40, which is relatively low in comparison with conventional concrete. With a low W/C, concrete durability is improved in all exposure conditions. Since VES concrete is expected to be in service in no more than 6 hours, the W/C selected might provide a discontinuous capillary pore system at about that age, as suggested by Powers et al.(1959).

The choice of an appropriate measure for frost durability is debatable and subjective. It is recognized that ASTM C 666, procedure A, which involves freezing and thawing in water, is a severe test, therefore durability criterion should not be unduly conservative. On the other hand, if HPC is to provide enhanced durability, it may be argued that higher standards are required. Since frost durability of concrete as measured by ASTM C 666, procedure A, is highly dependent on the air void system, and since freezing concrete of low permeability at the very high rate required in the test procedure tends to discriminate against concrete with low W/C, the specified durability factor of 80% at 300 cycles of freezing and thawing is considered appropriate. This is in contrast to the durability factor of 60% commonly expected of quality conventional concrete according to ASTM C 666.

## **1.2 Potential Applications of Very Early Strength Concrete**

Potential applications of VES concrete include situations in which the construction time is critical and the cost of materials is only marginally important when compared with the costs of closing a bridge or a section of pavement to traffic. The use of this concrete would be limited to full-depth pavement patches, short stretches of new pavement, bridge decks, or overlays, and would probably be inappropriate for most structural applications.

## Objective and Scope

The objective of this investigation was to develop and analyze basic data on the mechanical properties of very early strength (VES) concrete for highway applications. The concrete would be produced *utilizing only conventional constituent materials and normal production and curing procedures*. In order for the results to be applicable in different regions, the study included four different types of coarse aggregates and three kinds of sand, as summarized in Table 2.1. The materials were chosen as representing a wide geographical area.

**Table 2.1      Types of coarse and fine aggregates**

Type	Symbol	Source
Marine Marl	MM	Castle Hayne, N.C.
Crushed Granite	CG	Garner, N.C.
Dense Crushed Limestone	DL	West Fork, Ark.
Washed Rounded Gravel	RG	Memphis, Tenn.
Sand		Lillington, N.C.
Sand		Memphis, Tenn.
Sand		Van Buren, Ark.

The initial research plan called for both laboratory experiments and field studies. The laboratory experiments would include seven different types of tests, namely compression, tension (both flexure and splitting), freezing-thawing, shrinkage, rapid chloride permeability, AC impedance, and concrete-to-concrete bond. The field studies would involve field installations in three states — North Carolina, Arkansas, and Illinois — during the summer of 1990. Subsequently, New York and Nebraska expressed interest, and these two states were included in the program.

Planning and negotiations with the various state highway departments and the selection of appropriate sites for field installations consumed more time than expected. It was not until the summer of 1991 that the first two field installations were constructed in New York and North Carolina. In the fall of 1991, two more field installations were placed in Illinois and Arkansas. By July of 1992, the fifth field installation was constructed in Nebraska. Unfortunately, the development of the VES mixture proportions and the corresponding laboratory experiments were delayed due to a series of modifications of the strength criterion for the VES concrete. As a result, it was not possible for the five field installations to include the VES mixtures as reported herein.

However, in the earlier laboratory studies of the HES concrete mixture, it was found that when the concrete was insulated, its strength development characteristics were quite similar to those of the VES concrete. Therefore, two comparable test pavement patches were constructed at each field installation. One patch was insulated to mimic the VES mixture, and one was not insulated as is standard for HES concrete. In North Carolina, an early version of the VES mixture was used. A full account of the field experience and the results of subsequent studies are given in volume 4 of this report series, *High Early Strength (HES) Concrete*.

The laboratory studies using crushed granite (CG), marine marl (MM), and washed rounded gravel (RG) were conducted at North Carolina State University, whereas the studies using dense crushed limestone (DL) were carried out at the University of Arkansas. Lillington sand was used for the concretes made with either CG or MM, but Memphis sand was used for the concrete made with RG. Arkansas River sand from Van Buren was used for the concrete made with DL.

## Characterizations of Constituent Materials

### 3.1 Cements

Type III cement was used for producing VES (A) concrete. The cement used at North Carolina State University (NCSU) was of low alkali content and met the requirements of ASTM C 150 specifications. It was supplied by Blue Circle Cement, Inc. from its plant in Harleyville, South Carolina. The cement used at the University of Arkansas was supplied by the same manufacturer, but from its plant in Tulsa, Oklahoma.

Pyrament PBC-XT cement is a proprietary product which was supplied by Lone Star Industries from its Greencastle, Indiana plant. It may be classified as an alkali activated system composed of about 60% portland cement, meeting ASTM C 150 specifications for Type III, and 35% fly ash, meeting ASTM C 618 Class C specifications for use as a mineral admixture in portland cement concrete. The remaining 5% is essentially a proprietary functional addition consisting of high range water reducers, citric acid, and potassium carbonate. No chloride compounds are used. The cement is manufactured under U.S. Patent 4,842,649.

Pyrament PBC-XT cement is very sensitive to moisture and is packaged in plastic-lined bags. It should be stored in a dry environment. According to the manufacturer, when stored under normal conditions the material should be used within six months of the date of manufacture. If the cement is stored in a room with relatively high humidity, its shelf life may be greatly reduced.

The results of physical and chemical analyses of the various types of cement are summarized in Tables 3.1 and 3.2, along with the requirements of relevant ASTM specifications for comparison.

It is important to note that although ASTM C 595 does not specify a limit, the total equivalent alkali content of PBC-XT is typically as much as three times greater than the limit specified by ASTM C 150 for Type I and Type III cements. This high alkali content of PBC-XT poses a potential for alkali-silica reactivity when used with deleteriously reactive aggregates. Investigation of this phenomenon is outside the scope of this research.

**Table 3.1 Results of physical and chemical analyses of Type III cement compared with ASTM C 150**

	ASTM C 150 Type III	Type III* NCSU	Type III+ Arkansas
Fineness			
Specific surface (Blaine)	—	4,575 cm <sup>2</sup> /g	5,590 cm <sup>2</sup> /g
Soundness			
Autoclave expansion	0.80%	-0.03%	0.02%
Time of setting (Gillmore)			
Initial	1 hr	3 hr	1 hr 48 min
Final	10 hr	6 hr	2 hr 43 min
Water required			
1 : 2.75 mortar cubes	—	48.5%	—
Air temperature	—	73°F	—
Relative humidity	—	70%	—
Compressive strength, 2 in. mortar cubes			
1 day	1,800 psi	3,400 psi	3,717 psi
3 days	3,500 psi	4,450 psi	5,258 psi
7 days	—	—	5,725 psi
Silicon dioxide (SiO <sub>2</sub> ), %	—	20.4	20.1
Aluminum oxide (Al <sub>2</sub> O <sub>3</sub> ), %	—	5.1	5.6
Ferric oxide (Fe <sub>2</sub> O <sub>3</sub> ), %	—	3.8	2.1
Calcium oxide (CaO), %	—	65.2	64.1
Magnesium oxide (MgO), %	6.0	1.0	2.4
Sulfur trioxide (SO <sub>3</sub> ), %	3.5	2.9	3.7
Loss on ignition, %	3.0	1.2	1.1
Sodium oxide (Na <sub>2</sub> O), %	—	—	0.2
Potassium oxide (K <sub>2</sub> O), %	—	—	0.7
Total equivalent alkali content, %	0.60	0.18	0.66
Tricalcium silicate, %	—	62.6	58.6
Dicalcium silicate, %	—	11.2	13.3
Tricalcium aluminate, %	15	7.2	11.4
Tetracalcium a umino ferrite, %	—	11.5	6.4
Insoluble residue, %	0.75	0.03	0.15

Note: 1 MPa = 145 psi

\* Tests performed by the Materials and Tests Unit of North Carolina DOT

+ Tests performed by the Materials Division of Arkansas DOT

**Table 3.2 Results of physical and chemical analyses of PBC-XT cement compared with ASTM C 595**

	ASTM C 595 Type IP	Typical Value* PBC-XT	PBC-XT+ NCSU
Fineness			
Specific surface (Blaine)	—	5,000 cm <sup>2</sup> /g	3,200 cm <sup>2</sup> /g
Soundness			
Autoclave expansion	0.50%	0.07%	—
Time of setting (Vicat)			
Initial	45 min	32 min	—
Final	7 hr	—	—
Water required			
1 : 2.75 mortar cubes	—	—	32.7%
Air temperature	—	—	73°F
Relative humidity	—	—	70%
Compressive strength, 2 in. mortar cubes			
1 day	—	—	1,800 psi
3 days	1,800 psi	4,470 psi	4,200 psi
7 days	2,800 psi	6,150 psi	4,500 psi
28 days	3,500 psi	7,700 psi	—
Silicon dioxide (SiO <sub>2</sub> ), %	—	23.6	23.5
Aluminum oxide (Al <sub>2</sub> O <sub>3</sub> ), %	—	9.6	12.5
Ferric oxide (Fe <sub>2</sub> O <sub>3</sub> ), %	—	3.5	3.8
Calcium oxide (CaO), %	—	48.1	48.5
Magnesium oxide (MgO), %	5.0	3.0	3.1
Sulfur trioxide (SO <sub>3</sub> ), %	4.0	2.9	2.0
Loss on ignition, %	5.0	4.6	3.7
Sodium oxide (Na <sub>2</sub> O), %	—	0.2	0.6
Potassium oxide (K <sub>2</sub> O), %	—	2.6	1.8
Total equivalent alkali content, %	—	1.9	1.8
Tricalcium silicate, %	—	—	—
Dicalcium silicate, %	—	—	—
Tricalcium aluminate, %	—	—	—
Tetracalcium aluminoferrite, %	—	—	—
Insoluble residue, %	—	—	8.2

Note: 1 MPa = 145 psi

\* Provided by Pyrament/Lone Star Industries, Inc.

+ Tests performed by the Materials and Tests Unit of North Carolina DOT



### 3.2 Coarse Aggregates

Four different types of coarse aggregates were used in this investigation. They were chosen as representing aggregates from a wide geographical area. Crushed granite (CG) is a strong, durable aggregate locally available in North Carolina. It was supplied by Martin Marietta Company from its quarry in Garner, North Carolina. Marine marl (MM) is a weaker and more absorptive aggregate available in the coastal area of North Carolina. It was also supplied by Martin Marietta Company from its quarry in Castle Hayne, North Carolina. Washed rounded gravel (RG) was provided by Memphis Stone and Gravel Company from its Pit 558 in Shelby County, Tennessee. Dense crushed limestone (DL) was supplied by McClinton-Anchor from its West Fork quarry just outside of Fayetteville, Arkansas.

The coarse aggregates used at NCSU met ASTM C 33 size #57 specifications, with most of the material passing the 1-in. (25-mm) sieve. The CG was a hard, angular aggregate of low absorption (0.6%). The MM was a cubical to subangular, relatively porous, and highly absorptive (typically over 4.5%) shell limestone. The RG, drawn from a river, was primarily siliceous and contained some crushed faces, but most of them were worn. The absorption was moderate (just under 3%) and hard chert particles were present. The maximum size of the coarse aggregate used at the University of Arkansas was slightly smaller and met ASTM C 33 size #67 specifications.

Mineralogically, the CG consisted of approximately 35% quartz, 30% potassium feldspar, 25% sodium-rich plagioclase feldspar, and 10% biotite. The MM was a sandy fossiliferous limestone with about 60% calcite, 35% quartz, and 5% other oxide and hydroxide minerals. The RG consisted of 25% quartz, 10% quartzite, 60% chert, and 5% sandstone. The DL contained 97% limestone and 3% clay minerals. It should be noted that the RG contained a large amount of chert, which could be a cause for alkali-silica reaction.

Physical analyses of the coarse aggregates were performed according to ASTM C 33, and the results are shown in Table 3.3.

### 3.3 Fine Aggregates

Three different kinds of sand were used in this test program. The sand used with CG and MM was obtained from Lillington, North Carolina. The sand used with RG was shipped from Memphis, Tennessee, and Arkansas River sand was used with DL.

The Lillington sand contained 75% quartz, 22% feldspar, and 3% epidote. The finer material (passing #10 sieve) of the Memphis sand consisted of 95% quartz, 4% opaque minerals (oxide and hydroxide minerals), and 1% other miscellaneous minerals; whereas the coarser material (retained on #10 sieve) of the sand consisted of 20% chert, 30% sandstone and shale fragments, and 50% quartz. The finer material of the Arkansas River sand consisted of 85% quartz, 4% chert, and 11% microcline, and less than 1% rock fragments and heavy minerals; whereas the

coarser material of the Arkansas River sand consisted of 62% quartz, 16% chert, 11% microcline, and 5% rock fragments. The physical properties of the three kinds of sand are shown in Table 3.4.

**Table 3.3 Properties of coarse aggregates**

	CG	MM	RG	DL
Specific gravity (SSD)	2.64	2.48	2.55	2.72
% absorption	0.6	6.1	2.8	0.69
DRUW (pcf)	93.6	78.4	94.8	99.0
Fineness modulus	6.95	6.92	6.99	6.43
% Passing				
1 in.	100	98	95	100
3/4 in.	90	85	72	100
1/2 in.	31	43	56	82
3/8 in.	13	19	26	48
#4	2	4	1	6
#8	0	0	2	3
L.A. abrasion, %				
Grading A			17.6	
Grading B	39.6	43.7		24
Sodium sulfate soundness, %	1.3	9.6	2.8	3
Less than 200 by washing, %	0.6	0.4	—	—

### 3.4 Chemical Admixtures

Chemical admixtures used in producing VES (A) concrete included an accelerator, a high range water reducer, and an air-entraining agent. Their brand names, suppliers, and respective reference specifications are identified in Table 3.5.

### 3.5 Mineral Admixtures

In a group of test specimens of freezing-thawing tests, silica fume was used in the concrete (see Section 6.3.2). The silica fume was in slurry form containing approximately 50% solids. It was EMSAC, Type F-100, supplied by Elkem Chemicals, Pittsburgh, Pennsylvania.

**Table 3.4 Properties of fine aggregates**

	Lillington Sand	Memphis Sand	Arkansas River Sand
Specific gravity (SSD)	2.57	2.62	2.62
% absorption	1.1	1.2	0.6
Fineness modulus	2.66	2.60	2.72
% passing			
#4	100	100	96
#8	97	93	88
#16	80	82	75
#30	47	55	55
#50	9	9	13
#100	1	1	0.4

**Table 3.5 Chemical admixtures used in the test program**

Admixture	Brand Name	Supplier	Reference Specifications
Accelerator	DCI (calcium nitrite), 30% solution	W. R. Grace	ASTM C 494, Type C
HRWR	Melment 33% (melamine base)	Cormix	ASTM C 494, Type F
AEA	Daravair (neutral vinsol resin), 17% solids	W. R. Grace	ASTM C 260

DCI = Darex Corrosion Inhibitor

## Mixture Proportions

In the early stage of this investigation, an extensive program of development work involving a total of 360 trial batches of concrete was conducted in search of appropriate mixture proportions for the various types of high performance concrete. A detailed discussion of this development work was presented in volume 2 of this report series, *Production of High Performance Concrete*. For VES concrete, the development work included 203 trial batches using four different kinds of coarse aggregate.

Proportioning of the concrete mixtures was based on the methods recommended by ACI Committee 211 (1993b). Selections of W/C, workability, and air content requirements were made first, and these constraints were incorporated in accordance with the ACI 211 guidelines, as was selection of aggregate quantities.

At NCSU, a nominal maximum size (NMSA) of 1 in. (25 mm) (ASTM C 33, size #57) was selected for the coarse aggregate as the most appropriate for a variety of applications. This aggregate size could be used for many structural members or pavements, although larger aggregates might be better for paving mixes in some locations. The maximum size of the coarse aggregate used at the University of Arkansas was slightly smaller and met ASTM C 33, size #67, specifications.

Similarly, although the quantity of coarse aggregate (volume of coarse aggregate per unit volume of concrete) could have been increased by about 10 percent for paving applications, the quantity initially selected was at or near the recommended value in ACI 211. These values were adjusted slightly in subsequent trial batches. The objective of selecting a less coarse mixture was to provide a mixture for more general purposes. A less coarse mixture would be easier to use in small, hand placed and finished applications.

Based on the evaluation of the results of the trial batches, the mixture proportions for the VES (A) and VES (B) concretes with four different types of aggregate were selected, and they are summarized in Tables 4.1 and 4.2.

**Table 4.1 Mixture proportions of VES (A) concrete with four different aggregate types**

Coarse aggregate type: Source of sand:	CG Lillington	MM Lillington	RG Memphis	DL Van Buren
Cement (Type III), pcy	870	870	870	870
Coarse aggregate, pcy	1,720	1,570	1,650	1,680
Sand, pcy	820	800	760	920
HRWR (melamine based), oz/cwt	5.0	5.0	10	4.0
Calcium nitrite (DCI), gcy	6.0	6.0	6.0	6.0
AEA, oz/cwt	3.0	2.5	4.0	2.5
Water, pcy	350	350	350	340
W/C	0.40	0.40	0.40	0.39
Slump, in.	5	7	6	5.75
Air, %	6.5	6.4	7.5	4.40
Strength at 6 hr, psi (insulated)	2,090	2,000	2,360	3,090
Concrete temperature at placement, °F	71	75	79	78

Note: 1 MPa = 145 psi

**Table 4.2 Mixture proportions of VES (B) concrete with four different aggregate types**

Aggregate type: Source of sand:	CG Lillington	MM Lillington	RG Memphis	DL Van Buren
Cement (Pyrament), pcy	850	850	850	855
Coarse aggregate, pcy	1,510	1,500	1,510	1,680
Sand, pcy	1,440	1,460	1,400	1,560
HRWR (Melamine Based), oz/cwt	0	0	0	0
Calcium nitrite (DCI), gcy	0	0	0	0
AEA, oz/cwt	0	0	0	0
Water, pcy	195	145	183	200
W/C	0.23	0.17	0.22	0.23
Slump, in.	6.5	4	3.5	7.0
Air, %	6.0	7.0	3.7	7.6
Strength at 4 hr, psi (insulated)	2,510	2,270	3,060	2,890
Concrete temperature at placement, °F	72	72	75	77

Note: 1 MPa = 145 psi

# 5

## Mixing and Curing Procedures

### 5.1 Mixing Procedures

Concretes made with crushed granite (CG), marine marl (MM), or rounded gravel (RG) were produced in the Concrete Materials Laboratory at NCSU using a tilt drum mixer with a rated capacity of 3.5 ft<sup>3</sup> (0.1 m<sup>3</sup>). Concretes using dense limestone were also produced in an identical mixer in the Concrete Laboratory at Arkansas. The normal laboratory mixing and batching procedures (ASTM C 192) were modified slightly to approximate typical concrete dry-batch plant operations. Whether the concrete was produced at NCSU or Arkansas, the same mixing procedures were generally followed as described below.

#### 5.1.1 VES (A) Concrete

VES (A) concrete used Type III portland cement and calcium nitrite (DCI) as an accelerator. The step-by-step mixing procedures are as follows:

1. Butter the mixer with a representative sample of mortar, composed of approximately 3 lbs (1.36 kg) of cement, 6 lbs (2.72 kg) of sand, and 2 lbs (0.91 kg) of water. Turn on the mixer to coat the inside of the mixer completely. (At Arkansas, only water was used to butter the mixer.) Empty the mixer and drain it for 1 minute.
2. Charge the mixer successively with approximately 25% of coarse aggregate, 100% of sand, 50% of water, and 100% of air-entraining agent added with the sand. Mix for 1 minute to generate air bubbles. (At Arkansas, the mixer was charged with 50% of coarse aggregate, 67% of sand, and 67% of water.)
3. Stop the mixer and add the remaining coarse aggregate and water. Mix for 1 minute (if needed) to equalize the temperature of the materials. Otherwise mix 10 seconds and add the entire amount of cement. Record the time as the beginning of the total mixing time. After mixing for one minute, stop the mixer; add the high range water

reducer and continue mixing for 5 minutes. During all mixing, cover the mixer with a lid to minimize evaporation.

4. Mix continuously for 20 minutes to simulate travel time for a ready-mix truck. Then stop the mixer and add DCI. Mix for an additional 5 minutes. (Total mixing time, beginning with the addition of cement, is approximately 30 minutes.)
5. Discharge the concrete into a wheelbarrow; measure the unit weight, air content, slump, and temperature; fabricate test specimens.

### **5.1.2 VES (B) Concrete**

VES (B) concrete used Pyrament PBC-XT cement without any admixtures. The step-by-step mixing procedures are as follows:

1. Butter the mixer with a representative sample of mortar composed of approximately 3 lbs (1.36 kg) of cement, 6 lbs (2.72 kg) of sand, and 2 lbs (0.91 kg) of water. Turn on the mixer to coat the inside of the mixer completely. (At Arkansas, only water was used to butter the mixer.) Empty the mixer and drain it for 1 minute.
2. Charge the mixer successively with the entire amount of coarse aggregate, sand, and water. Mix for 10 seconds (but 1 minute at Arkansas) to coat the rock and sand with water. Ensure that the materials are of the same temperature.
3. Stop the mixer and add the entire amount of Pyrament XT cement. Record the time as the beginning of the total mixing time. During all mixing, cover the mixer with a lid to minimize evaporation.
4. Mix continuously for 30 minutes to simulate travel time for a ready-mix truck. (The concrete may appear dry initially, but will gradually improve. The total mixing time, beginning with the addition of Pyrament PBC-XT cement, is 30 minutes.)
5. Discharge the concrete into a wheelbarrow; measure the unit weight, air content, slump, and temperature; fabricate test specimens.

## **5.2 Curing Procedures**

Curing procedures differed for the different categories of high performance concrete. For VES concrete, whether using Type III portland cement or Pyrament XT blended cement, insulation was used to achieve rapid strength gain in the first few hours.

For each batch of concrete produced, an appropriate number of control cylinders were cast in 4 x 8-in. (100 x 200-mm) plastic molds. The cylinders were immediately placed in a Styrofoam block serving as an insulating jacket.

At NCSU, the Styrofoam block was made by gluing together a stack of eight sheets of 1-in. (25-mm) thick Styrofoam board. Through the 8-in. (200-mm) thickness of this block, a number of 4.25-in. (106-mm) holes were bored. This block was then glued to a base sheet of 1-in. (25-mm) thick Styrofoam which was, in turn, backed by a 0.5-in. (13-mm) sheet of plywood. Each control cylinder, together with its plastic mold, was stored in the bored hole within the Styrofoam block. The block was then covered with a top Styrofoam sheet similar to the base sheet. Figure 5.1a shows a view of the Styrofoam block used at NCSU. The Styrofoam block used at Arkansas was constructed of six sheets of 2-in. (50-mm.) Styrofoam board glued together as shown in Figure 5.1b.



**Figure 5.1a** Styrofoam insulation block used for curing concrete cylinders at NCSU



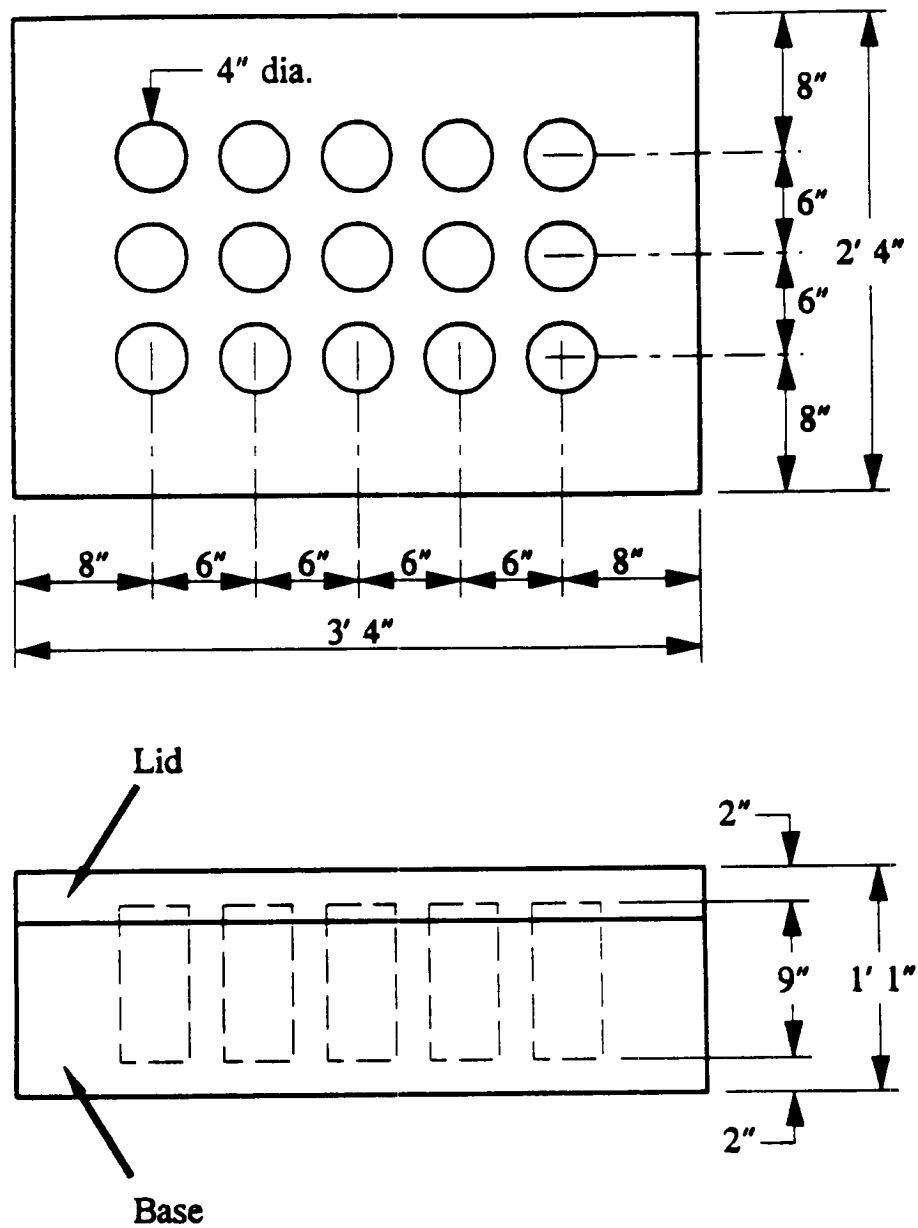


**Figure 5.1b Styrofoam insulation block used for curing concrete cylinders at the University of Arkansas**

After the cylinders were stored in the Styrofoam block for 6 hours for VES (A) or 4 hours for VES (B), they were removed from the insulation block and stripped from their molds. Several of the cylinders were tested immediately for compressive strength, and the remaining cylinders were stored in sealed plastic bags under normal laboratory conditions for testing at later ages.

The cylinders were placed in the plastic bags not so much to ensure continued curing as to control the rate of evaporation of the specimens. Although concrete at a job site would be covered with curing compound, opening a pavement structure to traffic at 4 or 6 hours would probably result in loss of the compound fairly soon. The concrete would therefore be exposed to evaporation of internal water soon after the design age. However, evaporation would be somewhat slowed since only one face of the pavement would be exposed. The plastic bag reduces evaporation compared to exposure of the specimen to laboratory air (50% relative humidity), but does not prevent it. Such curing does not provide unrealistically optimistic strength values nor does it unrealistically reproduce strength gain characteristics.

In addition to the 4 x 8-in. (100 x 200-mm) cylinders, three 6 x 12-in. (150 x 300-mm) cylinders (only two at Arkansas) were also cast for each batch of concrete. These large cylinders were cured inside an insulation block (as were the small cylinders) and were also tested for compressive strength at 6 hours for VES (A) or 4 hours for VES (B), for comparison with the results from the small cylinders. The comparison was used to investigate possible size effects.

Beam specimens for flexure or freeze-thaw tests were cast in steel forms, as were their companion cylinders. After they were cast, these specimens and cylinders were kept in an insulation box for 6 or 4 hours. Once removed from the insulation box and stripped from their forms, some were tested immediately and others were stored in sealed plastic bags for testing at later ages.

The inside dimensions of the insulation box are 40-in. (100-cm) wide, 43-in. (107.5-cm) long, and 21-in. (52.5-cm) deep. The side walls of the box are made of 1.5-in. (38-mm) Styrofoam insulation sandwiched between two sheets of 0.75-in. (19-mm) plywood. The base and the cover of the box are also made of 1.5-in. (38-mm) Styrofoam insulation sandwiched between two sheets of 0.5-in. (13-mm) plywood. Figure 5.2 shows a view of the insulation box.



**Figure 5.2** Insulated curing box for concrete specimens at NCSU

## 6

### Laboratory Experiments

The laboratory investigation consisted of tests for both the fresh or plastic concrete and the hardened concrete. The plastic concrete tests included tests for slump, air content, unit weight, and concrete temperature, and the results of these tests have been presented in volume 2 of this report series, *Production of High Performance Concrete*. The laboratory tests for hardened concrete included compression tests for strength and modulus of elasticity, tension tests for tensile strength and flexural modulus, freezing-thawing tests for durability factor, shrinkage tests, rapid chloride permeability tests, tests for AC impedance, and tests for concrete-to-concrete bond. The testing program for the mechanical properties of hardened concrete is outlined in Tables 6.1 through 6.4\*.

#### 6.1 Compression Tests

The compression tests were conducted on 4 x 8-in. (100 x 200-mm) cylinders at different ages to obtain stress-strain, strength-time, and modulus-time relationships for VES concrete with four different types of coarse aggregates (MM, CG, DL and RG). These tests were conducted for the VES (A) concrete (with portland cement) and VES (B) concrete (with Pyrament cement). A limited number of compression tests were also conducted on 6 x 12-in. (150 x 300-mm) cylinders to investigate the size effect.

##### 6.1.1 Test Setup and Procedure

The compression tests were conducted in a 2000-kip (8900-kN) compression machine with a hydraulic feedback system and a MTS 436 controller unit. The compression machine was equipped with both load and displacement controls. The testing for strength and the modulus of elasticity was done under the load control option.

---

\*The testing for the fatigue properties of plain concrete (Group IV) was not conducted because of the change of the scope of the project.

**Table 6.1 Test program for compressive strength and modulus of elasticity — Group 1**

Category of HPC	Aggregate Type	No. of 4 x 8-in. Cylinders				No. of 6 x 12-in. Cylinders			
		Age at testing (Days)				Age at testing (Days)			
		1	3	7	28	1	3	7	28
VES (A)	MM	3	3	3	3	2	—	—	—
	CG	3	3	3	3	2	—	—	—
	DL	3	3	3	3	2	—	—	—
	RG	3	3	3	3	2	—	—	—
VES (B)	MM	3	3	3	3	2	—	—	—
	CG	3	3	3	3	2	—	—	—
	DL	3	3	3	3	2	—	—	—
	RG	3	3	—	3	2	—	—	—

**Table 6.2 Test program for modulus of rupture, tensile strain capacity, and split tensile strength — Group 2**

Category of HPC	Aggregate Type	No. of Rupture Specimens Age at testing			No. of Split Tensile Specimens at Design	No. of 4 x 8-in "Control" Cylinders at 24 hrs
		design	7 days	28 days		
VES (A)	MM	2	2	2	2	2
	CG	2	2	2	2	2
	DL	2	2	2	2	2
	RG	2	2	2	2	2
VES (B)	MM	2	2	2	2	2
	CG	2	2	2	2	2
	DL	2	2	2	2	2
	RG	2	2	2	2	2

**Table 6.3 Test program for frost durability, shrinkage, and chloride permeability — Group 3**

Category of HPC	Aggregate Type	No. of Freezing - Thawing Specimens at 14 days	No. of Shrinkage Specimens at Design to 90 days	No. of Chloride Permeability Specimens at 14 days	No. of 4 x 8-in. "control" Cylinders at 24 hrs
VES (A)	MM	3	3	2	2
	CG	3	3	2	2
	DL	—	—	—	—
	RG	3	3	2	2
VES (B)	MM	3	3	2	2
	CG	3	3	2	2
	DL	3	—	—	—
	RG	3	3	2	2

**Table 6.4 Test program for bond strength — Group 5**

Category of HPC	Aggregate Type	No. of Specimens C-C Bond Test at Design	No. of Specimens C-S Bond Test at Design	No. of 4 x 8-in. "Control" Cylinders at 24 hrs
VES (A)	MM	—	—	—
	CG	2	—	2
	DL	—	—	—
	RG	—	—	—
VES (B)	MM	—	—	—
	CG	2	—	2
	DL	—	—	—
	RG	—	—	—
NCDOT (control)	CG	2	—	—

The compression tests were conducted according to AASHTO T-22-86 and ASTM C 39 with minor modifications: the use of an unbonded capping system, such as steel caps lined with neoprene pads, and the use of a deformation measuring fixture that included linear voltage differential transducers (LVDTs). The two LVDTs used in the compressive tests were Lucas Schaevitz MHR 050, with a sensitivity of 2.500 mV/V/0.001". The voltage was converted by a National Instruments AT-MIO-16 12-bit analog-to-digital converter.

An aluminum mounting jig was built to facilitate mounting the LVDTs on the test cylinder. The jig ensured that the LVDTs were placed 180 degrees apart and in the central 4 in. (100 mm) of the test cylinders. The device for mounting the transducers on the 4 x 8-in. (100 x 200-mm) cylinders is shown in Figure A.1. First, the specimens were placed in the device and the bottom of the cylinder was aligned with the alignment mark. A line of superglue was applied at each of the four locations where the transducers were to be attached. The metallic contact area of the LVDT holder was sprayed with a zip kicker (a product for speeding up the reaction between the metal and the concrete surface with superglue), and the LVDT holders (together with LVDTs) were attached with the wires of the LVDT sticking out toward the bottom of the cylinder. After about a minute, the cylinder was removed from the transducer mounting device. To ensure a good bond between the LVDT holders and the concrete surface, additional superglue was applied all around the contact surface and sprayed with the zip kicker. The unbonded caps were put on the cylinders, and the specimen was placed in the compression testing machine. The LVDTs used to measure the axial deformation of the cylinders had a maximum range of  $\pm 0.05$  in. (1.3 mm), and the gage length for the axial deformation measurements was 4 in. (100 mm). The core of the LVDTs could be moved up or down by a specially designed screw-thread mechanism (machined to become a part of the core of the LVDT) to adjust the output voltage to zero or near zero.

The test specimen with the two mounted LVDTs was placed inside a steel jacket, which rested between the two platens of the compression testing machine. Figure A.2 shows the steel jacket for protecting the transducers during the compression testing. The steel jacket prevented damage to the transducers from the brittle failure of the specimens at the maximum load.

The test cylinders were loaded and unloaded up to a load of 5,000 lbs (22.2 kN) at least twice prior to loading the cylinders to failure. This initial loading and unloading was done for seating purposes and to properly zero out the LVDTs. After the initial loading and unloading, the cylinders were loaded to failure. For 4 x 8-in. (100 x 200-mm) cylinders, a loading rate of 26,500 lbs/min (118 kN/min) was used, and for the 6 x 12-in. (150x300-mm) cylinders, a loading rate of 59,400 lbs/min (264 kN/min) was used. The loading rates were within the range of 20 to 50 psi/sec (0.14 to 0.34 MPa/sec), as specified in AASHTO T 22-86 and ASTM C 39.

The data acquisition system used was an OPTIM system (Megadec 100) with a capability of recording up to 40 channels of output. The load output and the output from the two displacement transducers were recorded by LabWindows software, in conjunction with the OPTIM data acquisition system. A view of the compression test setup is shown in Figure A.3.

### *6.1.2 Specimen Preparation*

The specimens were prepared according to ASTM C 192. Specimens used specifically for determining the compressive strength and modulus of elasticity were 4 x 8-in.(100 x 200-mm) cylinders cast in plastic molds. Companion 6 x 12-in.(150 x 300-mm) cylinders were also cast to investigate the size effect.

For the VES (A) concrete, the specimens inside the molds were placed after casting in a Styrofoam curing block, which protected the specimens from rapid heat loss. The Styrofoam curing block was made by gluing together a stack of eight 1-in. (25-mm) Styrofoam boards. The Styrofoam block was then bored to create 4.25-in. (106-mm) diameter holes in which the 4 x 8-in. (100 x 200-mm) cylinders with molds were placed for curing. The Styrofoam block was then glued to a Styrofoam base piece of 1-in.(25-mm) thickness, which was backed by a plywood sheet 0.5 in. (13 mm) thick. The top side of the Styrofoam block was covered in the same fashion as the bottom side. The Styrofoam curing block was very effective in maintaining the heat generated from the cement hydration process and preventing rapid heat loss. The 6 x 12-in. (150 x 300-mm) cylinders were cured inside a Styrofoam curing box similar to that used for the 4 x 8-in. (100 x 200-mm) cylinders. The 6 x 12-in. (150 x 300-mm) cylinders were tested at design ages of 6 and 4 hours for the VES (A) and VES (B) concretes respectively.

After casting, the VES (A) specimens inside the molds were stored in the Styrofoam curing block for curing until the design test age of 6 hours; the VES (B) specimens for 4 hours. Upon removal from the Styrofoam curing box, the cylinders were stripped of their molds and tested immediately for the compressive strength and modulus of elasticity; the remaining cylinders were stored in sealed plastic bags for testing at later ages. The specimens were air dried for 10 to 15 minutes before the LVDTs were mounted on the two sides of the specimens.

### *6.1.3 Test Results and Discussion*

There are three categories of test results. They include the stress-strain relationships, strength-time and modulus-time response, and the strength comparisons of 4 x 8-in. (100 x 200-mm) cylinders with 6 x 12-in. (150 x 300-mm) cylinders.

#### *6.1.3.1 Stress-Strain Relationships*

The stress-strain curves shown in Figures 6.1a and 6.1b were obtained from the load-deformation curves by dividing the load by the nominal area of the cylinders and the axial deformation by the gage length. Figure 6.1a shows typical stress-strain curves of VES (A) concrete at the design age of 6 hours with different types of coarse aggregates. From these figures, it appears that the stress-strain curve for VES (A) concrete with MM, RG, and CG coarse aggregate is relatively more nonlinear than that with DL coarse aggregate. The strain capacity corresponding to the maximum strength is about 1,200 microstrains for VES (A) concrete with DL coarse aggregate as



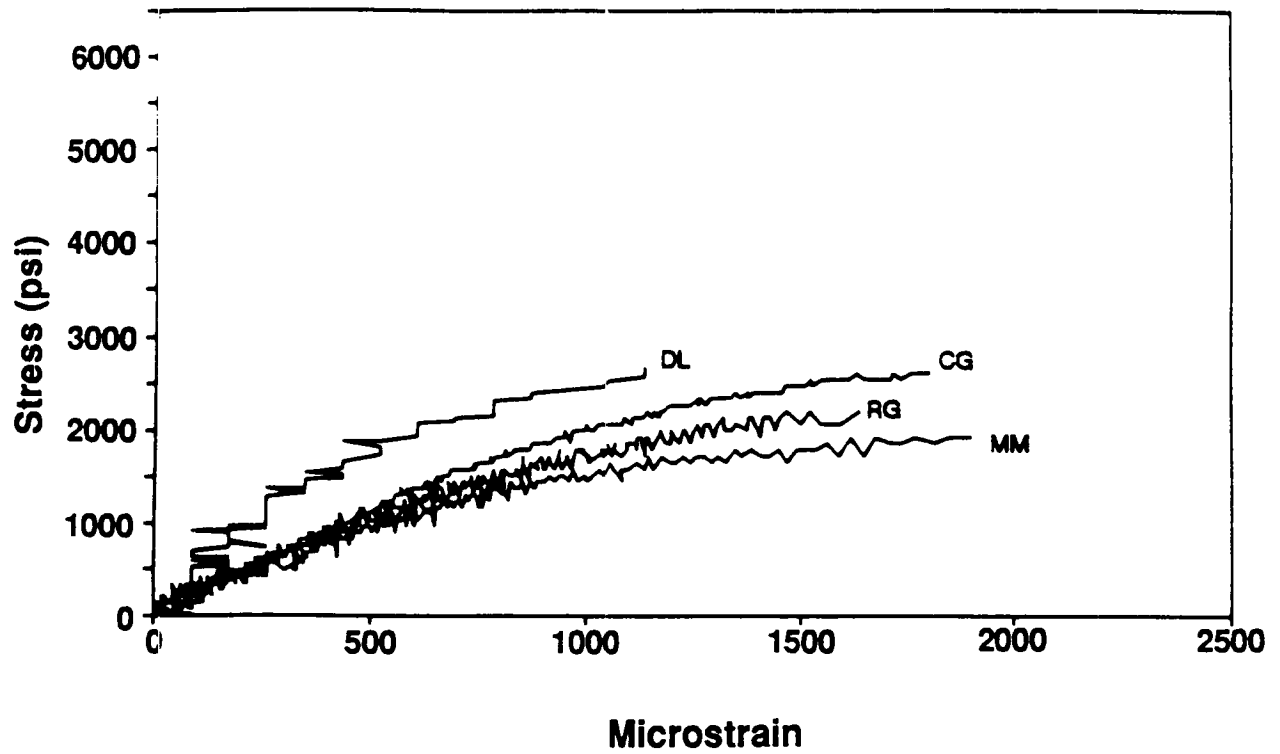


Figure 6.1a Stress-strain relationship of VES (A) concrete at design age of 6 hrs

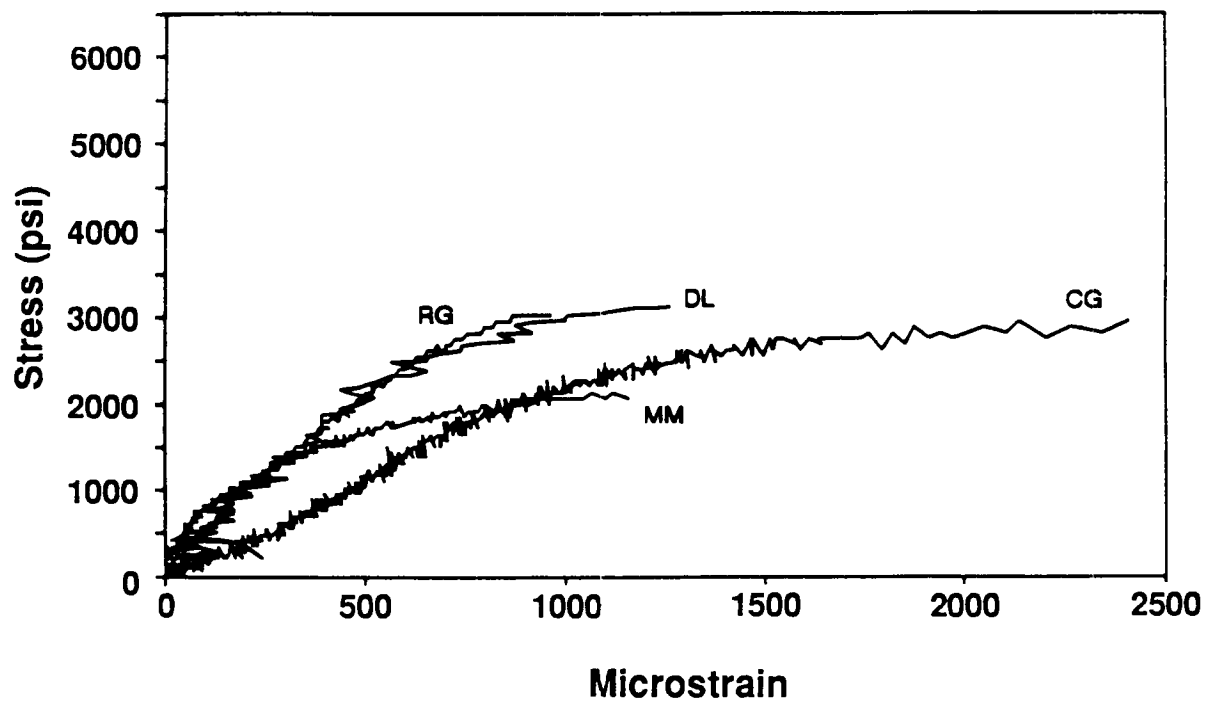


Figure 6.1b Stress-strain relationship of VES (B) concrete at design age of 4 hrs

compared to about 1,600 to 1,800 microstrains for VES (A) concrete with MM, RG, and CG coarse aggregates.

Figure 6.1b shows typical stress-strain curves of VES (B) concrete at design age of 4 hours with different types of coarse aggregates. From these figures, it appears that the stress-strain curve for VES (B) concrete with RG and DL coarse aggregate is slightly, stiffer than those with MM and CG aggregates. The strain capacity corresponding to the maximum strength is about 900 to 1,000 microstrains for the VES (B) concrete with MM, RG and DL coarse aggregates, as compared to about 2,000 microstrains for the VES (B) concrete with CG coarse aggregate.

The effect of coarse aggregate on the stress-strain relationship at 28 days is shown in Figure 6.2a and 6.2b; it can be seen that softer coarse aggregate such as MM exhibits softer response in the initial portion of the curve, translating into a lower modulus of elasticity. The compressive strain capacity at the age of 28 days ranges between 1,900 and 2,100 microstrains for the VES (A) concrete, see Figure 6.2a; and between 1,800 to 2,200 microstrains for VES (B) concrete, see Figure 6.2b.

The effect of age on the stress-strain curve for the VES (A) and VES (B) concretes with one type of coarse aggregate (MM) is shown in Figure 6.3a and 6.3b. These figures show that the initial portion of the stress-strain curve becomes more linear as the concrete matures; there is also a slight increase in the strain capacity during the early age (up to 3 days), after which the age of the concrete has insignificant effect on the strain capacity. These figures also show that for VES (A) concrete (with portland cement), the initial stiffness shown by the stress-strain curve at the design age of 6 hours is noticeably less than at later ages, whereas for the VES (B) concrete (with Pyrament cement), the initial stiffness is comparable to the stiffness at later ages. Note that the stiffening of the behavior over time shown by the initial portion of the stress-strain curve results in an increase in the modulus of elasticity with time.

### 6.1.3.2 Strength-Time and Modulus-Time Relationships

The test results of strength and modulus of elasticity for VES concrete (Options A and B) are summarized in Tables 6.5a and 6.5b. The values shown in the tables are averages for three replicate specimens. The strength-time relationships for VES concrete (Options A and B) with different types of coarse aggregate in a nondimensional form are shown in Figures 6.4a and 6.4b. Each point on the curve is based on an average of three replicate specimens. From Figure 6.4a, it can be seen that for the VES (A) concrete, the strength gain with respect to time for different types of coarse aggregates is similar. The figure indicates that at the design age of 6 hours, the strength achieved is about 30 to 45% of the 28-day strength and that during the early age (up to 3 days), the concrete with softer aggregate reaches a lower fraction of its 28-day strength. This figure also shows that the comparison of the observed strength-time relationships of VES (A) concrete with those predicted by ACI Committee 209 (1993a). The comparison shows that the strength gain is much faster in the first 3 days for the VES (A)

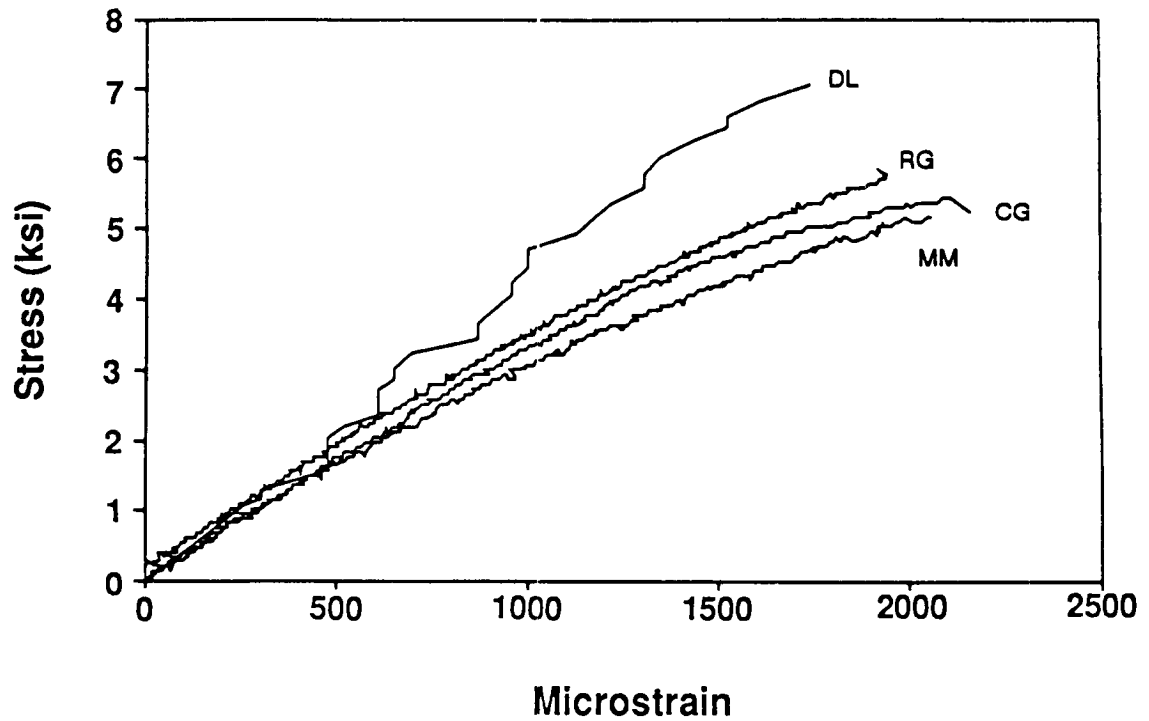


**Figure 6.2a** Effect of coarse aggregate on VES (A) stress-strain relationship at 28 days

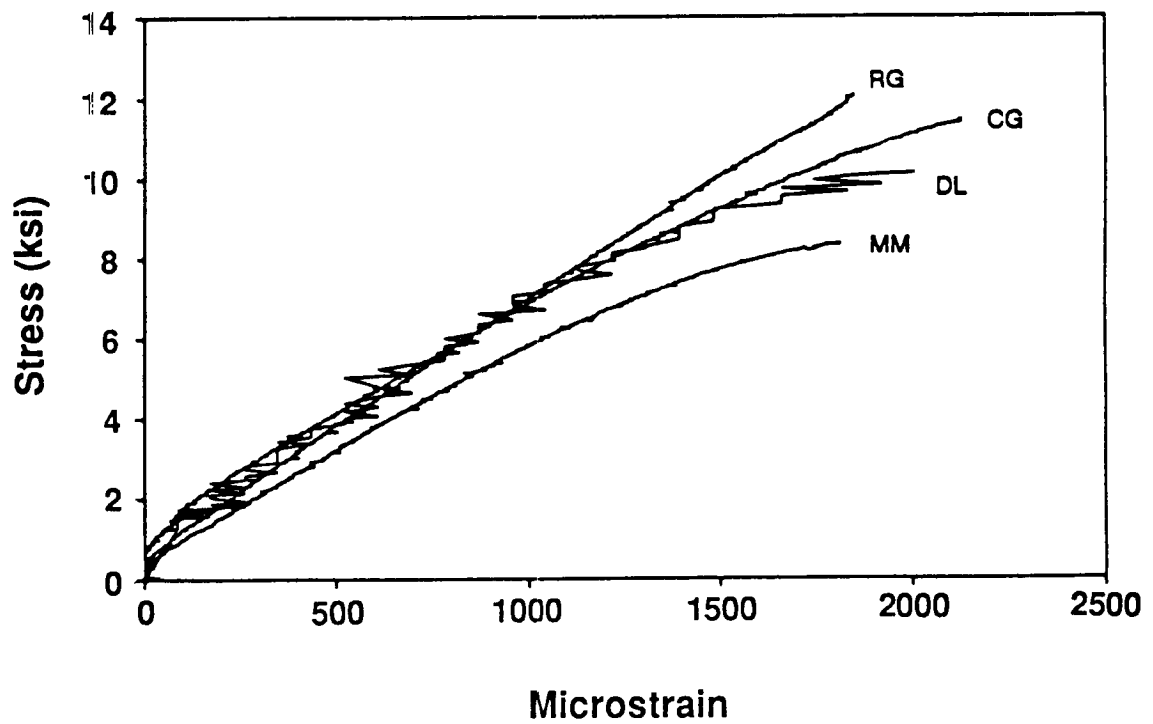


**Figure 6.2b** Effect of coarse aggregate on VES (B) stress-strain relationship at 28 days

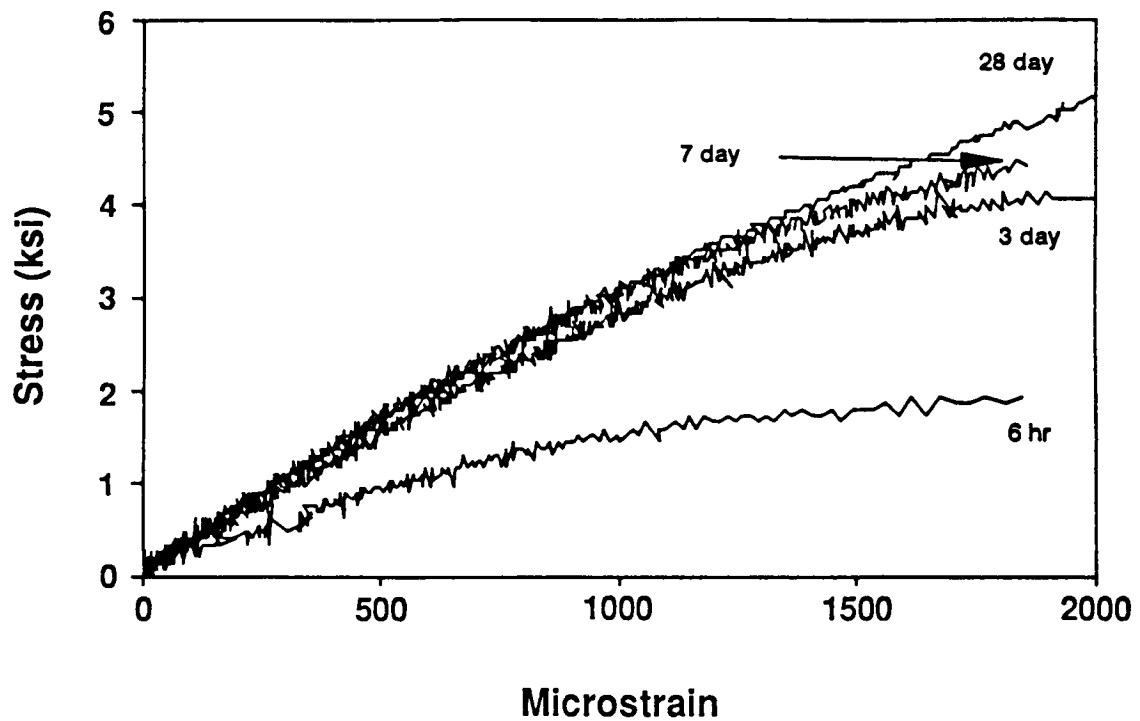


**Figure 6.3a** Effect of age on stress-strain relationship of VES (A) MM (6hrs, 3d, 7d, 28d)

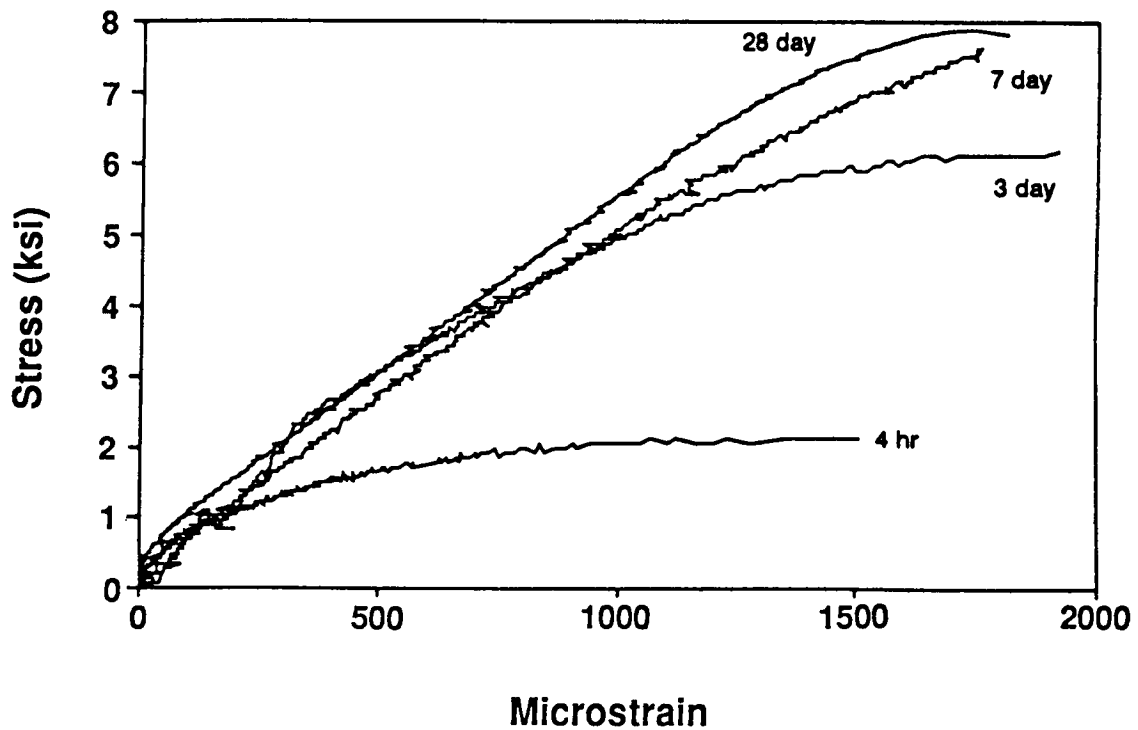


**Figure 6.3b** Effect of age on stress-strain relationship of VES (B) MM (4hrs, 3d, 7d, 28d)

**Table 6.5a Summary of test results for compressive strength (psi) and modulus of elasticity (10<sup>6</sup> psi) at different test ages for VES (A) concrete**

Age	MM	CG	DL	RG
Compressive Strength (psi)				
6 hrs (1)	1450	1690	1292	1450
6 hrs (2)	1540	1710	2205	1870
6 hrs (3)	1930	2540	2349	2130
3 days	3780	4400	—	4310
7 days	4360	4520	7226	- -
28 days	5230	5450	7884	5550
Modulus of Elasticity (10 <sup>6</sup> psi)				
6 hrs (1)	1.91	1.63	—	1.64
6 hrs (3)	1.69	2.05	4.42	1.72
3 days	3.15	2.92	—	3.00
7 days	3.13	3.07	4.83	- -
28 days	3.14	3.28	5.02	3.36

- (1) 4 x 8-in. companion cylinders of flexural strength testing  
(2) 6 x 12-in. companion cylinders of compressive strength testing  
(3) 4 x 8-in. cylinders of compressive strength testing

**Table 6.5b      Summary of test results for compressive strength (psi) and modulus of elasticity (10<sup>6</sup> psi) at different test ages for VES (B) concrete**

Age	MM	CG	DL	RG
Compressive Strength (psi)				
4 hrs (1)	2680	2890	2372	2580
4 hrs (2)	1670	2210	2432	2670
4 hrs (3)	1970	2980	3034	3140
3 days	6690	8440	—	8800
7 days	7560	9810	9498	10200
28 days	7930	11820	10189	12190
Modulus of Elasticity (10 <sup>6</sup> psi)				
4 hrs (1)	3.24	3.96	—	3.96
4 hrs (3)	3.25	3.07	4.41	4.40
3 days	4.67	4.54	—	5.53
7 days	5.05	5.43	7.31	6.14
28 days	5.49	5.28	6.26	6.21

- (1) 4 x 8-in. companion cylinders of flexural strength testing  
(2) 6 x 12-in. companion cylinders of compressive strength testing  
(3) 4 x 8-in. cylinders of compressive strength testing

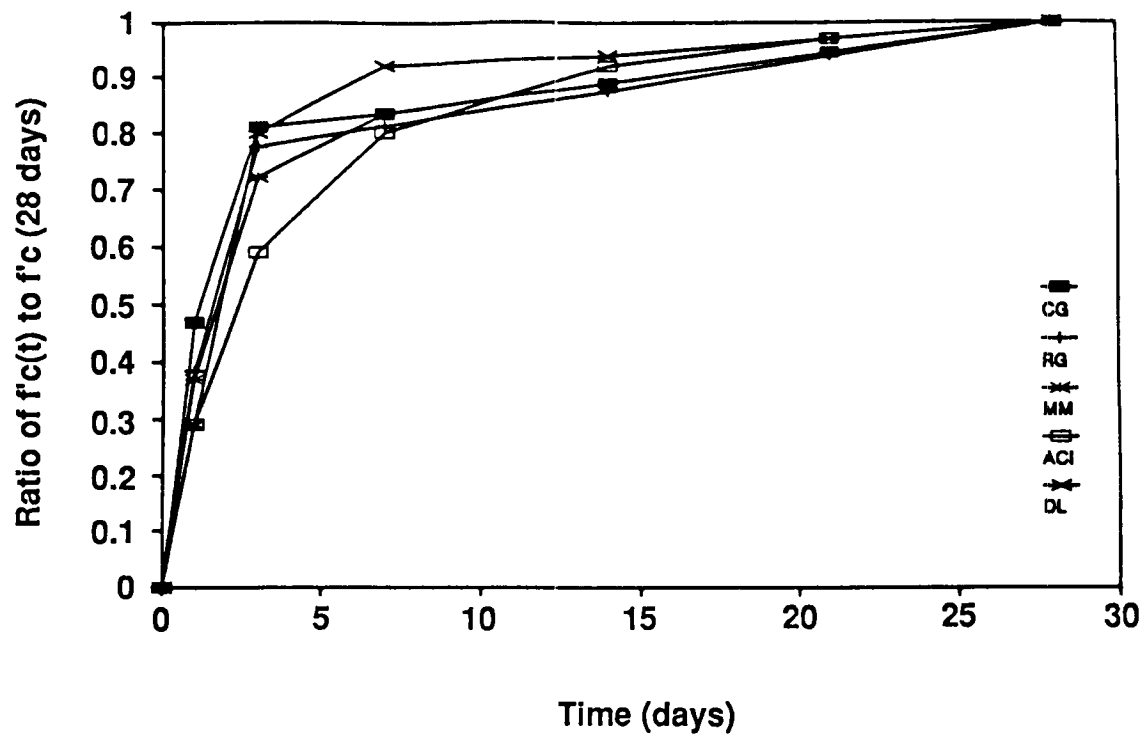


**Figure 6.4a** Variation of compressive strength with time for VES (A)

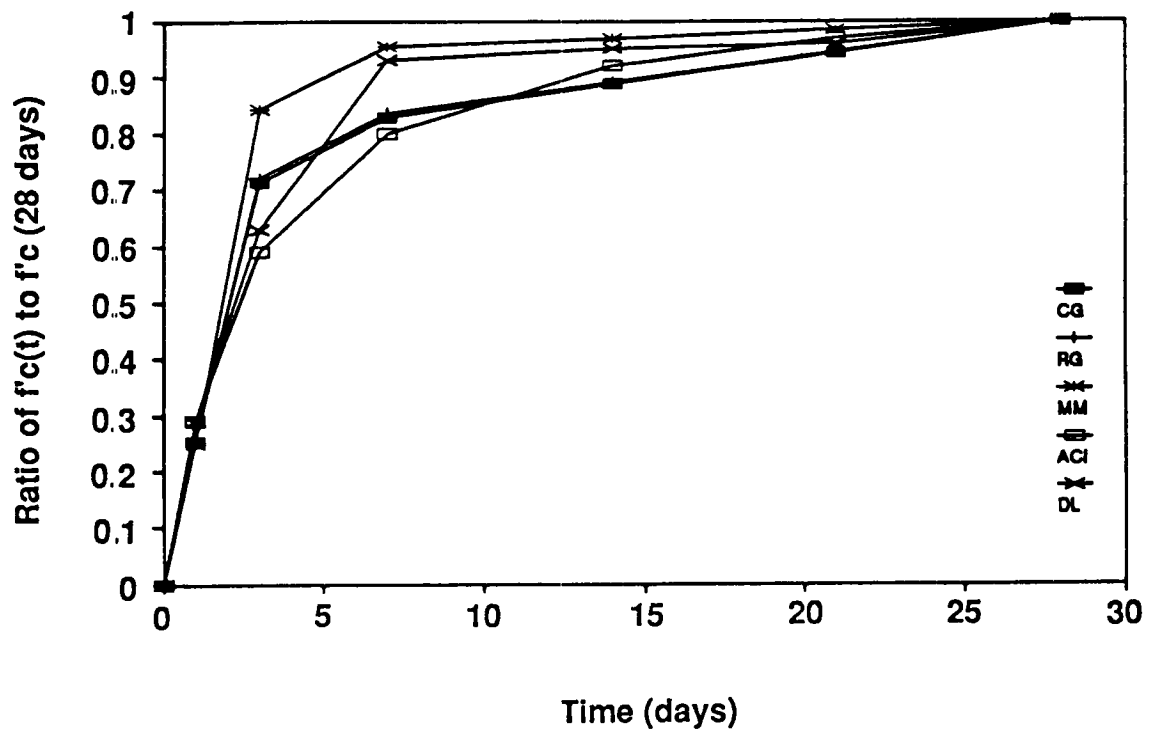


**Figure 6.4b** Variation of compressive strength with time for VES (B)

concrete than predicted by ACI committee 209. It should be noted that the equation of ACI Committee 209 was developed from experimental data for concretes with strengths up to 6,000 psi (42 MPa) at 28 days. The nondimensional strength-time relationship for VES (B) concrete shown in Figure 6.4b indicates that at the design age of 4 hours, the strength achieved is about 25 to 30% of the 28-day strength and that the strength gain with time for the MM aggregate is higher than for CG, RG, and DL coarse aggregates. The comparison with the prediction of the ACI committee 209 (see Figure 6.4b) shows that the strength gain is much faster in the first 7 days for the VES (B) concrete than predicted. The comparison of Figure 6.4a and Figure 6.4b shows that the strength-time relationship is more sensitive to the type of coarse aggregate for VES (B) concrete than for VES (A) concrete.

The modulus-time relationships for VES concrete (Options A and B) with all four different types of coarse aggregate are shown in Figures 6.5a and 6.5b. Each point on the curve is an average of three replicate specimens. The results indicate a lower modulus for the softer coarse aggregate, such as MM; however, the rate of increase in the modulus with time is comparable to VES concrete with other types of coarse aggregates.

The predictions of the various published equations for the modulus of elasticity are compared with the observed modulus of elasticity of VES concrete at different ages up to 28 days (Figures 6.6a and 6.6b). The ACI 318 equation (1993c) uses a premultiplier of 57,000 to the square root of the compressive strength in psi units. It can be seen that for VES (A) concrete, ACI 318, ACI 363, and Ahmad et al. (1993c, 1984, 1985) underpredict the observed values by 10 %, whereas the predictions by Cook (1989) are very close to the observed values. For VES (B) concrete, the predictions suggested by ACI 318, ACI 363, and Ahmad et al. overestimate the observed results by 3 to 10%, whereas the predictions by Cook overestimate the observed results by about 18%. Note that the ACI 318 equation was developed for lower strength concretes up to 6,000 psi (42 MPa) at 28 days, whereas the other equations were developed primarily for concretes with strengths exceeding 10,000 psi (70 MPa) at 28 days or older. Also note that the modulus of elasticity does not change significantly after the design age of 6 hours for VES (A) concrete and 4 hours for VES (B) concrete, see Figures 6.5a and 6.5b.

#### 6.1.3.3 Strength Comparison between 4 x 8-in. and 6 x 12-in. Cylinders

The summary of the results of strength comparisons between the 4 x 8-in. (100 x 200-mm) cylinders and the 6 x 12-in. (150 x 300-mm) cylinders for the VES concrete (Options A and B) are presented in Tables 6.6a and 6.6b. These tables indicate that the ratio of the 6 x 12-in. (150 x 300-mm) cylinder strengths to the 4 x 8-in. (100 x 200-mm) cylinder strengths varies with the type of the coarse aggregate used. The ratios of 6 x 12-in. (150 x 300-mm) cylinder strength to 4 x 8-in. (100 x 200-mm) cylinder strength varies between 0.67 and 0.94 for VES (A) concrete, and between 0.74 and 0.85 for VES (B) concrete. Values reported in the literature for concretes with 28-day strength ranging from 5,000 psi (35 MPa) to 12,000 psi (84 MPa) vary from 0.90 to 0.95 (Carrasquillo et al. 1991; Leming 1988; and Moreno 1990).



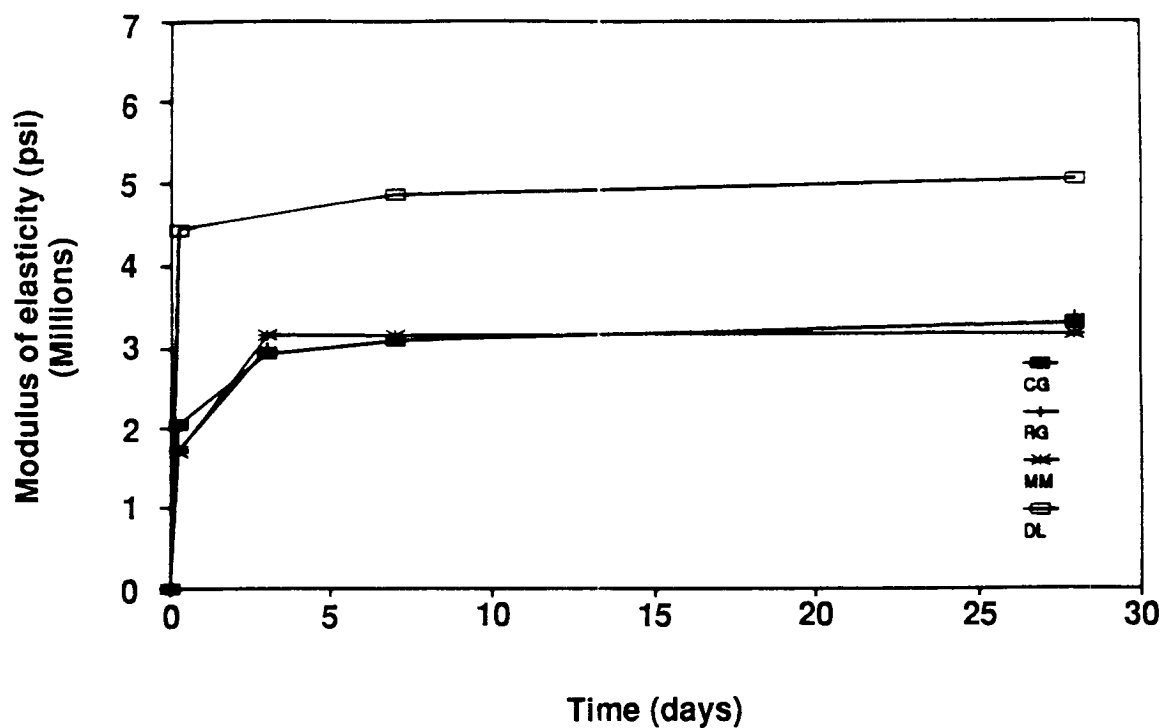


Figure 6.5a Variation of modulus of elasticity with time for VES (A)

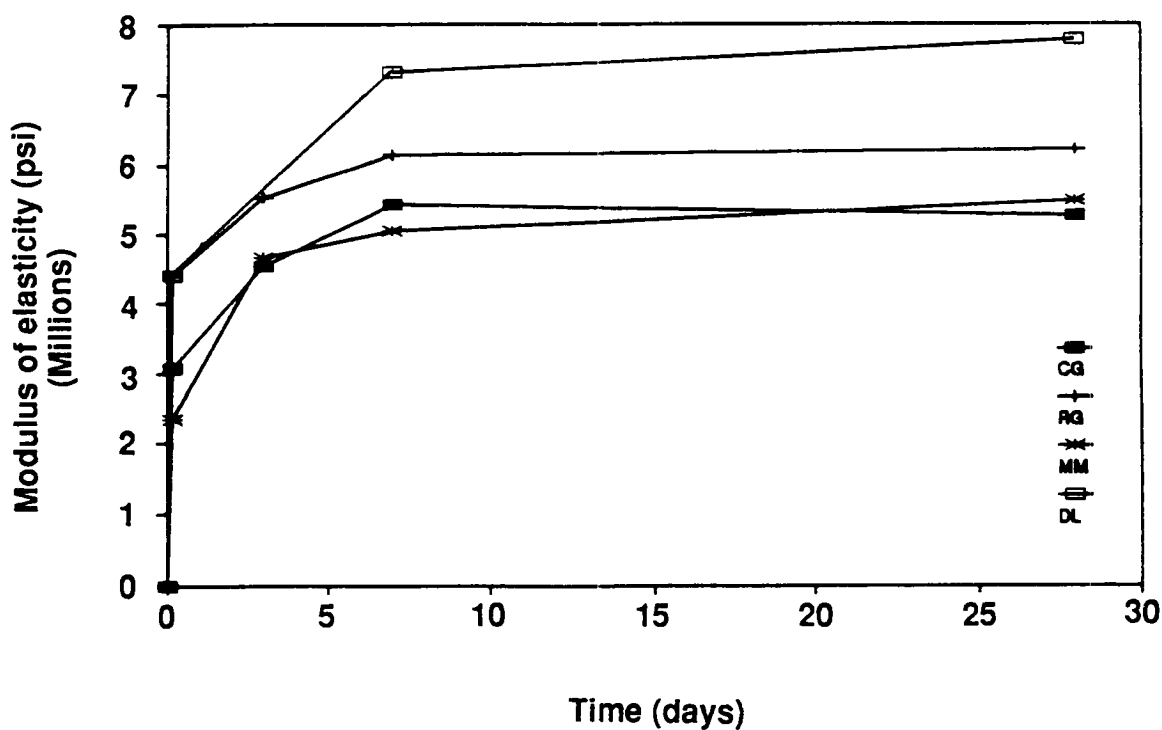
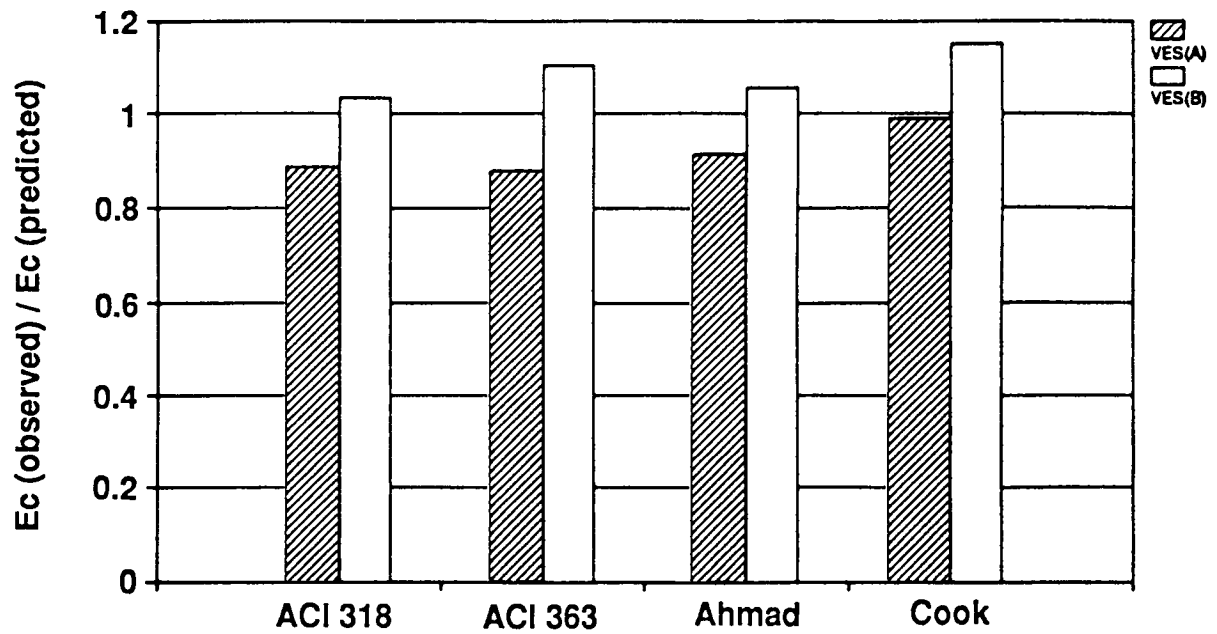
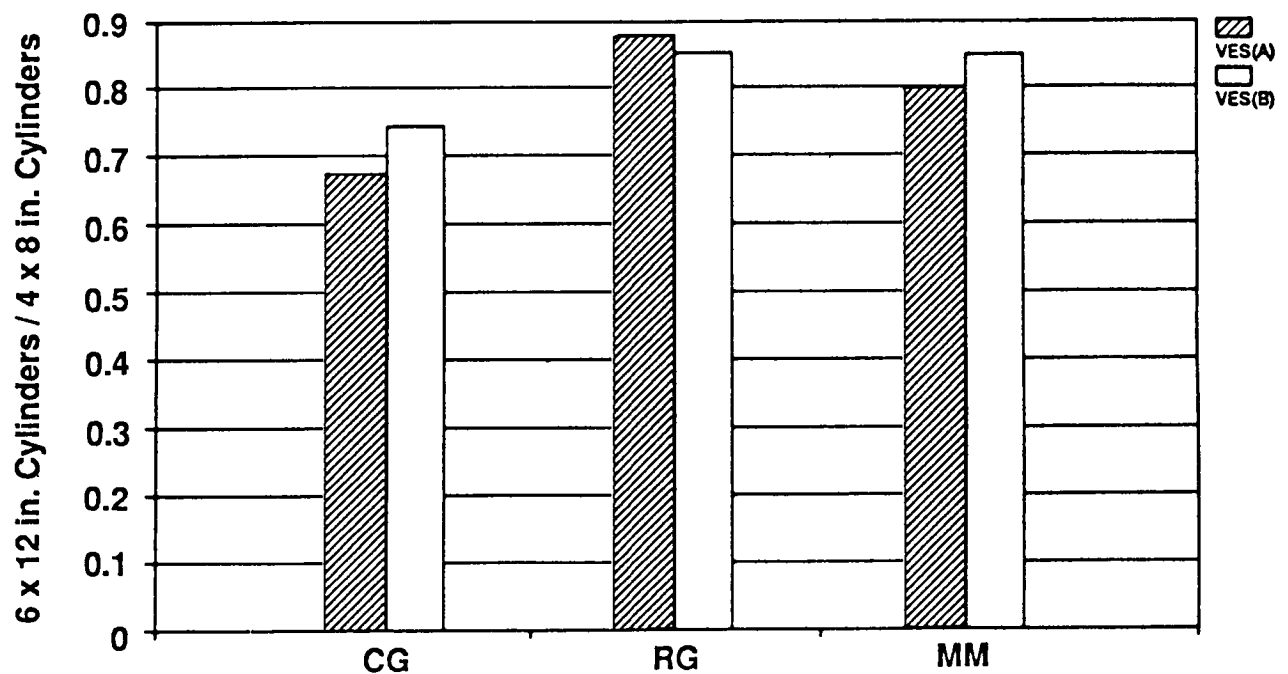


Figure 6.5b Variation of modulus of elasticity with time for VES (B)



**Figure 6.6a** Comparison of observed versus predicted modulus of elasticity of VES concrete considering all test ages



**Figure 6.6b** Average size effect of VES concrete at design age

**Table 6.6a      Summary of test results for 4 x 8-in. cylinder strength (psi)  
and 6 x 12-in. cylinder strength (psi) for VES (A) concrete**

Specimen size	No. of specimens	Test Age (hours)	Coarse Aggregate Type			
			MM	CG	DL	RG
A: 4 x 8 in.	3	6	1930	2540	2349	2130
B: 6 x 12 in.	2	6	1540	1710	2205	1870
B / A			0.80	0.67	0.94	0.88

**Table 6.6b      Summary of test results for 4 x 8-in. cylinder strength (psi)  
and 6 x 12-in. cylinder strength (psi) for VES (B) concrete**

Specimen size	No. of specimens	Test Age (hours)	Coarse Aggregate Type			
			MM	CG	DL	RG
A: 4 x 8 in.	3	4	1970	2980	3034	3140
B: 6 x 12 in.	2	4	1670	2210	2432	2670
B / A			0.85	0.74	0.80	0.85

## 6.2. Tension Tests

The tensile strength was obtained by two types of tests, a split cylinder test and a flexural tensile test. The split cylinder tests were conducted on 4 x 8-in. (100 x 200-mm) cylinders and the flexural tensile tests were conducted on 4 x 4 x 17.5-in. (100 x 100 x 438-mm) beams.

### 6.2.1 Test Setup and Procedure

The split cylinder tests were conducted according to ASTM C 496. The cylinders were loaded at a rate of 7500 lbs/min (33.4 kN/min) until failure. This rate of loading was within the ASTM specified range of 100 to 200 psi/min (0.69 to 1.38 MPa/min). The split cylinder tests were conducted on a 300 kip (1335 kN) compression machine.

The flexural tests were conducted on a universal testing machine with a capacity of 120 kips (534 kN). The universal testing machine was equipped with a SATEC System M120BTE automated control for programming loading rate. The flexural tensile strength test was conducted in accordance with AASHTO T 97-86 and ASTM C 78 with some modifications. The modifications were necessary to incorporate the ability to monitor the tensile strain capacity and the load-deflection response of the test specimen during the flexural test. To measure the tensile strain and the midspan deflection of the test specimen, a mounting frame (fixture) was designed and fabricated. The mounting frame is capable of holding five LVDTs (two on each side of the beam and one at midspan). To prevent damage to the transducers, a No. 2 smooth reinforcing bar was placed along the centroidal axis of the beam. This prevented the sudden collapse of the specimen upon reaching the maximum load and protected all the transducers.

Several preliminary tests indicated that using a No. 2 smooth reinforcing bar along the centroidal axis did not have any detectable effect on the strength and behavior of the test specimens. The test specimens were first placed in a transducer mounting device to facilitate mounting the four transducers to monitor the tensile and the compressive strains during the flexural test. The device for mounting the transducers is shown in Figure A.4.

Preliminary testing revealed that the combination of slight imperfections in the steel mold for the beams and in the rigid supports introduced a torsional effect which changed the mode of failure of the test specimen. A special beam supporting unit was then designed and fabricated. The beam support unit accommodates slight imperfections in steel molds used for casting the test specimens. In the beam support unit used for the flexural tests, both of the supports are restrained against motion along the centroidal axis of the beam; however, in the transverse direction, one of the supports is allowed to rotate (see Figure A.5).

The mounting frame on the flexural test beams for monitoring the midspan deflections is shown in Figure A.6. The beams were tested in third point loading over a clear span of 12 in. (300 mm) according to AASHTO T 97-86 and ASTM C 78. The loading arrangement for the flexural testing is shown in Figure A.7.

The beams were tested at different ages, and companion 4 x 8-in. (100 x 200-mm) cylinders were also tested at the same time. The test beams were loaded and unloaded up to a load of 500 lbs (2.2 kN). This process was done twice for seating and zeroing the LVDTs. After the initial loading and unloading process, the test beams were loaded to failure. A loading rate of 800 lbs/min (3.6 kN/min) was used.

The four LVDTs used to measure displacements in the flexural tests were Trans-Tek # 0270-0000, with a sensitivity of 3.189 vAC/in./volt input. A gage length of 4 in. (100 mm) was used to monitor the compressive and tensile deformation near the extreme fibers. The voltage output from the LVDTs was converted by an OPTIM data acquisition system (Megadec System 100). This system eliminated electronic noise in order to record accurately the small displacements encountered. An aluminum jig was used to mount the four LVDTs in the middle third of the beam and 5/8 in. (15.9 mm) from the top and bottom fibers on the front and back of the beam. A view of the test setup is shown in Figure A.8.

### *6.2.2 Specimen Preparation*

Specimens used for flexural strength tests were 4 x 4 x 17.5-in. (100 x 100 x 438-mm) beams, cast in steel molds with a No. 2 bar placed along the centroidal axis. The No. 2 bar was placed in the specimen to keep it from collapsing at failure so as to avoid damaging LVDTs. The concrete was placed into molds and vibrated internally with a needle vibrator. The finish was completed with a magnesium float. Companion 4 x 8-in (100 x 200-mm) cylinders were cast in plastic molds. After casting, the specimens inside the molds were maintained at 60° to 80°F (15.6° to 26.7°C) and protected from moisture evaporation by a plastic sheet cover for 20 to 24 hours. Then they were stripped of their molds and either tested immediately or placed in sealed plastic bags until testing at later ages. Since the tests involved measuring tensile strains and midspan deflections, transducers were mounted on the test specimens. The specimens were air dried for 10 to 15 minutes before the LVDTs were mounted on the two sides of the specimens.

### *6.2.3 Test Results and Discussion*

The results of the split cylinder tests for VES concrete (Options A and B) are shown in Tables 6.7a and 6.7b. The values shown in the table are the average of two replicate specimens. The ratio of the observed to the predicted split cylinder strength for VES concrete (Options A and B) with different types of coarse aggregates is shown in Figure 6.7. The equation suggested by ACI 318 (1993c) uses 6.7 as a premultiplier to the square root of the compressive strength in psi units. From this figure it appears that the split cylinder strength of VES (A) concrete at design age of 6 hours is not adequately predicted (underprediction of 18%) by the empirical equation of ACI 318, since the equation was developed for concretes with strength of up to 6,000 psi (42 MPa) at 28 days of age; however, for the VES (B) concrete, the ACI predictions are very good. Although the equation suggested by Ahmad and Shah (1985) was primarily for concretes with strength greater than 6,000 psi (42 MPa) at 28 days, the prediction is relatively good (within 11%) for

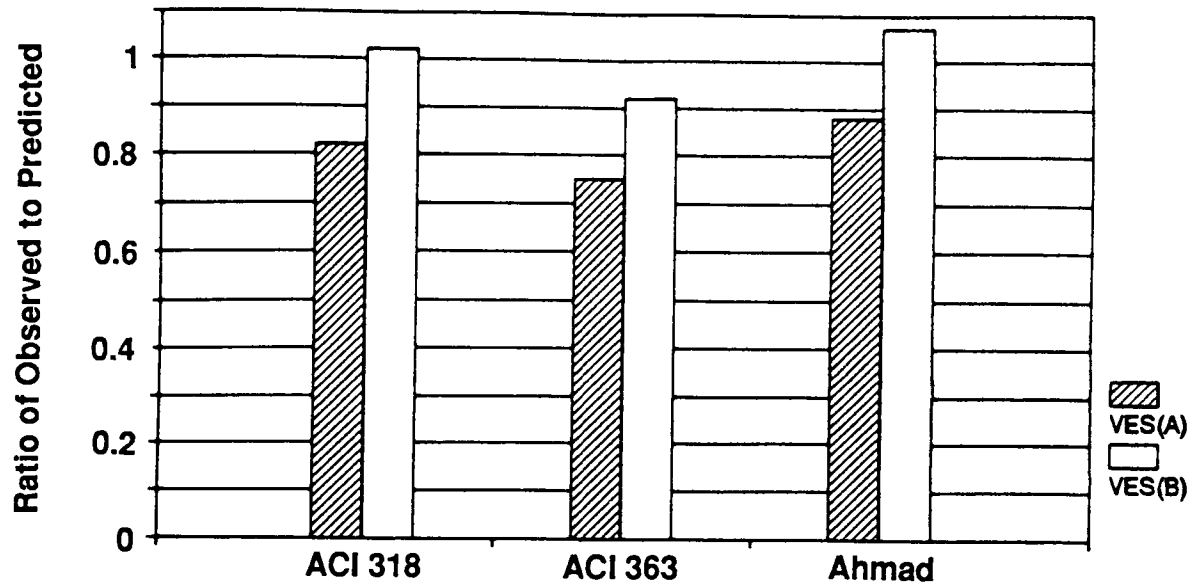


**Figure 6.7** Comparison of observed versus predicted split cylinder strength of VES concrete at design age

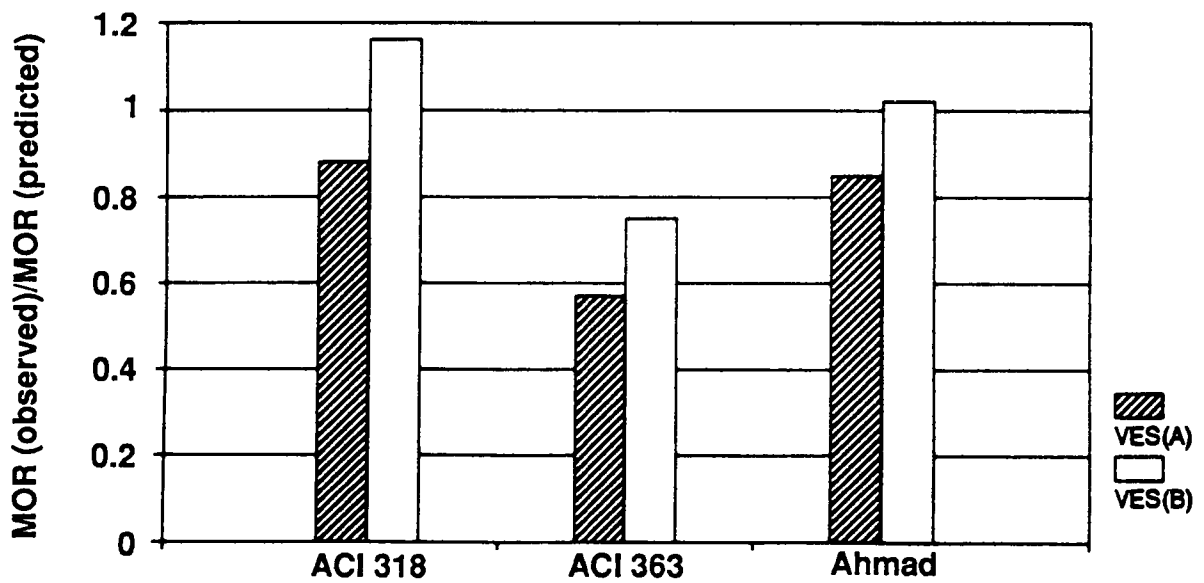


**Figure 6.8** Comparison of observed versus predicted modulus of rupture of VES concrete at design age

**Table 6.7a Summary of test results for modulus of rupture, tensile strain capacity, and split cylinder tensile strength for VES (A) concrete**

Coarse Aggregate Type	Age	Modulus of Rupture (psi)	Tensile Strain Capacity (microstrains)	Split Cylinder Strength (psi)	4 x 8-in. "Control" Cylinder Strength (psi)
MM	6 hours	260	-180	160	1450
	7 days	420	-200		
	28 days	540	-200		
CG	6 hours	290	-175	280	1696
	7 days	500	-200		
	28 days	530	-200		
DL	6 hours	259	—	207	1292
	7 days	485	—		
	28 days	479	—		
RG	6 hours	230	-100	210	1450
	7 days	380	-225		
	28 days	430	-150		

**Table 6.7b Summary of test results for modulus of rupture, tensile strain capacity, and split cylinder tensile strength for VES (B) concrete**

Coarse Aggregate Type	Age	Modulus of Rupture (psi)	Tensile Strain Capacity (microstrains)	Split Cylinder Strength (psi)	4 x 8-in. "Control" Cylinder Strength (psi)
MM	4 hours	450	-115	320	2680
	7 days	790			
	28 days	620	-200		
CG	4 hours	430	-160	420	2890
	7 days	890	-130		
	28 days	770			
DL	6 hours	582	—	288	2372
	7 days	575	—		
	28 days	590	—		
RG	4 hours	460	-115	330	2580
	7 days	1000	-175		
	28 days	930	-175		



VES (A) concrete at design age of 6 hours and within 5 % for VES (B) concrete. The prediction using the equation recommended by ACI Committee 363 (1984) is least satisfactory, since this equation was developed for concretes with strengths well over 10,000 psi (70 MPa) at 28 days of age.

The test results for the flexural modulus of VES concrete (Options A and B) are presented in Tables 6.7a and 6.7b. The comparison of the experimental results with some of the empirical equations of ACI 318 (1993c), ACI 363 (1984), Ahmad and Shah (1985) is shown in Figure 6.8. The equation suggested by ACI 318 uses 7.5 as a premultiplier to the square root of the compressive strength in psi units. From this figure, it can be seen that the predictions from the equation recommended by Ahmad and Shah are closer to the observed values than the predictions from ACI 318 and ACI 363. The equations suggested by ACI 318 underpredict the results for VES (A) concrete by about 10% and overpredict the results of VES (B) concrete by about 15%. The prediction using the equation recommended by ACI 363 is least satisfactory, since the equation was developed for concretes with strengths well over 10,000 psi (70 MPa) at 28 days of age.

The variations of the modulus of rupture with time for the VES concrete (Options A and B) are shown in Figures 6.9a and 6.9b. For VES (A) concrete, the modulus of rupture increases rapidly up to an age of 7 days, after which it essentially remains constant up to 28 days of age; the modulus of rupture for VES (A) concrete with RG aggregate is lower than that for VES (A) concretes with CG, RG, and DL aggregates (see Figure 6.9a). For VES (B) concrete, the modulus of rupture also increases rapidly up to an age of 7 days, after which it decreases until the age of 28 days (see Figure 6.9b). Also, this figure shows that the modulus of rupture for the VES (B) concrete with DL aggregate is lower than that for VES (B) concrete with MM, CG, and RG aggregates. The trend of decreasing modulus of rupture after the initial 7 days for the VES (B) concrete (with Pyrament cement) is unexpected. This phenomenon is believed to be due to the drying of the test specimens. It is recalled that the W/C for VES (B) concrete with four different types of coarse aggregates (CG, MM, RG, and DL) varied from 0.17 to 0.23. With such low W/C, it is probable that self-dessication would have taken place. According to the ASTM C 192, "relatively small amounts of drying of the surface of flexural strength specimens will induce tensile stresses in extreme fibers that will markedly reduce the indicated flexural strength." Studies on concrete made with Pyrament XT cement, conducted at the Army Corps of Engineers Waterways Experiment Station, also showed that the flexural strength of specimens continuously stored in the air was much lower than the strength of the specimens continuously stored in water, especially at later ages (Husbands and Wakely 1991).

The relationships of load versus midspan deflection at design age of 6 hours for VES (A) concrete and at design age of 4 hours for VES (B) concrete with all four types of coarse aggregates are shown in Figures 6.10a and 6.10b. These figures show that the aggregate type does not seem to have an appreciable effect on the initial stiffness of the load versus midspan deflection response for either VES concrete (Option A or B) beams when tested in flexure. The effect of age on the load versus midspan deflections for VES (A) concrete with one type of coarse aggregate is shown in Figure 6.11a. The figure indicates that with age, the response tends to become stiffer in the initial stage, and the flexural deformation capacity first increases with

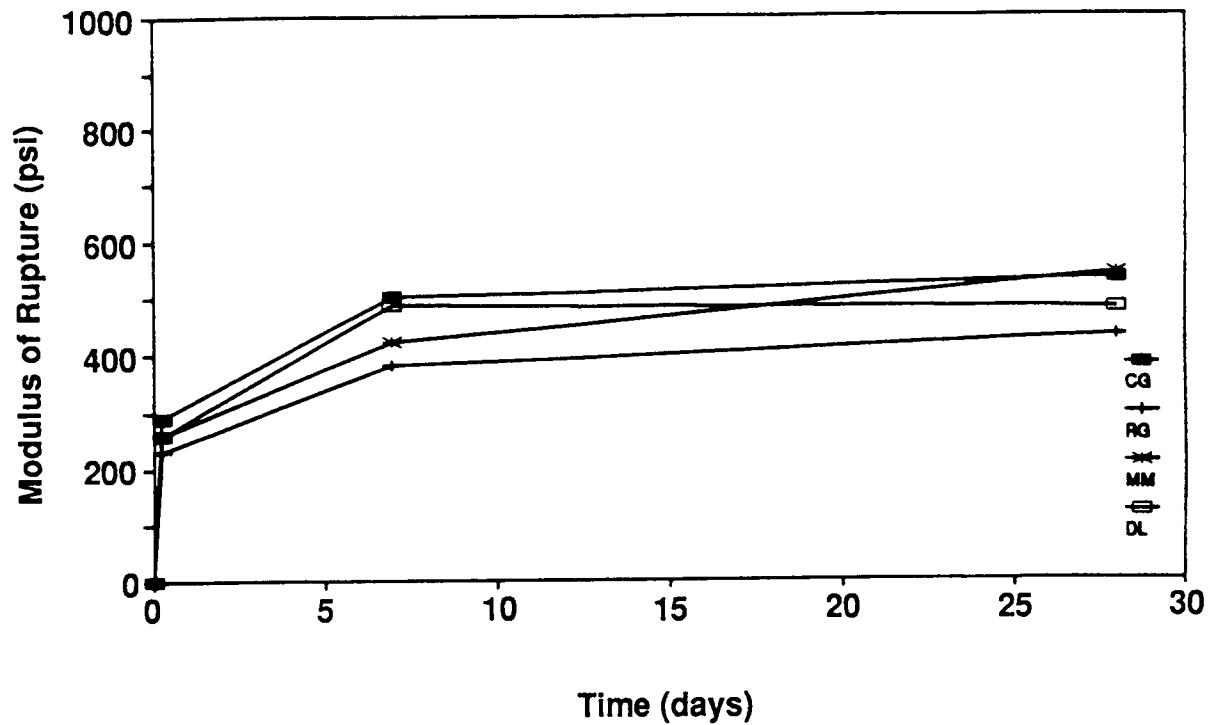


Figure 6.9a Variation of modulus of rupture with time for VES (A) concrete

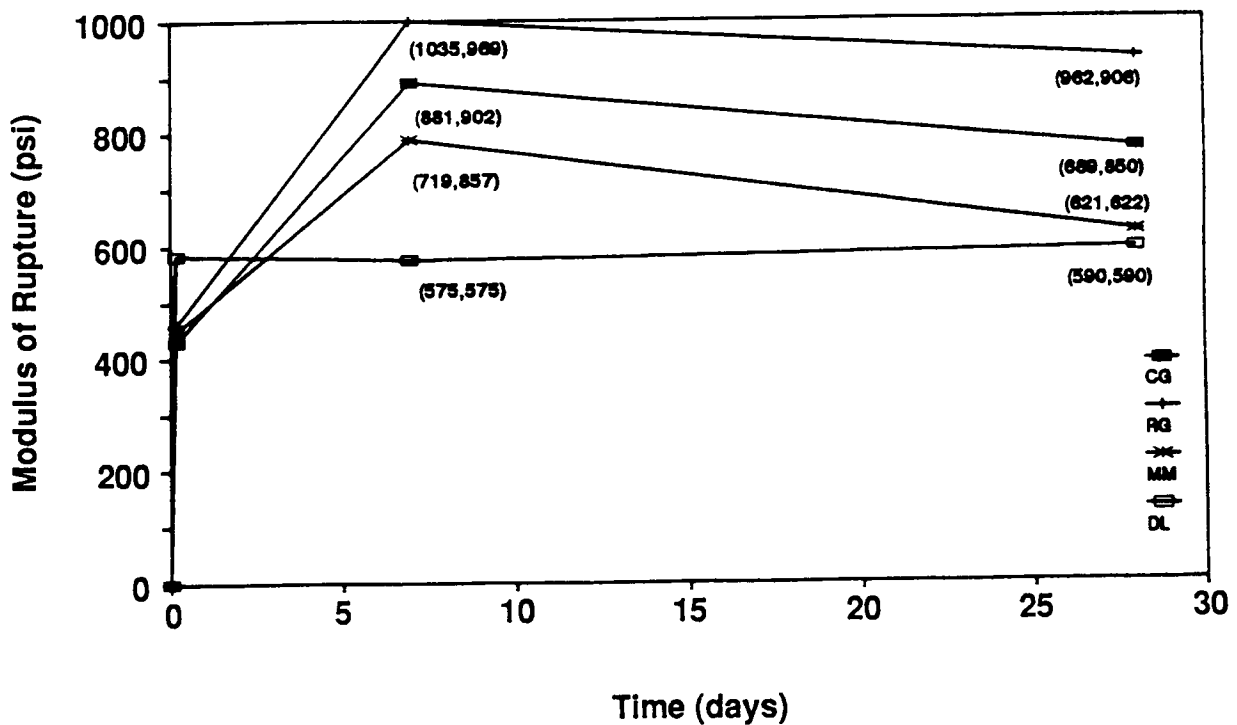


Figure 6.9b Variation of modulus of rupture with time for VES (B) concrete

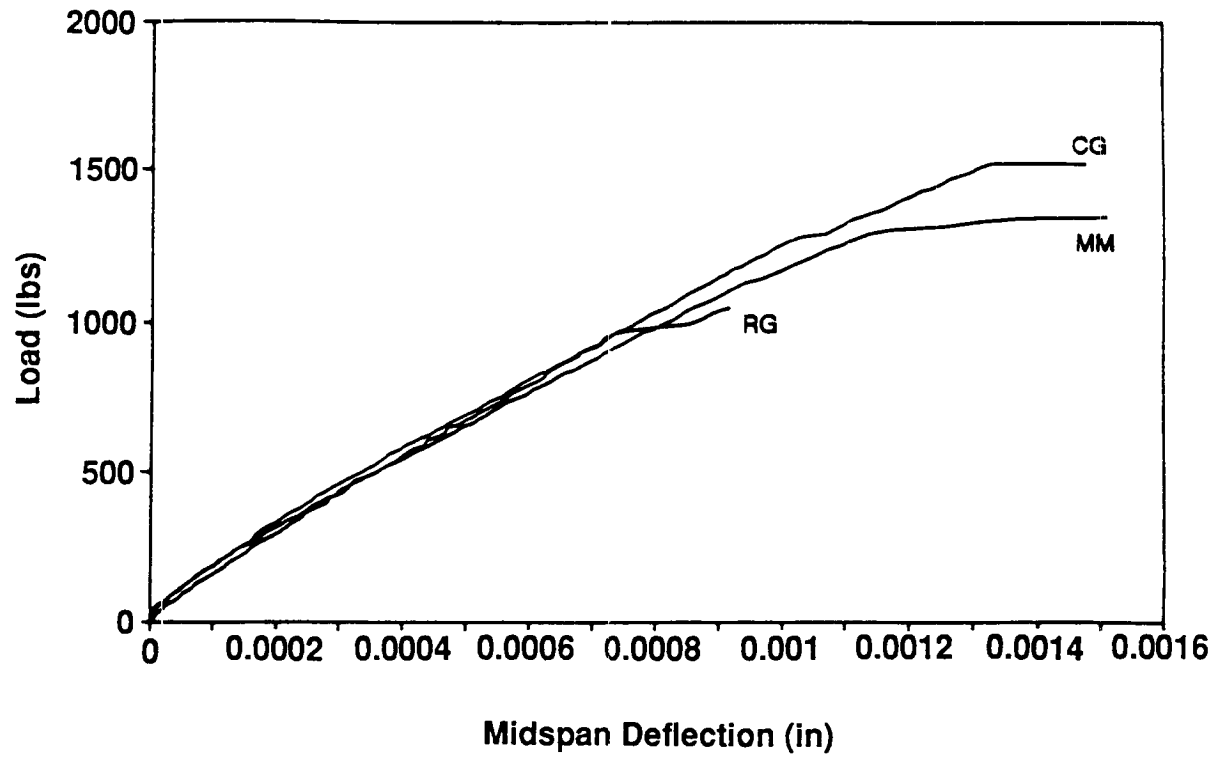


Figure 6.10a Load-midspan deflection of VES (A) at design age of 6 hrs

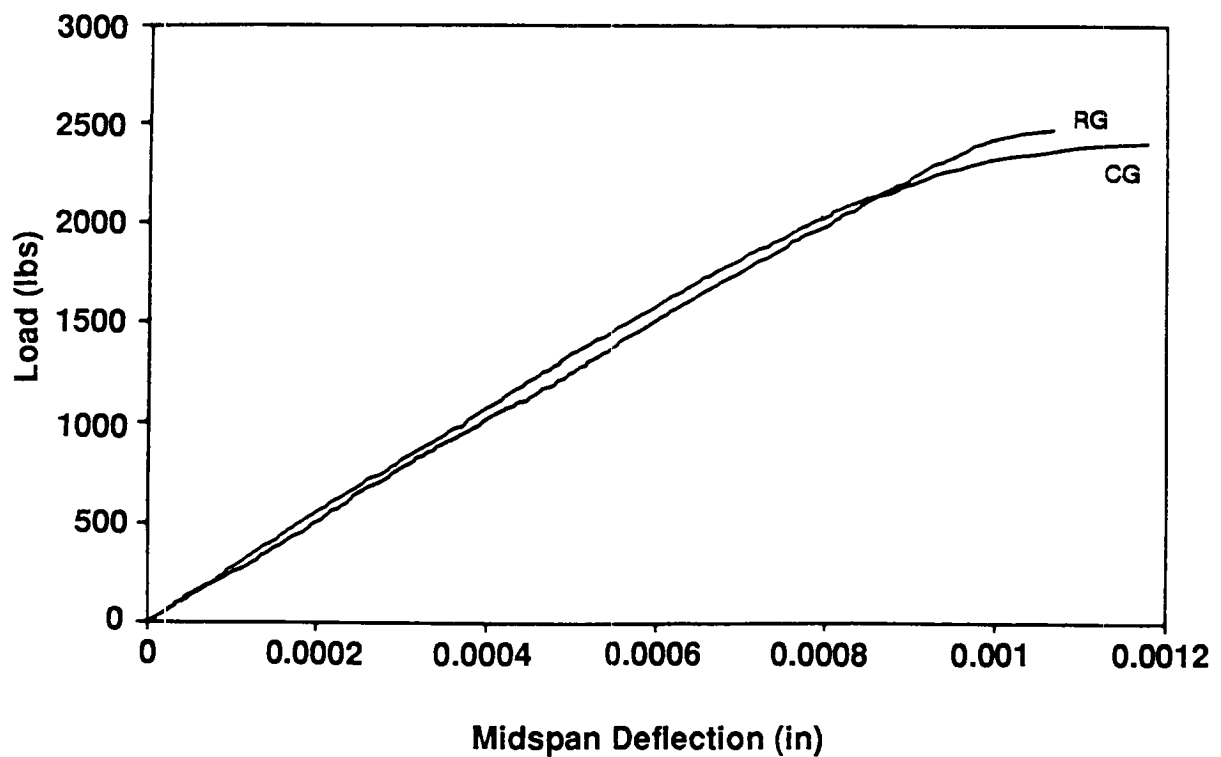


Figure 6.10b Load-midspan deflection of VES (B) at design age of 4 hrs

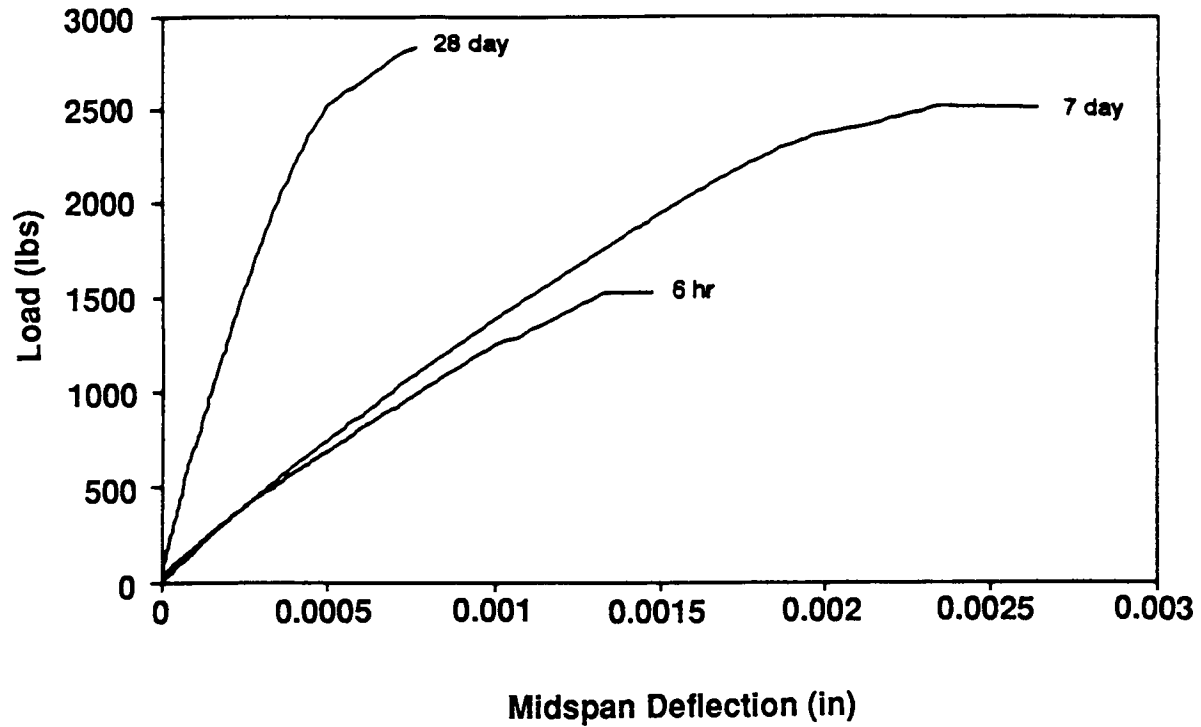


Figure 6.11a Load-midspan deflection of VES (A) CG (6hrs, 7d, 28d)

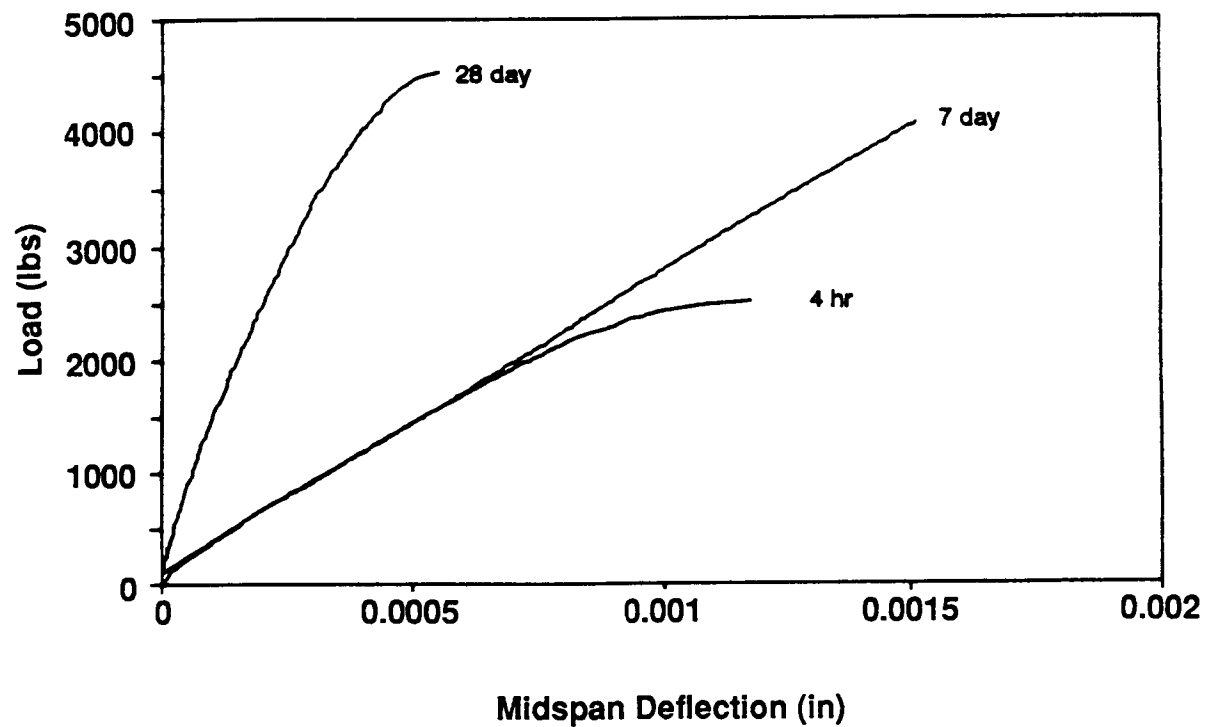


Figure 6.11b Load-midspan deflection of VES (B) CG (4hrs, 7d, 28d)

age up to 7 days and then significantly reduces for the age of 28 days. The effect of age on the load versus midspan deflections for the VES (B) concrete with one type of coarse aggregate is shown in Figure 6.11b. The figure shows that the trend for this type of concrete is similar to the trend observed above for the VES (A) concrete.

The relationships of load versus tensile strain for VES concrete (Options A and B) with different types of coarse aggregates at the design age of 6 and 4 hours, respectively, are shown in Figures 6.12a and 6.12b. The results for VES (A) concrete indicate that at an early age of 6 hours, the tensile strain capacity depends on the type of coarse aggregate used. The tensile strain capacity is lowest for the VES (A) concrete with MM coarse aggregate and highest for the VES (A) concrete with CG coarse aggregate. The results for the VES (B) concrete show that at an early age of 4 hours, the tensile strain capacity does not seem to be significantly affected by the type of the coarse aggregate (see Figure 6.12b). These results indicate that even at an early age of 4 hours, the paste characteristics of the VES (B) concrete are dominant in controlling the failure mode and in determining the tensile strain capacity. The load versus tensile strain at different ages (6 hours, 7 days, 28 days) for VES (A) concrete with CG coarse aggregate is shown in Figure 6.13a. The results indicate that tensile strain capacity of concrete at the age of 6 hours is about 150 microstrains and that the tensile strain capacity does not change significantly with the age of the VES (A) concrete up to an age of 28 days. The load versus tensile strain at different ages for VES (B) concrete with CG coarse aggregate (see Figure 6.13b) indicates that the tensile strain capacity of concrete at the age of 4 hours is about 125 microstrains and that tensile strain capacity does not change significantly with the age of the VES (B) concrete, up to an age of 28 days.

## **6.3 Freezing-Thawing Tests**

### ***6.3.1 Test Setup and Procedure***

The freezing-thawing tests were performed in accordance with ASTM C 666, procedure A, using a programmable freezing-thawing chamber as shown in Figure A.9. The chamber housed twelve rectangular aluminium containers, each measuring 4.25 in. (106 mm) wide, 16.25 in. (406 mm) long, and 6 in. (150 mm) deep, surrounded by antifreeze liquid, which served as heat exchange medium for the freezing-thawing cycle.

Two narrow vertical slits were cut in each side of the container to reduce the rigidity of the container. The slits were then filled with silicon to make the container watertight. Inside the container, small strips of plexiglas were attached to the two longitudinal side walls and the bottom to support the specimen so that the specimen would be completely surrounded by water.

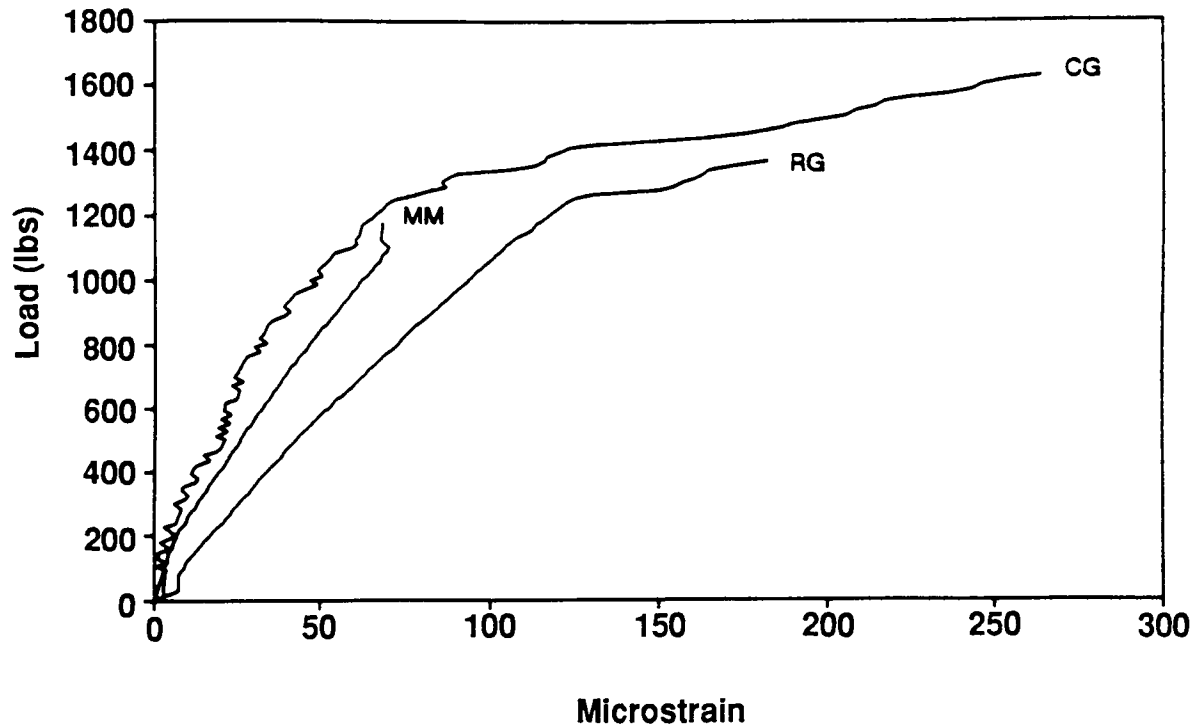


Figure 6.12a Load-tensile strain of VES (A) at design age of 6 hrs

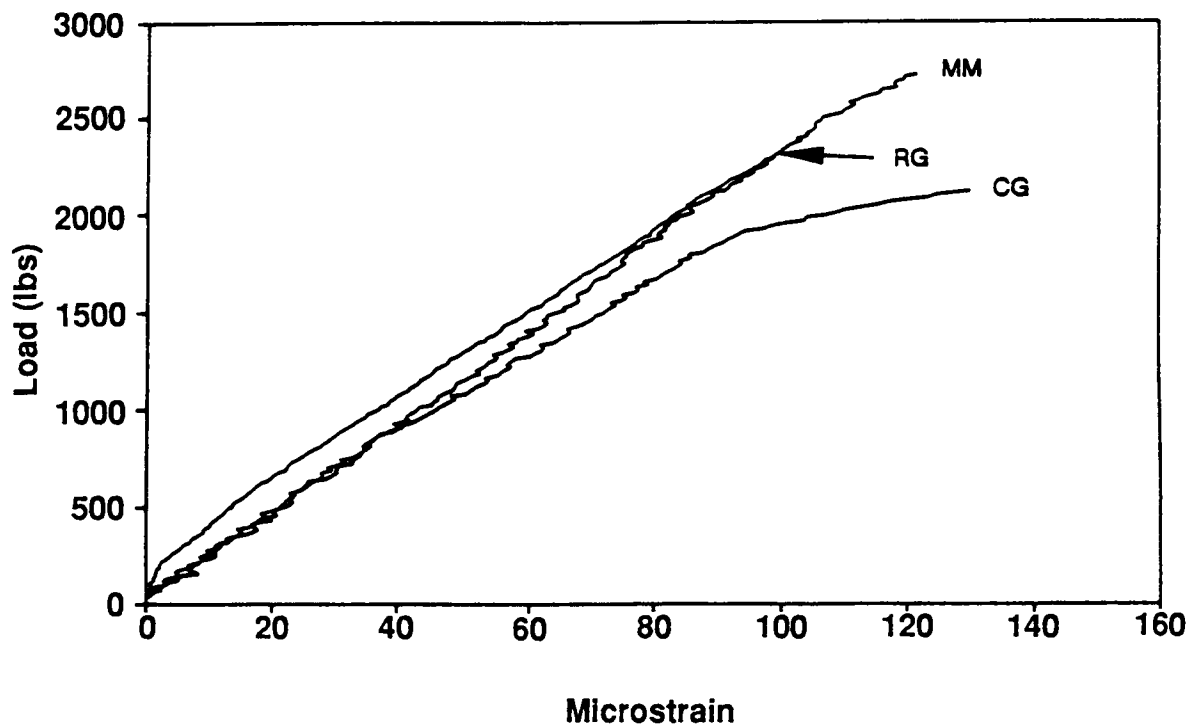


Figure 6.12b Load-tensile strain of VES (B) at design age of 4 hrs

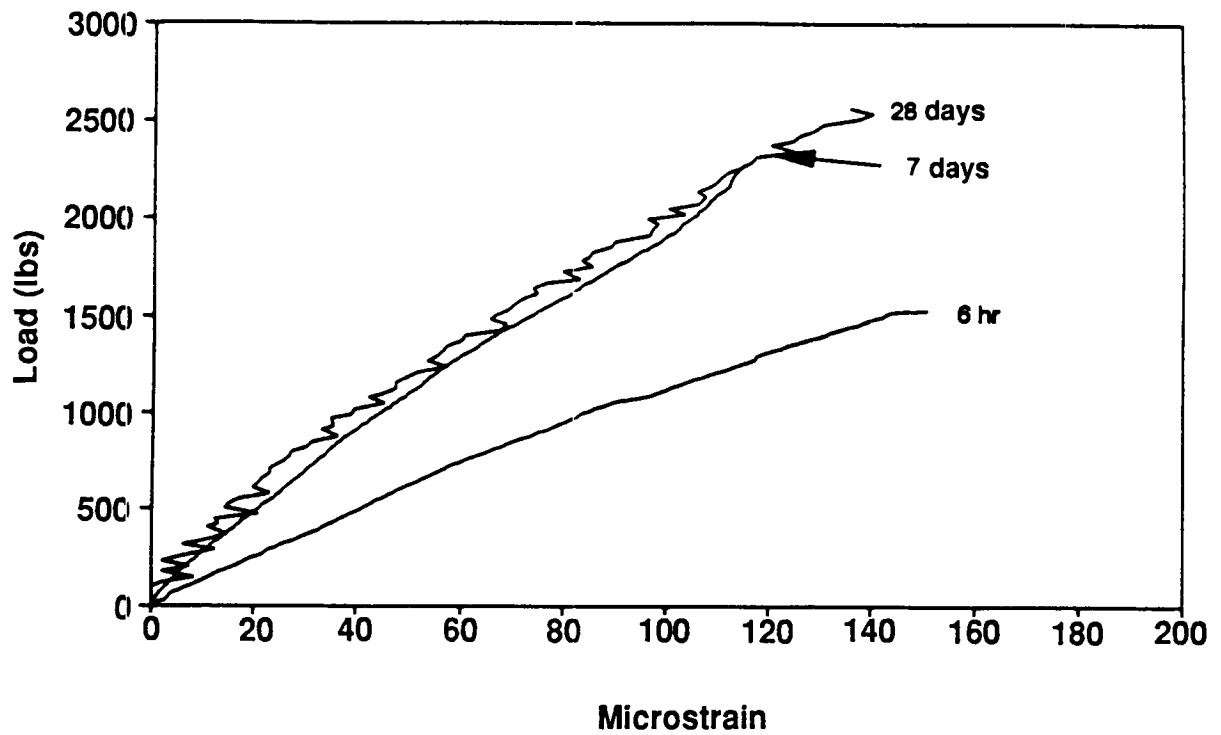


Figure 6.13a Load-tensile strain of VES (A) CG at 6hrs, 7d, 28d

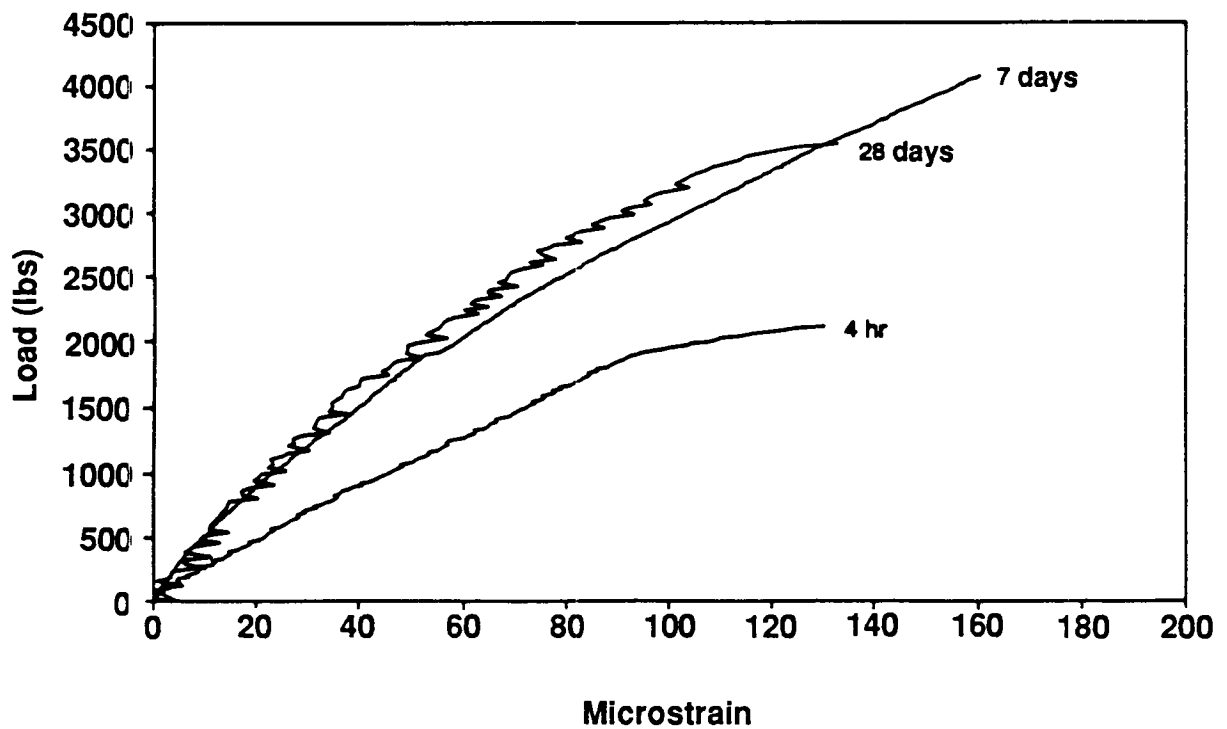


Figure 6.13b Load-tensile strain of VES (B) CG at 4hrs, 7d, 28d

The thickness of the side supports was 1/16 in. (1.6 mm) and that of the bottom supports was 1/8 in. (3.2 mm). These supports ensure proper spacing and clearance of the submerged specimens. The size of each specimen was 3 x 4 x 16 in. (75 x 100 x 400 mm). The specimens were placed inside plastic bags filled with water, then placed in the containers. This was to prevent aluminium from reacting with the lime (CaOH) in the concrete.

When the specimens were 14 days old, they were placed, with the finished surface up, in the freezing-thawing chamber and subjected to freezing and thawing between 0° and 40°F (-17.8° and 4.4°C), +/- 3°F (+/- 1.7° C). Each freezing-thawing cycle required approximately 2.5 hours to complete. The exact amount of time was somewhat influenced by the ambient temperature in the laboratory.

At intervals of not more than 36 freezing-thawing cycles, the specimens were removed from the freezing-thawing chamber, brought to saturated-surface-dry condition, and weighed in grams. The weight was automatically converted to pounds by the computer program used for data analysis. The dimensions of each specimen were measured to the nearest 1/8 in. (3.2 mm). Each specimen was then tested for its fundamental transverse frequency.

The fundamental transverse frequency of the specimen was determined by using an impact resonance device in accordance with the proposed revision of ASTM C 215. The equipment used for the test is shown in Figure A.10. The impactor used to excite the specimen for frequency measurement was a 1 x 0.5 x 7.75 in. (25 x 13 x 194 mm) steel bar with a weight of 1.034 lbs (470 gm). The steel bar was used for convenience instead of a spherical impactor. Results obtained using both the spherical and prismatic impactors were compared beforehand and no appreciable difference was found.

Soft rubber pad supports were placed at the estimated nodal points of the specimen, at approximately 0.224 of the length of the specimen from each end, to allow the specimen to vibrate freely. A small piezometric accelerometer (Model 303A02, PCB Piezotronics, Depew, NY) weighing 0.113 oz was placed at midheight on the specimen near one end. The accelerometer had a calibrated operating frequency range of 10 to 10,000 Hz, a self-resonant frequency of 100 kHz, and a voltage sensitivity in excess of 10 mV/g. Amplitude deviation was within 3% full range.

Since the specimen was moist and adhesion to its surface was difficult, the accelerometer was held tightly against the specimen with a rubber band. Soft wax with good acoustic properties was used between the accelerometer and the specimen surface, which frequently was rough, to ensure good mechanical contact. The soft wax also provided some adhesion and kept the accelerometer from slipping.

The specimen was struck lightly at midheight near its middle, in the same direction as the primary axis of the accelerometer. The latter was connected to a power unit supplied by the same manufacturer. The output signal from the power unit was sent to a digital acquisition (DAQ) board in a PC computer. The board, Model AT-MIO-16L-9, was supplied by National Instruments, Austin, Texas. It is a 12-bit, multipurpose, multiple gain, 16 single-ended or 8



differential channel, input-output, plug-in board, with a 9 microsecond analog-to-digital converter (ADC), permitting sampling rates of up to 90 to 100 thousand samples per second. The board was used within a 80386-based 20 MHz stand-alone microcomputer.

The software used to set up and operate the DAQ board was also provided by National Instruments. This software, LabWindows (version 2.0), with the Advanced Analysis Library option, permitted standard programming languages to be used (together with special function calls provided with the software) to control or program data acquisition, to perform optional analysis on the data, and to save the data or analysis to computer files. The programming language used in this application was Microsoft QuickBASIC (version 4.0).

The program was written so that data acquisition of the output from the accelerometer was self initiating, i.e., a jump in voltage from the accelerometer would initiate data acquisition. The sampling rate was 50 kHz with 2,048 sample points collected. The program transformed the data to time-based values and, using a LabWindows function call, conducted a Fast Fourier Transform (FFT) on the first 1,024 data points. The program examined the FFT output and selected the frequency with the largest amplitude as the fundamental (or resonant) frequency.

The program then used the resonant frequency, in combination with the mass of the specimen, to compute the dynamic modulus of elasticity of the specimen, based on the following equation given in ASTM C 215:

$$E = CWn^2$$

where W = weight of specimen, lbs  
n = fundamental transverse frequency, Hz  
C = 0.00245 (L<sup>3</sup>T/bt<sup>3</sup>), sec<sup>2</sup>/in<sup>2</sup>, for a prism  
L = length of specimen, in.  
t, b = dimensions of cross section of prism, in (t being in the direction in which the prism is driven)  
T = a correction factor obtained from a table given in ASTM C 215 = 1.4  
(T depends on the ratio of the radius of gyration to the length of the specimen, and on Poisson's ratio)

The resonant frequency test was repeated twice to observe the repeatability of the results. If any one reading deviated from the average of three measurements by more than 10%, the test was repeated. The average of the three final readings was then recorded.

After all the specimens were tested, they were returned to the freeze-thaw chamber and placed at different locations before the freezing-thawing cycles were resumed. Each specimen was subjected to the freezing-thawing test for 300 cycles or until its dynamic modulus became less than 80% of its original value, whichever occurred first.

A set of control specimens kept in water at room temperature was also tested for resonant frequency at the same time as the freezing-thawing specimens. The change in dynamic modulus of the control specimen reflected the effect of strength variation of the concrete.

### 6.3.2 Specimen Preparation

Thirteen groups of specimens of VES concrete using Type III cement or Pyrament XT cement with CG, MM, and RG as aggregate were produced for the freezing-thawing tests. Each group consisted of a set of three freezing-thawing specimens and one or two control specimens. In addition to the freezing-thawing specimens, a prism measuring 6 x 6 x 24 in. (150 x 150 x 600 mm) was also cast, from which the specimens for the rapid chloride permeability test and the AC impedance test were later obtained.

The mixture proportions, strength, and plastic properties of the concrete used for the test specimens are detailed in Tables 6.8a through 6.8d. The concrete was placed in the molds, vibrated with a needle vibrator, and finished with a magnesium float. A thermocouple wire was placed in one of the freezing-thawing specimens to measure the concrete temperature in the freezing-thawing chamber. For curing, all specimens were kept in separate plastic bags at room temperature for 14 days before they were subjected to the freezing-thawing test.

### 6.3.3 Test Results and Discussion

The results of the freezing-thawing tests expressed in terms of durability factor are summarized in Table 6.9. Durability factor is defined as

$$DF = (E/E_o) \times (N/300)$$

in which  $E_o$  = initial dynamic modulus of specimen  
 $N$  = number of cycles of freeze-thaw up to 300  
 $E$  = dynamic modulus of specimen after  $N$  cycles of freeze-thaw

Figures 6.14 through 6.17 show the typical behavior of selected groups of test specimens in terms of the effect of freezing-thawing on the relative dynamic modulus of each specimen.

It is noted from Table 6.9 that five groups of test specimens failed the freezing-thawing test. The failure of C/VE(CS)/3N (with silica fume but no entrained air) and C/VE(CC)/3 (with 1% calcium chloride as accelerator and 3.4 % air) was due to inadequate air content.

The failures of R/VE(C)/.34 and R/VE(C)/32 were due to the weakness of the coarse aggregate used in the concrete. There was a clear evidence of disintegration of the coarse aggregate at failure. The RG from Memphis, Tennessee, had an absorption of about 5 % and pore sizes of

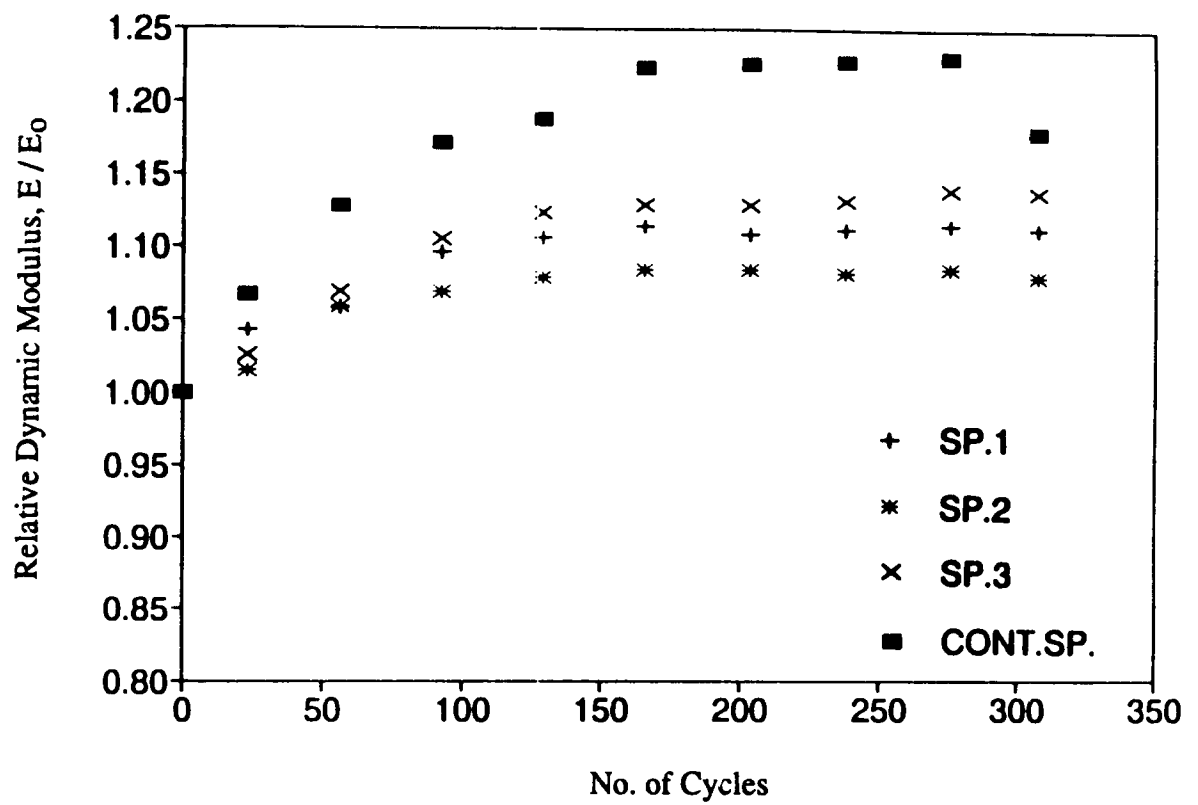


**Figure 6.14** Relative dynamic modulus vs number of freezing-thawing cycles for C/VE(C)/3

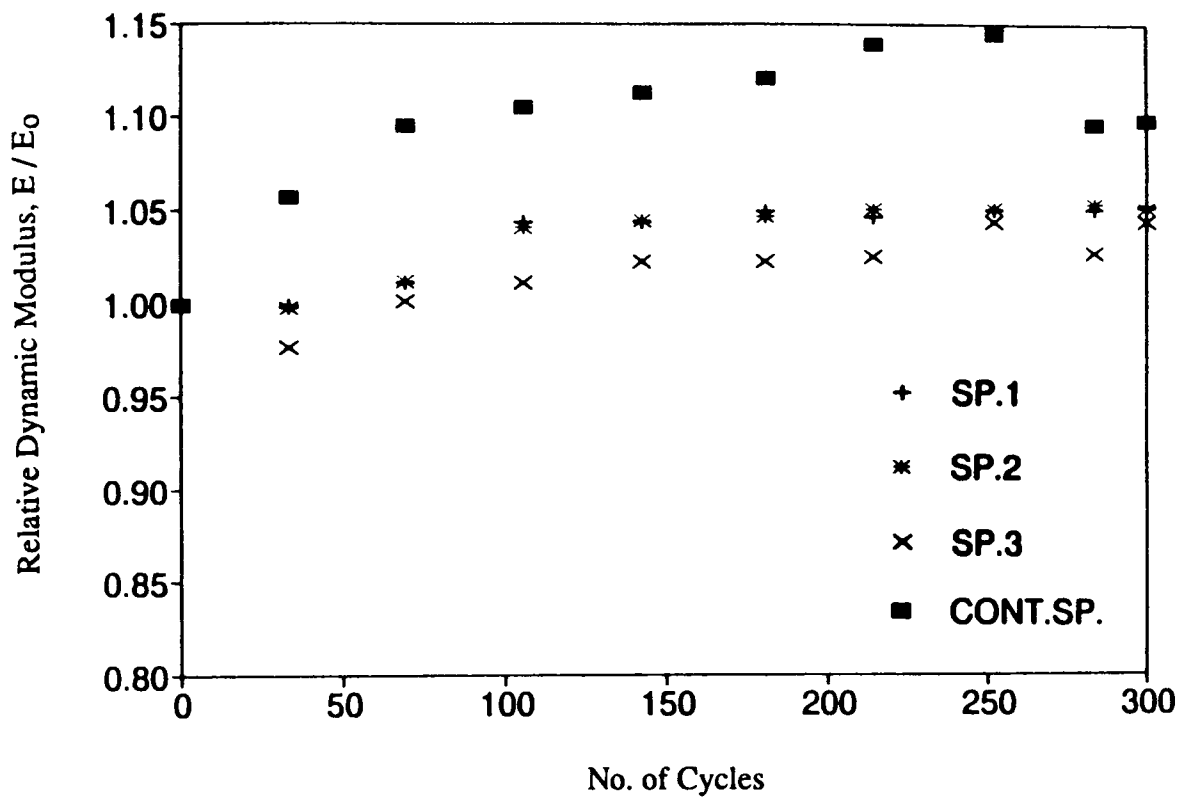


**Figure 6.15** Relative dynamic modulus vs number of freezing-thawing cycles for C/VE(C)/.34

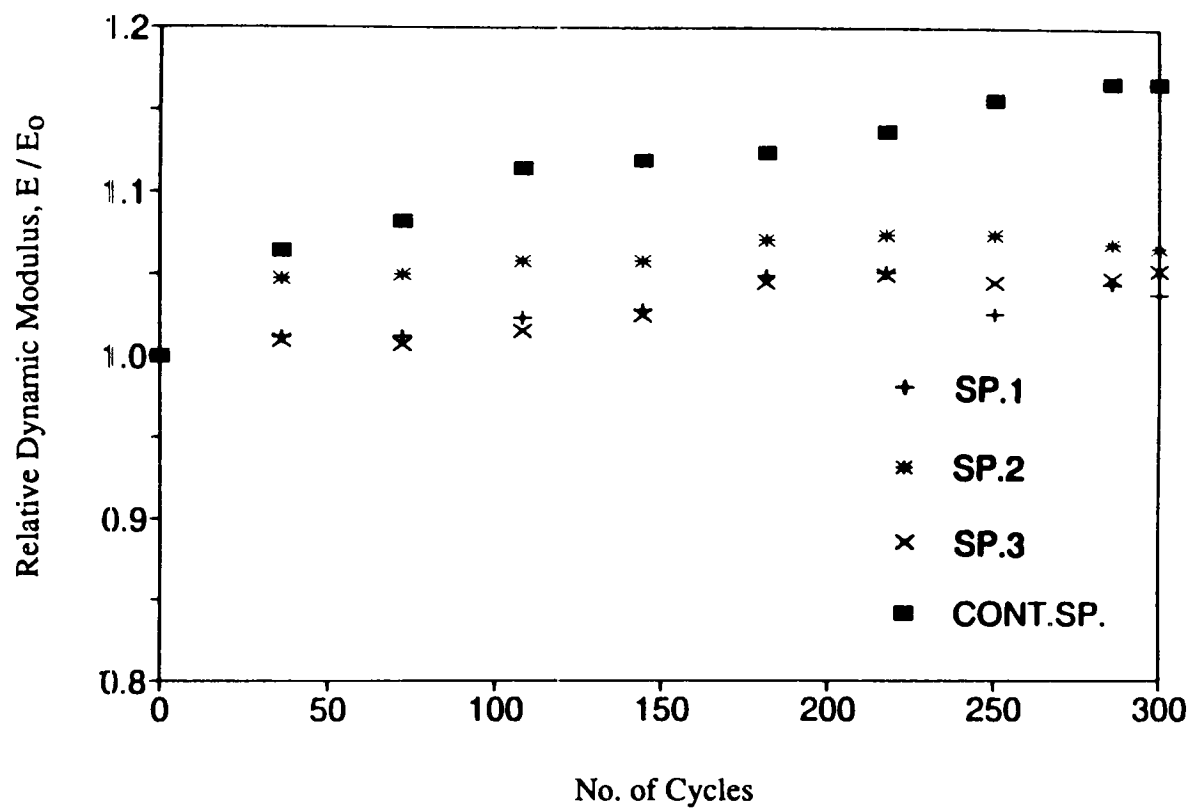


**Figure 6.16** Relative dynamic modulus vs number of freezing-thawing cycles for C/VE(C)/3R6

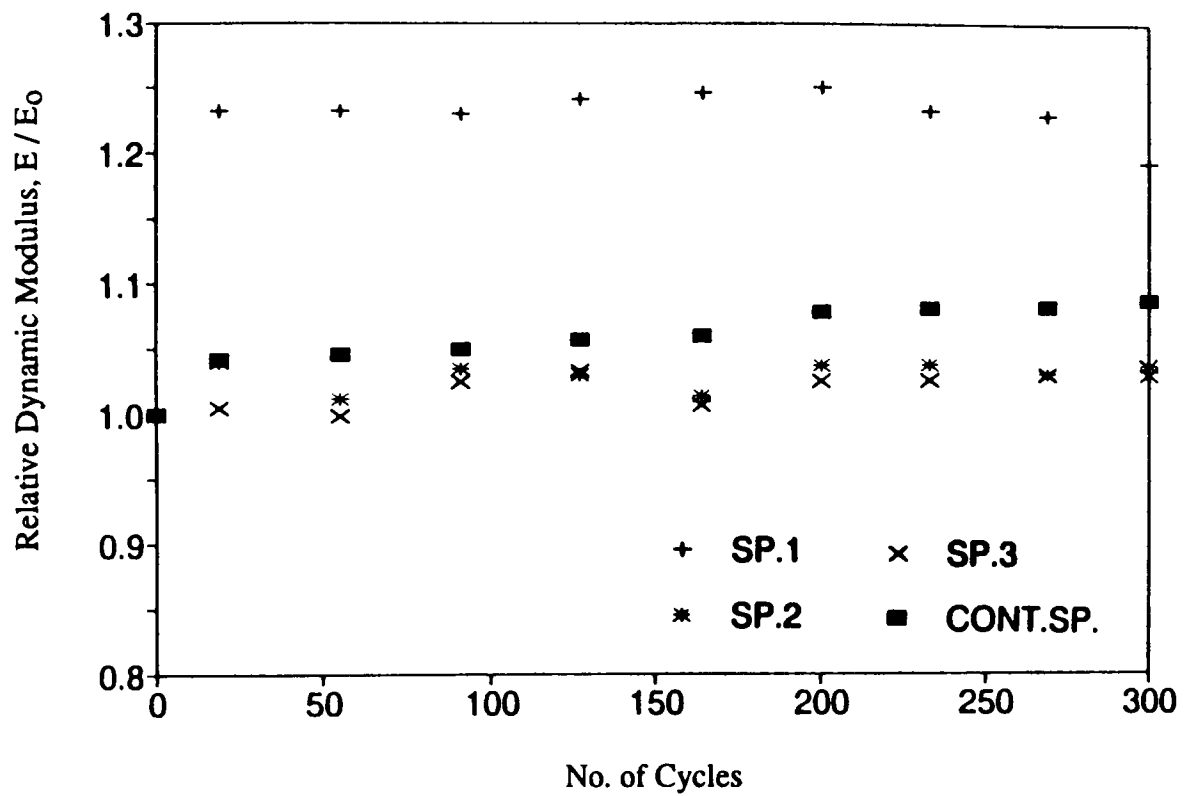


**Figure 6.17** Relative dynamic modulus vs number of freezing-thawing cycles for C/VE(PYR)/3

**Table 6.8a Mixture proportions, strength, and plastic properties of VES concrete used for freezing-thawing test specimens**

Ref. No.*	46	67	45	28
Batch ID	C/VE(C)/.34	C/VE(C)/3R6	C/VE(C)/3	CVALT25
Cement Type	III	III	III	III
Aggregate Type	CC	CG	CG	CG
Sand Type	Lillington	Lillington	Lillington	Lillington
No. of F/T Specimens	3	3	3	3
No. of Control Specimens	1	1	1	1
Cement, pcy	940	870	940	870
Silica fume, pcy	—	—	—	—
Coarse aggregate, pcy	1,720	1,720	1,720	1,720
Sand, pcy	800	820	650	909
HRWR (melamine based), oz/cwt	12	5	—	30
Calcium nitrite (DCI), gal/cy	6.0	6.0	6.0	4.0
AEA, oz/cwt	5	3	1.8	10
Water, pcy	320	350	380	300
W/C	0.34	0.40	0.40	0.34
Slump, in	1.5	6.5	3.75	1.75
Air, %	4.8	10.1	7	7.4
Strength, psi @				
4 Hrs	2,680	—	2,210	—
5 Hrs	4,040	—	2,980	—
6 Hrs	5,150	2,460	3,380	1,190
14 Days	9,070	5,230	6,290	7,320
28 Days	10,150	5,810	—	7,540
Concrete temperature at placement, °F	99	82	90	82

\* Ref. No. relates to tables in Appendixes of volume 2 of this report series.

**Table 6.8b Mixture proportions, strength, and plastic properties of VES concrete used for freezing-thawing test specimens**

Ref. No.*	73	60	23	71
Batch ID	C/VE(CS)/3N	C/VE(PYR)/3	C/VE(CC)/3	C/VE(C*)/3 <sup>+</sup>
Cement Type	III	Pyrament XT	III	III
Aggregate Type	CG	CG	CG	CG
Sand Type	Lillington	Lillington	Memphis	Lillington
No. of F/T Specimens	3	3	3	3
No. of Control Specimens	1	1	2	1
Cement, pcy	940	870	940	870
Silica fume, pcy	43.5	—	—	—
Coarse aggregate, pcy	1,720	1,510	1,720	1,720
Sand, pcy	910	1,440	860	780
HRWR (melamine based), oz/cwt	10	—	18	5
Calcium nitrite (DCI), gal/cy	6.0	—	5.0	6.0
AEA, oz/cwt	—	—	4	2.5
Water, pcy	360	195	285	350
W/C	0.40	0.23	0.34	0.40
Slump, in	7	3.75	3	7
Air, %	1.2	3.6	3.4	9.3
Strength, psi @				
4 Hrs	—	2,680	2,680	—
5 Hrs	—	—	—	—
6 Hrs	2,810	—	—	2,490
14 Days	8,520	9,090	—	—
28 Days	—	—	—	—
Concrete temperature at placement, °F	85	76	90	86

\* Ref. No. relates to tables in Appendixes of volume 2 of this report series.

<sup>+</sup> C/VE(C\*)/3 was moist cured for 14 days before testing.



**Table 6.8c Mixture proportions, strength, and plastic properties of VES concrete used for freezing-thawing test specimens**

Ref. No.*	207	219	226
Batch ID	R/VE(C)/.34	R/VE(C)/32	R/VE(PYR)/3
Cement Type	III	III	Pyrament XT
Aggregate Type	RG	RG	RG
Sand Type	Memphis	Memphis	Memphis
No. of F/T Specimens	3	3	3
No. of Control Specimens	1	1	1
Cement, pcy	940	870	850
Silica fume, pcy	—	—	—
Coarse aggregate, pcy	1,650	1,650	1,510
Sand, pcy	790	760	1,410
HRWR (melamine based), oz/cwt	12	10	0
Calcium nitrite (DCI), gal/cy	6.0	6.0	0
AEA, oz/cwt	5	4	0
Water, pcy	320	350	183
W/C	0.34	0.40	0.22
Slump, in	3	7.75	—
Air, %	4.5	14	4.5
Strength, psi @			
4 H's	1,190	—	1,610
5 H's	2,390	—	—
6 H's	3,680	1,730	—
14 Days	5,900	4,410	—
28 Days	7,290	—	—
Concrete temperature at placement, °F	89	84	—

\* Ref. No. relates to tables in Appendixes of volume 2 of this report series.

**Table 6.8d Mixture proportions, strength, and plastic properties of VES concrete used for freezing-thawing test specimens**

Ref. No.*	176	182
Batch ID	M/VE(C)/3	M/VE(PYR)/3
Cement Type	III	Pyrament XT
Aggregate Type	MM	MM
Sand Type	Lillington	Lillington
No. of F/T Specimens	3	3
No. of Control Specimens	1	1
Cement, pcy	870	850
Silica fume, pcy	—	—
Coarse aggregate, pcy	1,570	1,500
Sand, pcy	800	1,460
HRWR (melamine based), oz/cwt	5	0
Calcium nitrite (DCI), gal/cy	6.0	0
AEA, oz/cwt	2.4	0
Water, pcy	350	145
W/C	0.40	0.17
Slump, in	8.25	4.25
Air, %	9	6.2
Strength, psi @		
4 Hrs	—	1,950
5 Hrs	—	—
6 Hrs	1,900	—
14 Days	—	—
28 Days	—	—
Concrete temperature at placement, °F	83	81

\* Ref. No. relates to tables in Appendixes of volume 2 of this report series.

**Table 6.9 Results of freezing-thawing test of VES Concrete**

Ref. No.*	Batch ID	Air Content %	No. of Cycles Completed	Specimen #1	Durability Factor % Specimen #2	Specimen #3
46	C/VE(C)/.34	4.8	300	105	105	104
67	C/VE(C)/3R6	10.1	300	104	107	105
45	C/VE(C)/3	7	300	111	108	114
28	C/VALT25	7.4	300	106	106	109
73	C/VE(CS)/3N	1.2	36	0	0	0
60	C/VE(PYR)/3	3.6	300	119	104	103
23	C/VE(CC)/3	3.4	36	9	9	8
71	C/VE(C*)/3 <sup>+</sup>	9.3	300	104	102	99
207	R/VE(C)/.34	4.5	63	9	5	10
219	R/VE(C)/32	14	20	1	1	5
226	R/VE(PYR)/3	4.5	300	**	**	83
176	M/VE(C)/3	9	300	100	101	99
182	M/VE(PYR)/3	6.2	300	98	98	97

\* Ref. No. relates to tables in Appendixes of volume 2 of this report series.

\*\* Failed after 70 cycles.

<sup>+</sup> C/VE(C\*)/3 was moist cured for 14 days before testing.

about 0.10 microns (as observed in SEM micrographs), the worst possible situation for freeze-thaw deterioration (Hansen 1993).

One of the specimens of R/VE(PYR)/3 made with Pyrament XT cement and rounded gravel did achieve a durability factor of 83 % at 300 cycles of freezing and thawing, barely meeting the durability requirement. However, the other two companion specimens failed the test after 70 cycles of freezing-thawing, again due to the deterioration of the rounded gravel.

The results of these tests indicate that, even with a very short curing period, VES concrete can be produced with enhanced durability if it has a minimum air content of 5 % and if the coarse aggregate used is not susceptible to freezing-thawing damage.

## **6.4 Shrinkage Tests**

The shrinkage tests were conducted on test specimens of 4 x 4 x 11.25-in. (100 x 100 x 281-mm) prisms for a period up to 90 days. Three replicate specimens were tested for each type of coarse aggregate. The overall program for the shrinkage tests is outlined in Table 6.3.

### *6.4.1 Test Setup and Procedure*

The shrinkage tests were conducted in accordance with the ASTM C 157. An OKO SOKKI model DG 154 digital dial gage was used to measure the length changes. The digital dial gage had a range of 2 in. (50 mm). A view of the shrinkage test setup is shown in Figure A.11.

### *6.4.2 Specimen Preparation*

The 4 x 4 x 11.25-in. (100 x 100 x 281-mm) prisms were cast in steel molds, internally vibrated with a needle vibrator, and finished with a magnesium float. The specimens with molds were protected from moisture loss by being covered with plastic sheets. The specimens were stripped at the design age of 24 hours. Upon removal of the specimens from the molds, the specimens and the standard calibration bar were placed in water maintained at 73°F (22.8°C) for a period of 30 minutes before the length was measured. This was done to equalize the temperature of the specimens and the bar. After the initial readings, the specimens were cured in lime-saturated water for at least 28 days. During the first 28 days, the specimens were periodically removed from the lime-saturated water for measurements and returned to the lime-saturated water after the measurements were taken. Subsequently, they were stored in air under normal laboratory conditions.

**Table 6.10a Summary of shrinkage test results for VES (A) concrete**

Coarse Aggregate Type	Batch ID	Age (days)	Shrinkage Strain (microstrains)	Avg. of No. of Specimens
MM	M/VE(C)/3	1	0	3
		40	-17	
		69	125	
		90	141	
		104	151	
CG	C/VE(C)/R6	1	0	3
		14	45	
		28	-150	
		90	321	
		96	367	
RG	R/VE(C)/32	1	0	3
		14	6	
		61	-20	
		90	59	

**Table 6.10b Summary of shrinkage test results for VES (B) concrete**

Coarse Aggregate.Type	Batch ID	Age (days)	Shrinkage Strain (microstrains)	Avg. of No. of Specimens
MM	M/VE/(PYR)/3	1	0	3
		28	-59	
		56	-59	
		90	-131	
CG	C/VE(PYR)/3	1	0	3
		28	59	
		90	52	
		94	52	
		118	66	
RG	R/VE(PYR)/3	1	0	1
		28	-79	
		35	-46	
		63	-138	
		90	-144	
		98	-144	

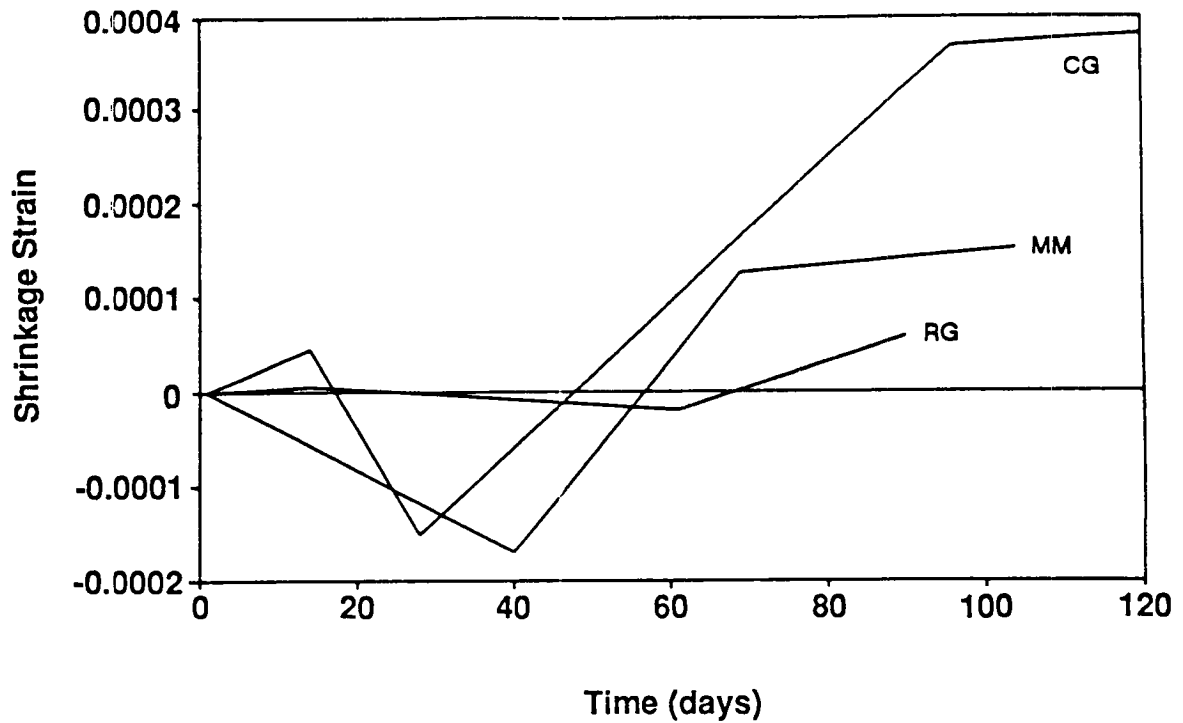


**Figure 6.18a** Variation of shrinkage strain with time for VES (A) concrete

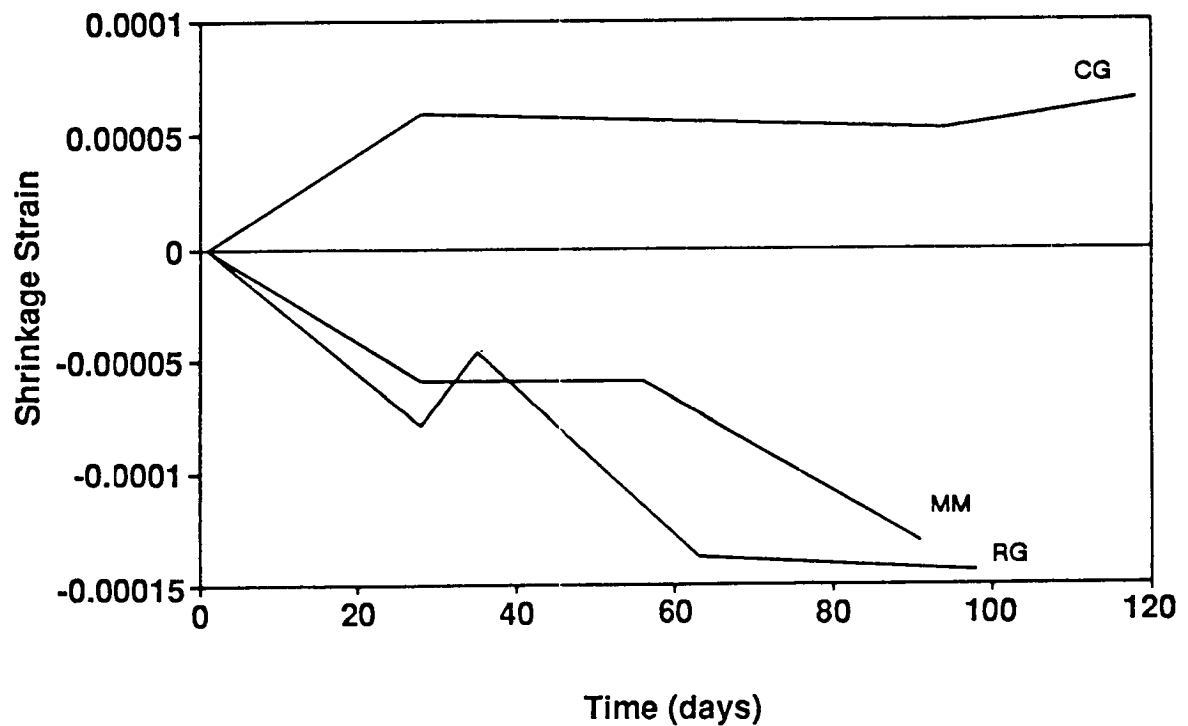


**Figure 6.18b** Variation of shrinkage strain with time for VES (B) concrete

### 6.4.3 Test Results and Discussions

The test results of the shrinkage tests for VES concrete (Options A and B) are summarized in Tables 6.10a and 6.10b. The results for VES (A) concrete indicate that at the age of 90 days, more shrinkage strains occurred with CG coarse aggregate than with the other types of coarse aggregates. The variation of the shrinkage strains with time for VES (A) concrete with different types of coarse aggregates is shown in Figure 6.18a. These curves are an average of three replicate specimens. It can be seen that three curves (with CG, MM, and RG coarse aggregates) show an initial expansion when readings were taken at early ages. This phenomenon is common for shrinkage specimens stored in water according to ACI Committee 209 (1993a). For VES (A) concrete with RG and MM coarse aggregates, the shrinkage strains at 90 days were much smaller (60 to 140 microstrains) than the generally accepted values (700 to 800 microstrains) for conventional concretes. The general trend of variation of shrinkage strains with time for VES (A) concrete was similar to that generally accepted for conventional concrete. The variation of the shrinkage strain with time for VES (B) concrete with different types of coarse aggregates is shown in Figure 6.18b. It is interesting to note that for VES (B) concrete with MM and RG coarse aggregates, the specimens do not exhibit any shrinkage strains up to an age of 90 days and the shrinkage strains for concrete with CG coarse aggregate are relatively small (about 50 microstrains). It should be noted that the shrinkage specimens were immersed in lime-saturated water for the first 28 days, according to the test procedures of ASTM C 157. Since the W/C was very low (0.17 to 0.23) for the VES (B) concrete using Pyrament XT cement, the concrete would absorb moisture in the lime water, resulting in a slight expansion. When the specimens with MM and RG aggregates (W/C equals 0.17 and 0.22, respectively) were removed from the lime water, they continued to experience a small amount of expansion because of the increased volume of the hydration products. They showed no shrinkage strains, probably because no evaporable water was available in the concrete due to the very low W/C. Tests on concrete using Pyrament XT cement, conducted at Army Corps of Engineers Waterways Experiment Station, have shown expansion in the order of 1,000 microstrains in specimens which were kept in water for a year (Husbands and Wakely 1991).

It should be noted that coarse aggregate in a concrete provides a restraining effect on the drying shrinkage of pure cement paste. The amount of restraint provided by the aggregate depends on the amount of coarse aggregate in the concrete, its stiffness, and the maximum size of the coarse aggregate (Mindess and Young 1981). The stresses due to drying shrinkage at the cement-paste aggregate interface increase as the maximum aggregate size increases (Mindess and Young 1981). The size and the shape of a concrete specimen determines the rate of moisture loss, and hence the rate and magnitude of drying shrinkage. Also, the absorption characteristics of the coarse aggregate have an influence on the shrinkage characteristics of the concrete, especially during the early ages. The length of the diffusion path also has a strong influence on the rate of moisture loss, which in turn affects the shrinkage characteristics.

ACI committee 209 (1993a) recommends a set of empirical equations that allow shrinkage strains to be estimated as a function of drying and relative humidity. The value of the ultimate shrinkage strain recommended by the ACI Committee 209 is  $730 \times 10^{-6}$  in/in. The magnitude of



the ultimate shrinkage strain is difficult to estimate since it depends on a number of factors including W/C, degree of hydration, presence of admixtures and cement content. The average shrinkage strains at 90 days for VES (A) concrete varied between 59 microstrains (for concrete with RG coarse aggregate) and 331 microstrains (for concrete with CG coarse aggregate). The average strains at 90 days for the VES (B) concrete varied from an expansion of 150 microstrains (for concrete with RG coarse aggregate) to a shrinkage of 50 microstrains (for concrete with CG coarse aggregate).

## **6.5 Rapid Chloride Permeability Tests**

### *6.5.1 Test Setup and Procedure*

The rapid chloride permeability test (RCPT) was performed in accordance with AASHTO T 277-83 and the identical ASTM C 1202. The typical specimen was a 2-in. (50-mm) thick slice of concrete sawn from the top of a 3.75-in. (94-mm) diameter core from a concrete prism cast at the same time as the freezing-thawing test specimens, as described in section 6.3.2. The top of the specimen, which would be exposed to chloride ions, was the finished surface.

### *6.5.2 Specimen Preparation*

The specimen was prepared by vacuum saturation and by soaking in water for 18 hours, as shown in Figure A.12. The specimen was then sealed in the test cells. The cell connected to the top surface of the specimen was filled with 3% sodium chloride (NaCl) solution; the other cell, connected to the bottom surface of the specimen, was filled with 0.3 N sodium hydroxide (NaOH), as shown in Figure A.13. Two replicate specimens were always tested concurrently. Both specimens were energized continuously with 60 V DC between the cells as shown in Figure A.14. The current flowing through the concrete specimen was measured and plotted on a strip chart recorder for 6 hours, as shown in Figure A.15. A switching unit was built to allow two measurements to be plotted alternately on one strip chart. The total time required to complete each test was about 33 hours. Described below are the step-by-step procedures for the test.

1. Obtain two 3.75-in. (94-mm) diameter concrete samples by coring through a 6 x 6-in. (150 x 150-mm) prism, oriented as cast, when the concrete is 12 days old. (Two days are allowed for specimen preparation so that the actual testing can be started at 14 days.) Keep the samples in a plastic bag.
2. Saw a 2-in. (50-mm) slice from the top of each core. Surface dry the specimens for 10 minutes after cutting. Mark an ID on each specimen and clearly identify its top surface. Keep the specimens in a plastic bag.

3. Boil two liters of water vigorously to de-air the water. Do not cap the boiling pot. Allow the water to cool.
4. Prepare clear epoxy, and brush it on the side surface of each specimen. Allow the epoxy to cure according to the manufacturer's instructions. Use a type that takes no longer than 1 hour to cure.
5. Place both specimens, slightly separated, in a tilted position in a beaker, then place the beaker in a *vacuum type* desiccator and start the vacuum (1 mm Hg abs., 133.3 Pa). Maintain the vacuum for 3 hours.
6. While the vacuum pump is running, fill the beaker with the boiled water until it submerges the specimens.
7. Continue running the vacuum pump for 1 additional hour.
8. Turn the pump off and allow air to enter the desiccator.
9. Allow both specimens to remain in the beaker, soaking in water for 18 hours.
10. Remove the specimens from the beaker, blot off water, and place the specimens in a plastic bag.
11. Place a small amount of silicon sealant on a brass shim around the inside perimeter of each cell. Place the specimen in a cell assembly, with its top side toward the NaCl cell. Apply liberal amounts of silicon sealant around the specimen to seal it to the cells. Allow the sealant to cure according to the manufacturer's recommendations (use a type that will cure in about 1 hour).
12. Fill the negative cell (top side) with 3% NaCl solution. Fill the positive cell with 0.3 N NaOH. Connect the wires as marked, with negative to NaCl and positive to NaOH. Turn on the power, set to 60.0 +/- 0.1 V DC, and turn on the plotter. [Setting: 1 volt full scale (this is actually 0.985 amp. full scale on the NCSU plotter), and 2 in./hr]. Record the time and ID number on plotter paper. Run the test for 6 hours.
13. Remove the specimens from the test cells. Rinse the cells and clean the assembly.
14. Integrate the area under the curve from the plotter in units of ampere-second (coulombs), and record the results.

### 6.5.3 Test Results and Discussion

A total of 21 groups of specimens of VES concrete were subjected to the RCPT, as shown in Tables 6.11a and 6.11b. Each group consisted of two replicate specimens which were tested concurrently in two separate RCPT cells. A typical output strip chart from the RCPT is shown in Figure A.16. The abscissa represents time, obtained at a chart rate of 5 cm/hr for approximately 6 hours. The ordinate represents the current flowing through the specimen, in amps, with a chart calibration of full scale being equal to 0.985 amps for the particular plotter used.

**Table 6.11a Results of rapid chloride permeability test of VES concrete**

Ref. No.*	Batch ID	W/C	Air %	F/T Cycles	Durability Factor %			Rapid Chloride Pene. Test	
					Sp #1	Sp #2	Sp #3	Initial Current (Amp.)	Total Charge (Coulomb)
153	MVALT4	0.30	5.0	—	—	—	—	0.271	9,800
153	MVALT4	0.30	5.0	—	—	—	—	0.192	5,290
153	MVALT4	0.30	5.0	—	—	—	—	0.134	3,620
23	C/VE(CC)/3	0.34	3.4	36	9	9	8	0.199	5,680
154	M/VE(CC)/3	0.30	4.2	—	—	—	—	0.190	6,160
28	CVALT25	0.34	7.4	300	106	106	109	0.125	3,490
45	C/VE(C)/3	0.40	7.0	300	111	108	114	0.216	7,810
46	C/VE(C)/.34	0.34	4.8	300	105	105	104	0.116	2,854
207	R/VE(C)/.34	0.34	4.5	63	9	5	10	0.136	3,570
67	C/VE(C)/3R6	0.40	10.1	300	104	107	105	0.294	11,890
67	C/VE(C)/3R6	0.40	10.1	300	104	107	105	0.293	12,300
67	C/VE(C)/3R6	0.40	10.1	300	104	107	105	0.208	7,620
60	C/VE(PYR)/3	0.21	3.6	300	119	104	103	0.113	2,960
219	R/VE(C)/32	0.40	14.0	20	1	1	5	0.194	7,300
176	M/VE(C)/3	0.40	9.0	300	100	101	99	0.335	>20,000

\* Ref. No. relates to tables in Appendixes of volume 2 of this report series.

**Table 6.11b Results of rapid chloride permeability test of VES concrete**

Ref. No.*	Batch ID	W/C	Air %	F/T Cycles	Rapid Chloride Pene. Test			Initial Current (Amp.)	Total Charge (Coulomb)
					Durability Factor %	Sp #1	Sp #2	Sp #3	
71	C/VE(C*)/3 <sup>+</sup>	0.40	9.3	300	104	102	99	0.252	12,320
71	C/VE(C*)/3	0.40	9.3	300	104	102	99	0.203	8,450
71	C/VE(C*)/3	0.40	9.3	300	104	102	99	0.231	9,550
73	C/VE(CS)/3N	0.40	1.2	36	0	0	0	0.174	5,600
226	R/VE(PYR)/3	0.22	4.5	300	**	**	83	0.099	1,350
182	M/VE(PYR)/3	0.17	6.2	300	98	98	97	0.094	2,670

\* Ref. No. relates to tables in Appendixes of volume 2 of this report series.

\*\* Failed after 70 cycles.

<sup>+</sup> C/VE(C\*)/3 was moist cured for 14 days before testing.

As described before, two replicate specimens were tested together and both were energized continuously for 6 hours. However, the current flowing through each specimen was measured and plotted alternately on the strip chart. The average area under the curve is the total charge, in coulombs, that passed through the specimen in 6 hours. The initial current, in amps, is the average ordinate just after the test was started.

It can be seen that the amount of current flowing through the specimen tended to increase during the RCPT due, at least in part, to the temperature increase in the specimen. This heating problem was caused by the current. The question was raised whether the initial current, which is also an indirect measure of the concrete conductance, could be used in lieu of the total charge as a more convenient data to obtain for the RCPT. If so, six hours of testing time would be saved. A comparison of the initial current with the total charge for each of the 21 groups of testing, as shown in Tables 6.11a and 6.11b, indicates a good correlation between the two measurements.

It should be observed that both the freezing-thawing test and the RCPT were performed for 17 of the 21 groups of specimens. As discussed in section 6.3.3, five of the seventeen groups failed the freezing-thawing test because of either inadequate air content or deterioration of the coarse aggregate (i.e., RG). However, even though they failed the freezing-thawing test, their total charge values from the RCPT were much lower in comparison with the majority of the total charge values of the remaining groups of test specimens. In fact, the coulomb values of these latter groups were in the very "high permeability" category according to the classifications of ASTM C 1202, but the specimens showed excellent freeze-thaw durability. This comparison indicates that VES concrete may have excellent freeze-thaw durability and yet exhibit high

permeability for chloride penetration, which can be greatly affected by the many additional ions introduced in the concrete through the various admixtures. These ions would cause the concrete to be more conductive electrically and make it *appear* to be more permeable than it really is.

It should also be noted that the three groups of specimens made with Pyrament XT cement (with very low W/C) had the lowest coulomb values, whereas the coulomb values for the remaining groups of test specimens were considerably higher. Furthermore, one can observe an expected trend that both the total charge value and the initial current value increase as W/C increases.

Several groups of test specimens—C/VE(C)/3R6, M/VE(C)/3, and C/VE(C\*)/3—showed very high total charge values, with one in excess of 20,000 coulombs. This was because the high current flowing through the specimen caused excessive heating of the specimen. The chemicals in the RCPT cells began to boil and the test was stopped.

## **6.6 AC Impedance Tests**

The objective of conducting the AC impedance tests was to examine its potential as a reasonable alternative to the RCPT method for determining concrete permeability. The goal was to explore a faster method that could be more versatile and portable. The method would also avoid elaborate test setups and specimen preparation, as well as expensive and time-consuming procedures. The use of external measurement terminals would allow more versatility than the internal terminals used for the RCPT method. A "point source" type of test, such as the AC impedance test, would also be more versatile since it could be adapted more easily to specimens of different shape.

The RCPT method measures total conductance of a specimen, rather than conductivity. Similarly, the AC impedance test measures total resistance in ohms, which may be more indicative of the gross concrete properties than resistivity. As long as the test could classify concrete as accurately as the RCPT, it would be a satisfactory alternative.

### ***6.6.1 Test Setup and Procedure***

Currently there are no AASHTO or ASTM standards for the AC impedance test. The test for this investigation was conducted using a Kohlrausch bridge instrument, Model 4000, manufactured by AEMC Instruments, Boston, Massachusetts. The Kohlrausch bridge uses 1,000 Hz AC with an accuracy of 1% on the impedance measurement. Eight impedance ranges are available for selection by pushbuttons, and usually the 1 to 10 Kohm range was used. The voltage actually placed across the specimen was measured to be about 0.20v. Six 1.5v "AA" batteries were used as power supply. The general setup is shown in Figure A.17.

A good electrical connection between the Kohlrausch bridge terminals and the concrete specimen was ensured by using potassium agar gel. The impedance (resistance) was measured at five

random points on each specimen, the same as for the RCPT; see Figure A.18. Rubber gloves were used to insulate fingers from the test specimen.

### 6.6.2 *Specimen Preparation*

The AC impedance test was conducted in conjunction with the rapid chloride permeability test at three different stages: (1) right after the specimens of RCPT were cut, but before they were subjected to the vacuum saturation process; (2) after the specimens were vacuum saturated, but before they were subjected to the RCPT; and (3) after the specimens had been subjected to the RCPT.

Therefore the specimens for the AC impedance test were prepared in exactly the same manner as for the RCPT. Described below are the step-by-step procedures used for the AC impedance test.

1. After the specimen is cut from a 3.75-in. (94-mm) concrete core, air dry the specimen to avoid wet surfaces which may distort the electrical measurement.
2. Connect two electrode wires to the Kohlrausch bridge (which is similar to a Wheatstone bridge), with the specimen placed one arm of the bridge. The free end of each wire should have a flattened piece of solder (about 0.25-in., 6.4-mm diameter) as an electrode. Virtually any type of electrical wire can be used to connect the concrete specimen into the bridge circuit since the current is very small. A wire length of about 18 in. (450 mm) is recommended.
3. Put a rubber glove on the hand which will press the electrodes onto the concrete specimen.
4. Dip the solder end of the wires into potassium agar gel to obtain a small amount of gel, ensuring good conductivity between the electrodes and the concrete.
5. Press the solder flat ends against the two flat surfaces of the test specimen and hold them in place with the thumb and middle finger of one hand. With a little practice, a good connection can be made by feel. Also, the gel "fingerprint" should be kept small and *consistent* through all of the testing.
6. Balance the Kohlrausch bridge circuit and record the impedance measurement in ohms.
7. Repeat the measurement at 5 random locations on the flat surfaces of each of the replicate specimens. Be careful to not allow the gel "fingerprint" to overlap, for this will affect the conductance.

### 6.6.3 Test Results and Discussion

AC impedance tests were conducted along with the RCPT on fifteen groups of VES concrete specimens, as summarized in Table 6.12. (The AC impedance test was not conducted on concrete with DL aggregate at the University of Arkansas.) As mentioned before, AC impedance was measured five times on each of two replicate specimens for a total of 10 measurements. Therefore each impedance value listed in Table 6.12 is the average of the 10 measurements.

The AC impedance was measured three times on the RCPT specimens: (1) just after the specimen was cut, but before vacuum saturation; (2) after vacuum saturation of the specimen; and (3) after the RCPT had been completed. It is worth noting that the degree of saturation is initially more varied in a specimen, so its conductance is lower and its impedance higher. After vacuum saturation, the degree of saturation of the specimen becomes more uniform, so its conductance is improved and its impedance reduced. After the RCPT is conducted on the specimen, its impedance becomes slightly higher again, since the test has affected the conductance of the specimen by driving some unknown amount of chloride ions into the concrete and by driving out some of the ions originally in the pore water of the concrete. Furthermore, any heating of the specimen may accelerate further hydration of residual cement, thereby changing the electrical conductance pathways through the concrete. Because of these effects, vacuum saturation is regarded as the best preparation of the specimen for the AC impedance test.

As discussed before, chloride permeability (measured in coulombs) is essentially a conductance test, whereas AC impedance (measured in ohms) is essentially a resistance test. Since the two properties are reciprocals, an inverse relationship could be expected between the data from these measurements. After evaluating the two sets of data in several ways, it was determined that the best correlation between the two properties is expressed by the inverse impedance (reciprocal of impedance) in terms of the initial current as shown in Figures 6.19a through 6.19d.

## 6.7 Concrete-to-Concrete Bond Tests

Concrete-to-concrete (C-C) bond tests were conducted to determine the interfacial bond strength and the corresponding interfacial deformation. For these tests, the specimen was designed so as to have a direct shear condition at the interface between the two segments of the specimen. The specimen used in the direct shear test was composed of an inverted L-shaped segment "A" bonded to an upright L-shaped segment "B" (see Figure A.19). Standard North Carolina Department of Transportation (NCDOT) concrete mixture, termed "control" mixture, was used for casting segment "A", and VES concrete was used to cast segment "B" of the C-C bond test specimen. This method of fabricating the test specimen simulated the condition of a HPC overlay on an existing pavement of "control" concrete.

**Table 6.12 Results of AC impedance test of VES concrete**

Ref. No.(a)	Batch ID	W/C	Air %	AC Impedance Test, Ohms			Rapid Chloride Pene. Test	
				Before Sat.(b)	After Sat.(c)	After Test(d)	Initial Current (Amp.)	Total Charge (Coulomb)
45	C/VE(C)/3	0.40	7.0	2,142	1,051	1,052	0.216	7,810
46	C/VE(C)/.34	0.34	4.8	3,594	2,254	1,947	0.116	2,854
207	R/VE(C)/.34	0.34	4.5	3,230	2,309	1,950	0.136	3,570
67	C/VE(C)/3R6	0.40	10.1	2,381	770	674	0.294	11,890
67	C/VE(C)/3R6	0.40	10.1	2,193	1,040	817	0.293	12,300
67	C/VE(C)/3R6	0.40	10.1	1,954	933	789	0.208	7,620
60	C/VE(PYR)/3	0.23	3.6	6,185	3,003	5,223	0.113	2,960
219	R/VE(C)/32	0.40	14.0	2,235	1,264	868	0.194	7,300
176	M/VE(C)/3	0.40	9.0	-	-	500	0.335	>20,000
71	C/VE(C*)/3	0.40	9.3	1,570	987	716	0.252	12,320
71	C/VE(C*)/3	0.40	9.3	1,905	1,143	728	0.203	8,450
71	C/VE(C*)/3	0.40	9.3	2,013	1,174	971	0.231	9,550
73	C/VE(CS)/3N	0.40	1.2	2,462	1,443	2,308	0.174	5,600
226	R/VE(PYR)/3	0.22	4.5	4,504	4,037	5,563	0.099	1,350
182	M/VE(PYR)/3	0.17	6.2	4,620	4,300	5,214	0.094	2,670

(a) Ref. No. relates to tables in Appendixes of volume 2 of this report series.

(b) Test conducted before specimen was vacuum saturated for rapid chloride permeability test.

(c) Test conducted after specimen was vacuum saturated for rapid chloride permeability test.

(d) Test conducted after completion of rapid chloride permeability test.



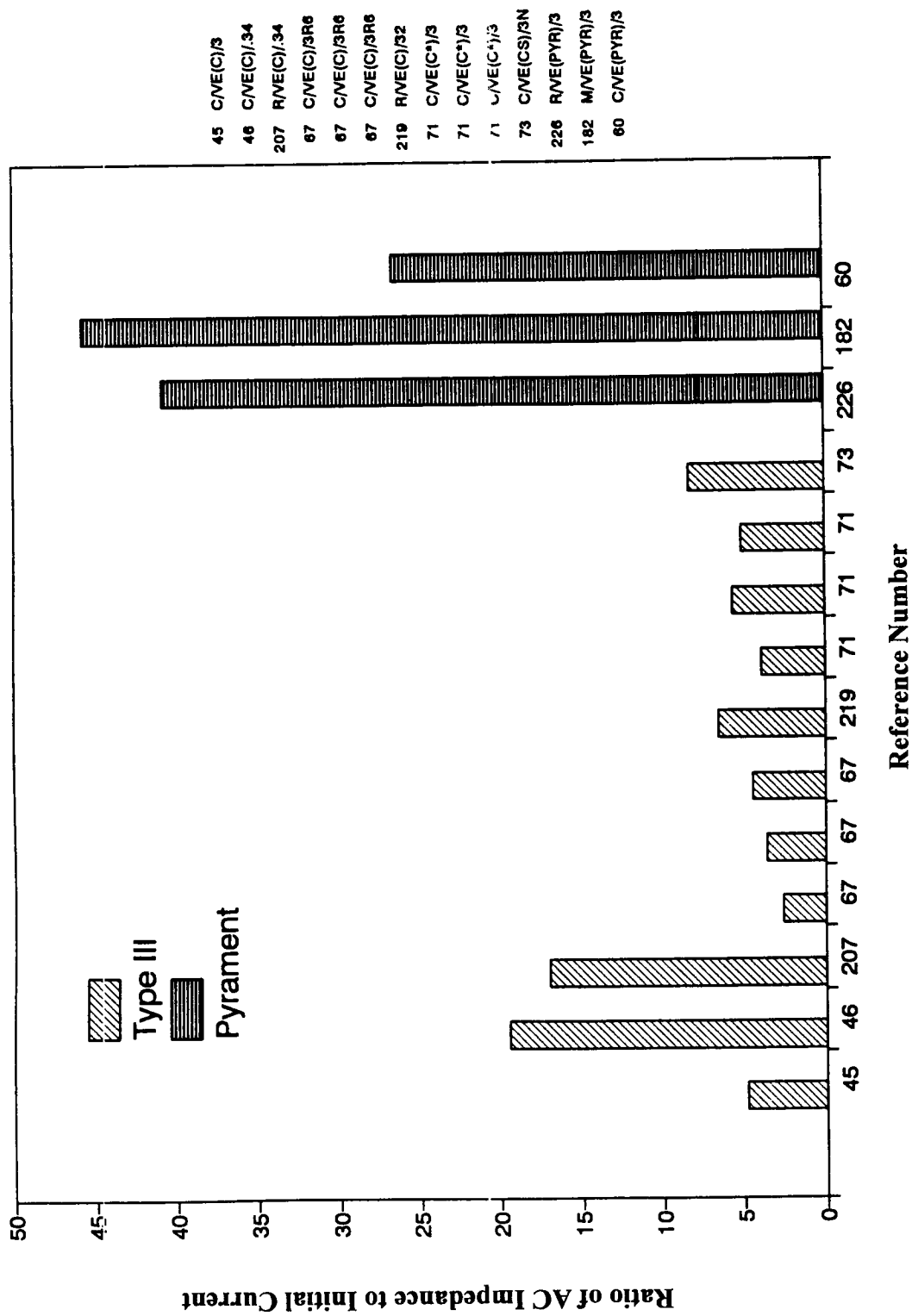


Figure 6.19a Comparison of AC impedance with initial current

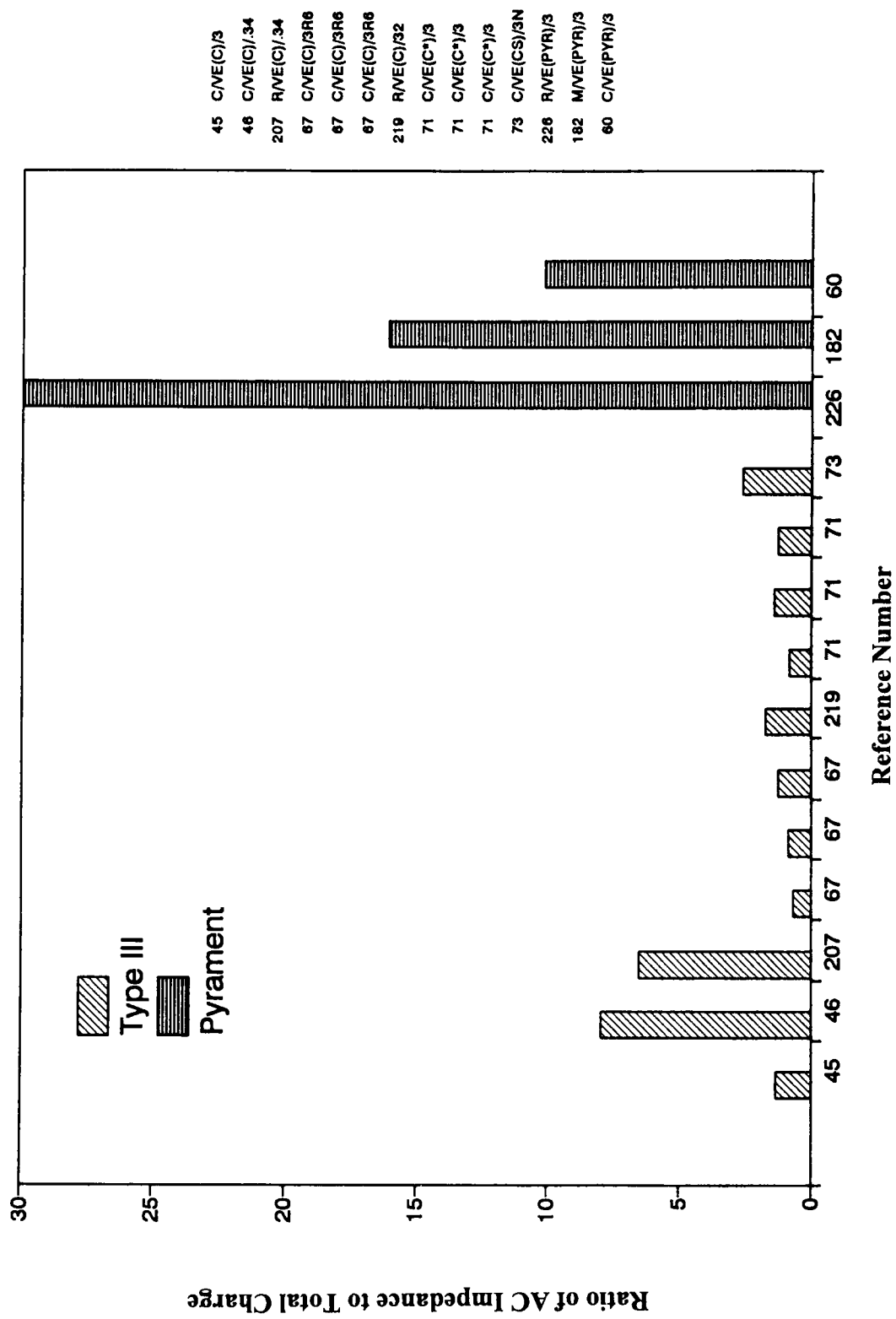


Figure 6.19b Comparison of AC impedance with total charge

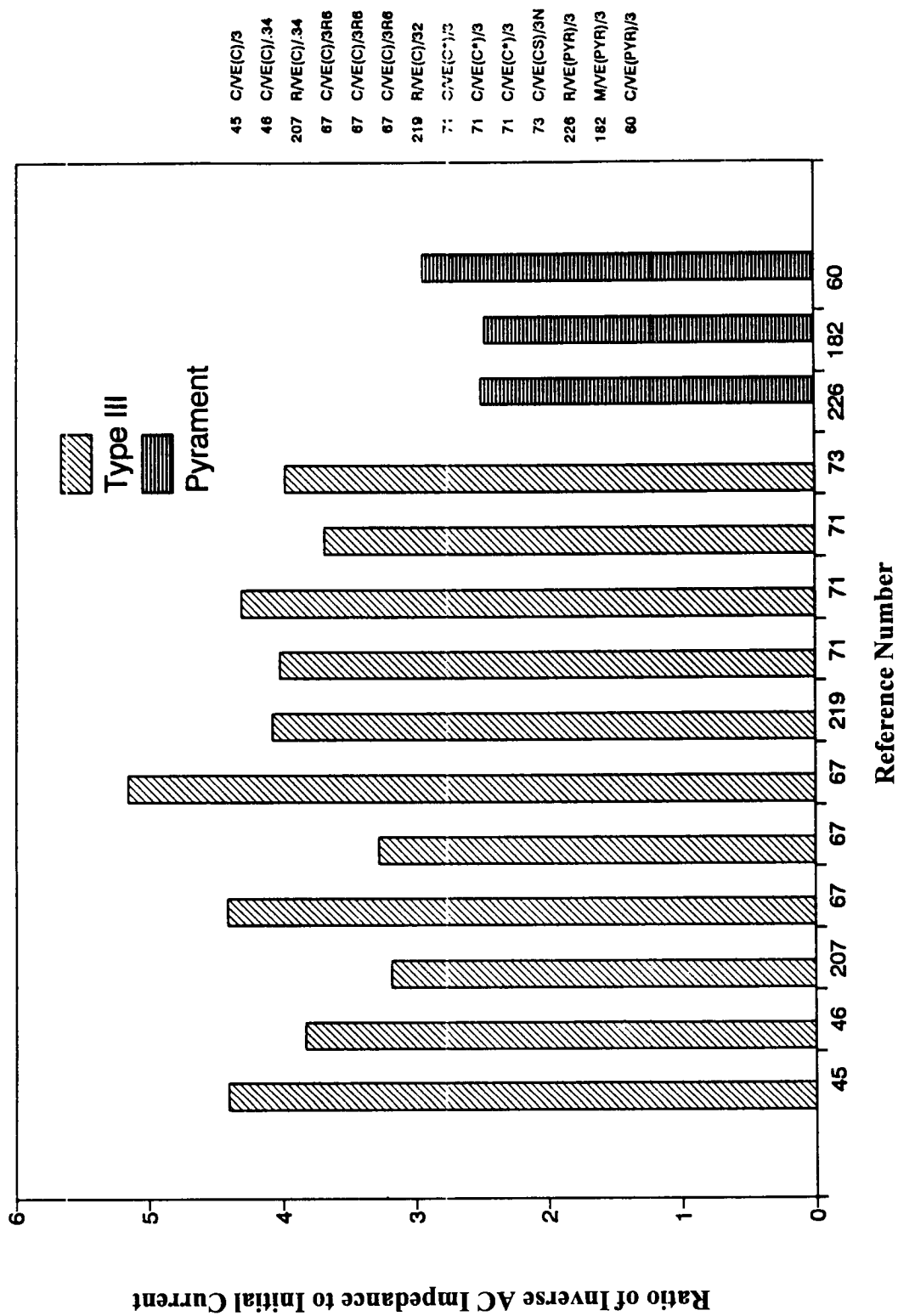


Figure 6.19c Comparison of inverse AC impedance with initial current

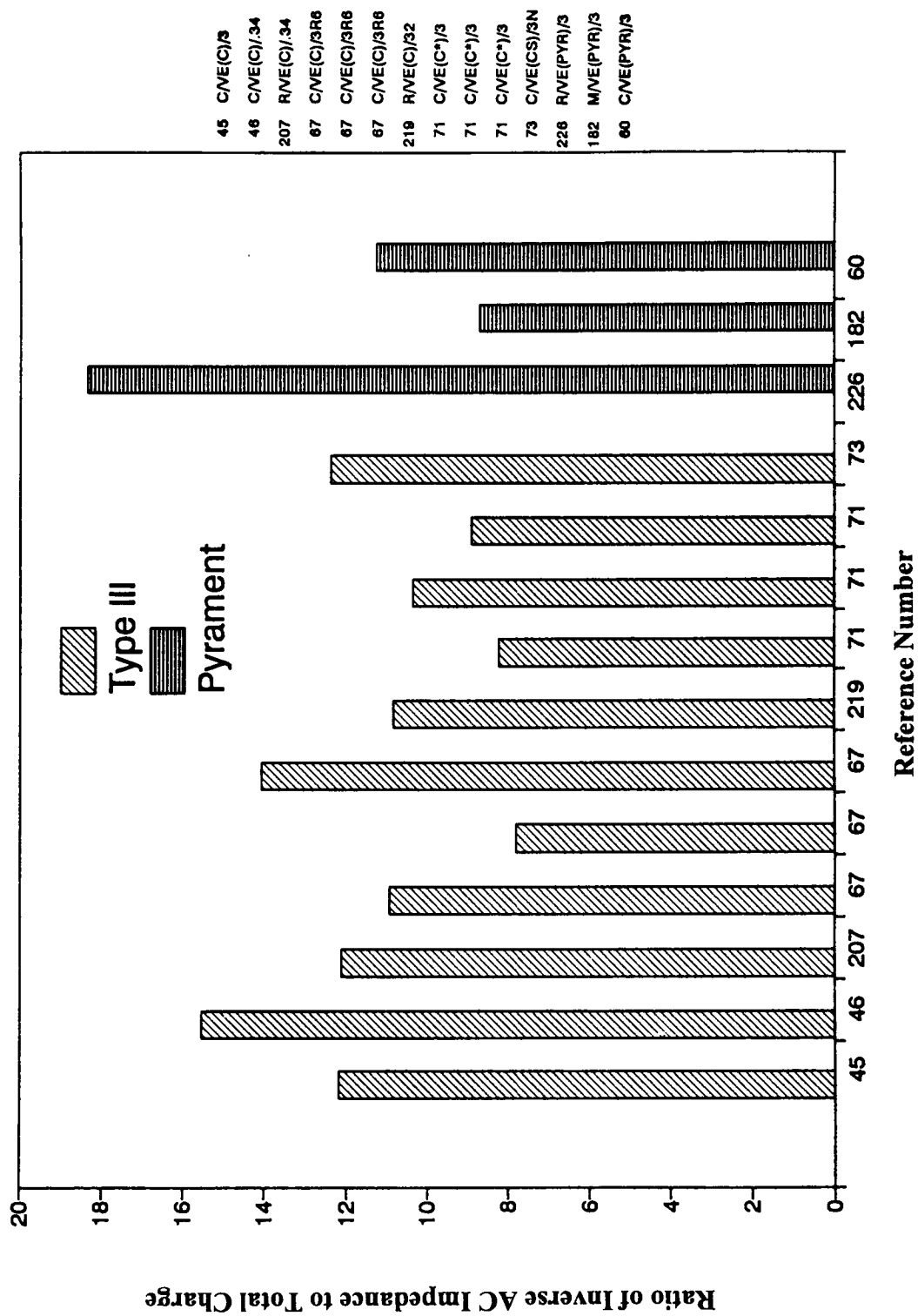


Figure 6.19d Comparison of inverse AC impedance with total charge

### *6.7.1 Test Setup and Procedure*

The direct shear tests were conducted in an 810 Material Test System (MTS) with a 200-kip (890-kN) capacity. The test was conducted at the design age (1 day) of the VES concrete. The age of the "control" concrete segment of the C-C bond specimen was well over 100 days.

The load was applied at the rate of 1,500 lbs/min (6.68 kN/min). During the test, the interfacial deformation along the shearing plane was measured by two LVDTs, one mounted at the front and the other mounted at the back of the specimen. The LVDT's had a gage length of 4 in. (100 mm) and were attached to angles which were then glued to the specimen. The load output and the outputs from the two LVDTs were recorded at 2-second intervals, using the OPTIM data acquisition system (Megadac System 100).

For safety reasons, wood blocks with a thickness of slightly less than 2 in. (50 mm) were inserted into the gaps between segment "A" and segment "B" of the test specimen. A chain was also used to loosely tie the lifting handles in the top segment of the test specimen to the loading head of the test machine. This was done to ensure that the top segment of the test specimen would not fall after failure. The test setup is shown in Figure A.20.

### *6.7.2 Specimen Preparation*

The direct shear L-shaped segments were reinforced with mild steel bars and were provided with lifting handles. The reinforcement in each L-shaped segment of the specimen consisted of two # 2 bars and two # 3 bars (see Figure A.19). The segment which used the "control" concrete (i.e., segment "A") was cured in a moist room for 28 days. After segment "A" was air dried, its bonding surface was sandblasted with extra-fine sand under 90 psi (0.62 MPa) pressure for a period of 20 seconds to simulate the field condition of an overlay installation. Segment "A" was then placed on its side with the bonding surface facing upward. Prior to casting segment "B", a wet cloth was placed on the sandblasted surface for 30 minutes; then segment "B" was cast using the VES concrete. After casting, the C-C bond specimen was protected from moisture loss by being covered with plastic sheets. The test specimens were cured till the time of testing. Companion 4 x 8-in. (100 x 200-mm) cylinders were also cast when casting segment "A" and segment "B" of the test specimens. The curing conditions of these companion cylinders were identical to the curing conditions of segments "A" and "B".

### *6.7.3 Test Results and Discussions*

The concrete-to-concrete bond strength test results are summarized in Table 6.13. The values of concrete strength of the NCDOT "control" concrete and the VES concrete reported in the table are the average compressive strength of two 4 x 8-in. (100 x 200-mm) replicate specimens. The load-interfacial deformations for VES concrete with CG and MM as coarse aggregates are shown in Figure 6.20. The result of each test specimen is shown separately. From these figures, it can

**Table 6.13 Summary of test results for concrete-to-concrete bond tests of VES concrete**

Test Type	Coarse Aggregate Type	Specimen	Age at Testing	Air Content %	Slump (in)	Concrete Temp. (deg. F)	$f'_c$ of HPC at Testing	$f'_c$ of NCDOT "Control" Mix at 28 Days (psi)	$f'_c$ of NCDOT Mix at Time of Testing
	CG	VES(A)(CG)/5A	6.0 hrs	9.0	5.5	68	1450*	6180	7100 @ 123 days
	CG	VES(A)(CG)/5B	6.5 hrs	9.0	5.5	68		6180	7300 @ 123 days
C-C	CG	VES(B)(CG)/5A	4.5 hrs	5.0	6.0	75	2250	6170	7150 @ 117 days
Bond Test	CG	VES(B)(CG)/5B	5.0 hrs	5.0	6.0	75		6190	7250 @ 117 days
	CG	NCDOT(CG)	7 days	5.8	3.4	69	4180	6175	7300 @ 137 days
	CG		7 days	6.0	3.5	69		6185	7500 @ 137 days

\* Did not meet the strength criteria for VES concrete (Option A), due to curing condition.

Notes: VES (A), VES (B) = Category of HPC      5A, 5B = Specimen No.

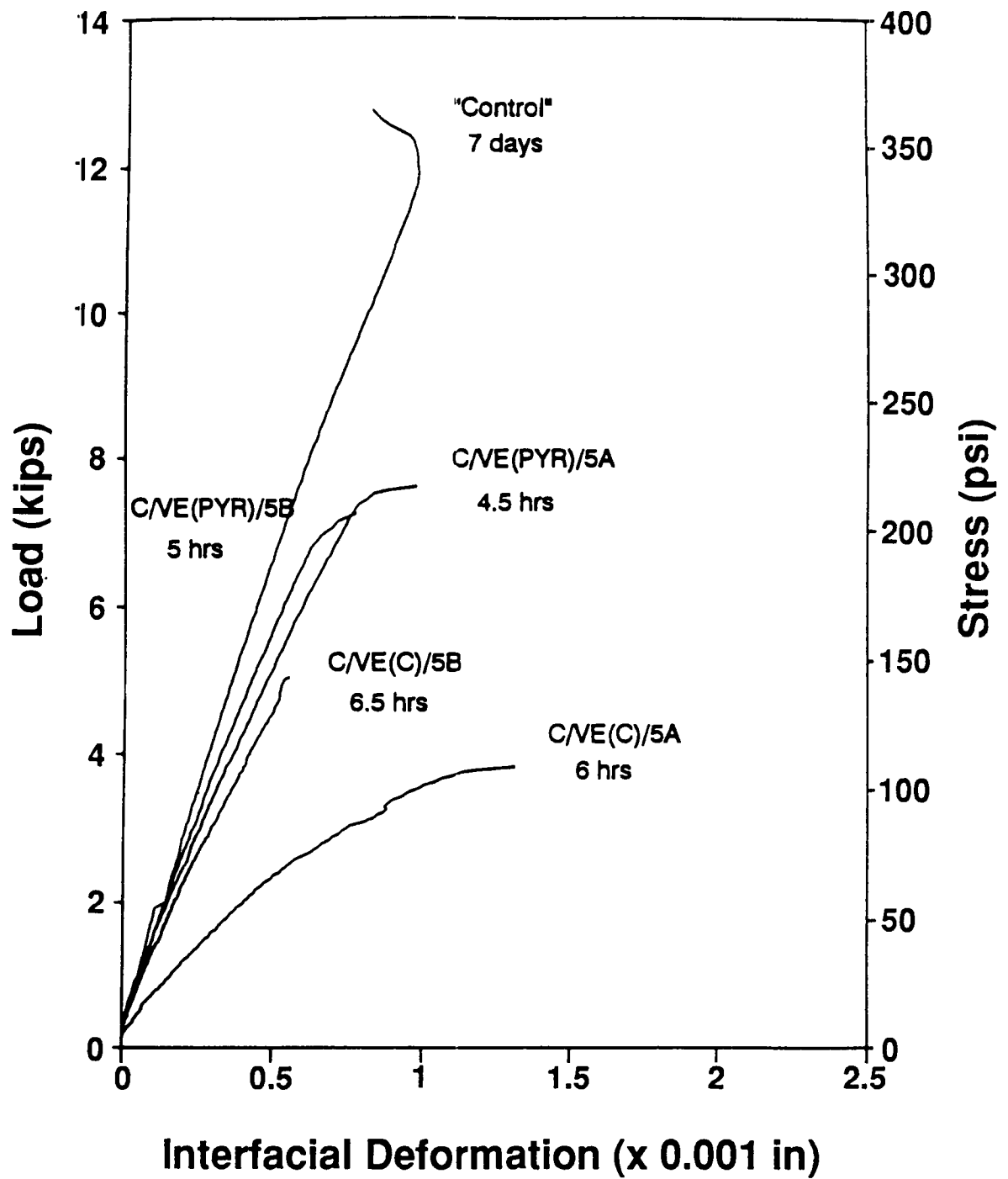


Figure 6.20 Load vs interfacial deformation for C-C bond of VES concrete

be observed that for specimens with an older test age, the stiffness of the load-interfacial deformation increased and remained linear, up to a larger strain value. Although these results are very limited, they indicate that interfacial bond strength is sensitive to the age of the concrete, especially during the early age.

The nominal bond stress between the "control" concrete and the VES concrete can be computed by dividing the maximum debonding load by the nominal bonding area of 36 sq. in. ( 225 cm<sup>2</sup>). The values of the nominal C-C bond stress range between 125 psi ( 0.86 MPa) for VES (A) concrete with CG aggregate, and 225 psi (1.55 MPa) for VES (B) concrete with CG aggregate.

A "control" specimen with both the L-shaped segments "A" and "B" made from standard NCDOT mix was also fabricated and tested at the age of 7 days. Figure 6.20 shows the test results of the "control" specimen. It should be pointed out the curved portion at the top of the load-interfacial deformation response is due to interfacial slip, which occurred just prior to the failure of the specimen. The nominal C-C bond stress in this case is 330 psi (2.27 MPa).



## Conclusions

This report has documented the results of an extensive program of laboratory studies on the performance of very early strength (VES) concrete, which is a class of high performance concrete designed for highway applications. The laboratory studies included seven different types of tests: compression, flexural and split tension, shrinkage, freezing-thawing, rapid chloride permeability, AC impedance, and concrete-to-concrete bond. Based on the results of this investigation, the following conclusions can be drawn:

1. Using conventional materials and equipment, but with more care than needed for conventional concrete, two options of VES concrete can be produced. VES (A) will achieve a minimum compressive strength of 2,000 psi (14 MPa) in 6 hours, and VES (B) will achieve a minimum compressive strength of 2,500 psi (17.5 MPa) in 4 hours. Such concretes can be produced with a variety of aggregates including crushed granite, marine marl, dense crushed limestone, and washed rounded gravel.
2. Insulation must be used to entrap the heat of hydration in order to accelerate the early strength development of the VES concretes.
3. Use of a larger amount of Type III cement or Pyrament XT cement in the VES concrete mixtures, along with a low W/C, leads to a more rapid strength development of these concretes in the first 3 days than predicted by the current ACI recommendation based on conventional concrete.
4. Since the VES concretes are kept moist only for the first 6 or 4 hours, followed by air curing in the laboratory, the strength development of the small laboratory samples is very rapid during the first 3 days; the subsequent rate of strength gain is greatly reduced. The same is true with the modulus of elasticity.
5. Since the design strength of both options of the VES concrete is within the range of conventional concrete, the mechanical behavior of the VES concrete, such as the modulus of elasticity and the compressive and tensile strain capacities, is similar to that of conventional concrete. The modulus of elasticity, the flexural modulus, and

the splitting tensile strength can all be predicted reasonably well by the ACI Code equations. At the early design ages (6 or 4 hours), the compressive strain capacity ranges between approximately 1,000 and 2,000 microstrains, and the tensile strain capacity varies between 100 and 180 microstrains. These strain values would increase somewhat as the concrete ages.

6. The stress-strain relationship of the VES concretes is more nonlinear at 6 or 4 hours than at later ages, and the modulus of elasticity is lower for concrete with softer aggregate, such as marine marl.
7. For VES (B) concrete with Pyrament XT cement, the flexural modulus may decrease after the first 7 days because of the drying of the test specimen, possibly due to self-dessication resulting from the very low W/C of the concrete.
8. Even with a very low W/C, the VES concretes should have an adequate amount of air entrainment to enhance their frost resistance, because the concretes are subject to moist curing for only a few hours. The test results indicate that if the VES concrete contains at least 5% entrained air, it will meet the stringent requirement of a durability factor of 80% after 300 cycles of freezing and thawing according to the ASTM C 666, procedure A. This is in contrast to a durability factor of 60% commonly expected of quality conventional concrete.
9. The VES concretes produced with washed rounded gravel from Memphis, Tennessee, failed the freeze-thaw test according to ASTM C 666, procedure A, because the aggregate had an absorption of about 5% and pore sizes of about 0.10 microns (as observed in SEM micrographs), the worst possible conditions for freezing-thawing deterioration.
10. Shrinkage of the VES (A) concrete follows the general trend of conventional concrete. The average shrinkage strain of the concretes at 90 days ranges from 59 to 321 microstrains, depending on the type of coarse aggregate used. These values represent 10 to 55% of the ultimate shrinkage strain recommended by ACI Committee 209 for conventional concrete. On the other hand, the 90-day shrinkage strain of the VES (B) concrete with crushed granite was only 52 microstrains; and the VES (B) concrete with marine marl or rounded gravel exhibited an expansion of approximately 140 microstrains, rather than shrinkage for the entire period of 90 days. The expansion is attributed to the lack of evaporable water in the concrete because of its very low W/C (0.17 for marine marl, and 0.22 for rounded gravel).
11. The normal procedure of the rapid chloride permeability test (RCPT) is to measure the total electrical charge in terms of coulombs flowing through a vacuum saturated concrete specimen in 6 hours. This measurement indicates chloride ion permeability of the concrete. The VES concrete may exhibit high permeability according to the RCPT, since many additional ions introduced in the concrete by the various

admixtures will cause the concrete to be more conductive electrically and make it appear more permeable than it really is.

12. The initial current in amperes flowing through the concrete specimen in a RCPT correlates consistently with the total charge measured in 6 hours. Therefore, the initial current, which is an indirect measure of the concrete conductance, can be used as an alternate measurement for the RCPT, thus shortening the total testing time by 6 hours.
13. The AC impedance test measures the total resistance of a concrete specimen in ohms. This test method is simpler and faster than the RCPT, and has the potential of substituting for the RCPT. The best correlation between the two test methods is expressed as the inverse impedance (reciprocal of impedance) in terms of the initial current measured in the RCPT.
14. Concrete-to-concrete bond strength can be determined by a direct shear test. The VES (A) concrete with crushed granite developed a nominal bond strength at 6 hours ranging from 120 psi (0.82 MPa) to 150 psi (1.03 MPa) with the normal NCDOT pavement concrete. The VES (B) concrete with crushed granite developed a 4-hour nominal bond strength of 225 psi (1.55 MPa) with the same NCDOT pavement concrete. These values are much lower than the corresponding value of 330 psi (2.28 MPa) obtained from the control test using NCDOT concrete. However, the control test was performed at the age of 7 days. Since the compressive strength of the VES concretes increases rapidly in the first 3 days, it is expected that its concrete-to-concrete bond strength will also increase substantially as the concrete ages. This should be verified in future tests.

## References

- ACI Committee 209. 1993a. Prediction of Creep, Shrinkage and Temperature Effects in Concrete Structures (ACI 209R-92). *ACI Manual of Concrete Practice*, part 1, 47 pp.
- ACI Committee 211. 1993b. Standard Practice for Selecting Proportions for Normal, Heavyweight, and Mass Concrete (ACI 211.1-91). *ACI Manual of Concrete Practice*, part 1, 38 pp.
- ACI Committee 318. 1993c. Building Code Requirements for Reinforced Concrete (ACI 318-89) and Commentary (ACI 318R-89), (Revised 1992). *ACI Manual of Concrete Practice*, part 3, 347 pp.
- ACI Committee 363. 1984. State-of-Art Report on High Strength Concrete. *ACI Journal*, vol. 81, no. 4, July-August, pp. 364-411.
- Ahmad, S.H., and Shah, S.P. 1985. Structural Properties of High Strength Concrete and its Implications for Precast Prestressed Concrete. *PCI Journal*, vol. 30, no. 6, Nov-Dec, pp. 91-119.
- America's Highways: Accelerating the Search for Innovation*. 1984. Special Report 202, Transportation Research Board, National Research Council, Washington, D.C.
- Berke, N.S.; Pfeifer, D.W.; and Weil, T.G. 1988. Protection Against Chloride-Induced Corrosion. *Concrete International*, vol. 10, no.12, December, pp. 45-55.
- Carrasquillo, R.L.; Slate, F.O.; and Nilson, A.H. 1991. Microcracking and Behavior of High Strength Concrete Subjected to Short Term Loading. *ACI Journal*, vol. 78, no. 3, May-June, pp. 179-186.
- Cook, J.E. 1989. Research and Application of High-Strength Concrete: 10,000 PSI Concrete. *Concrete International*, vol. 11, no. 10, October, pp. 67-75.
- Hansen, M.R. 1993. *Durability of High Performance Concrete*. Ph.D. Dissertation, North Carolina State University, Raleigh, N.C., May, 224 pp.

Husbands, T.B., and Wakely, L. D. 1991. Working with Concretes Based on High-Performance Blended Cements. Paper presented at the annual meeting of the ASCE, Orlando, Florida, October 20-24.

Leming, M. L. 1988. *Properties of High Strength Concrete: An Investigation of High Strength Concrete Characteristics Using Materials in North Carolina*. Research Report No. FHWA/NC/88-006, Department of Civil Engineering, North Carolina State University, Raleigh, N.C, July, 202 pp.

Mindess, S., and Young, J.F. 1981. *Concrete* Prentice Hall, Inc., Englewood Cliffs, New Jersey, 671 pp.

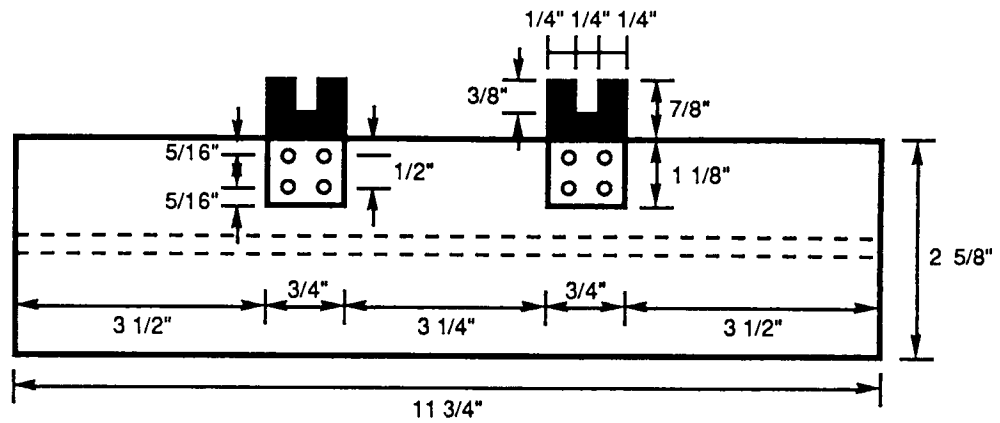
Moreno, J., 1990. The State-of-the-Art of High-Strength Concrete in Chicago: 225 W. Wacker Drive. *Concrete International*, vol. 12, no. 1, January, pp. 35-39.

Powers, T.C.; Copeland, L.E.; and Mann, H.M. 1959. Capillary Continuity or Discontinuity in Cement Pastes. *Journal of the PCA Research and Development Laboratories*, vol. 1, no. 2, May, pp. 38-48.

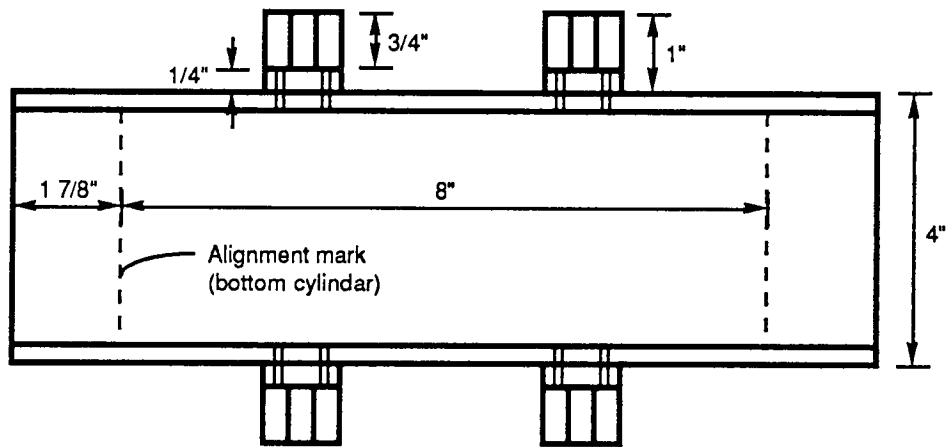
# Appendix

## List of Figures

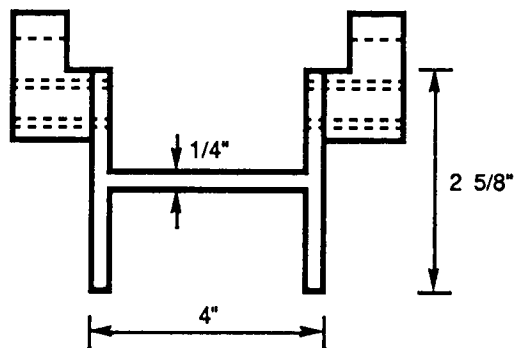
- |             |                                                                                |
|-------------|--------------------------------------------------------------------------------|
| Figure A.1  | Device for mounting transducers on 4 x 8-in. cylinders                         |
| Figure A.2  | Steel jackets for protecting transducers during the compression testing        |
| Figure A.3  | A view of the compression test setup                                           |
| Figure A.4  | Mounting device of transducers for flexural testing                            |
| Figure A.5  | Beam support for flexural testing                                              |
| Figure A.6  | Frame mounting on the flexural test beams for recording the midspan deflection |
| Figure A.7  | Loading arrangement for flexural test                                          |
| Figure A.8  | A view of the flexural test setup                                              |
| Figure A.9  | Freezing-thawing chamber                                                       |
| Figure A.10 | Measuring dynamic modulus of elasticity                                        |
| Figure A.11 | A view of the shrinkage test setup                                             |
| Figure A.12 | RCPT vacuum saturation setup                                                   |
| Figure A.13 | RCPT specimens sealed in two test cells                                        |
| Figure A.14 | RCPT test cells attached to power supply                                       |
| Figure A.15 | RCPT output being recorded                                                     |
| Figure A.16 | RCPT output being recorded on strip chart                                      |
| Figure A.17 | AC impedance test setup                                                        |
| Figure A.18 | AC impedance test in progress                                                  |
| Figure A.19 | Test setup for concrete-to-concrete bond                                       |
| Figure A.20 | A view of the concrete-to-concrete bond test setup                             |



Elevation

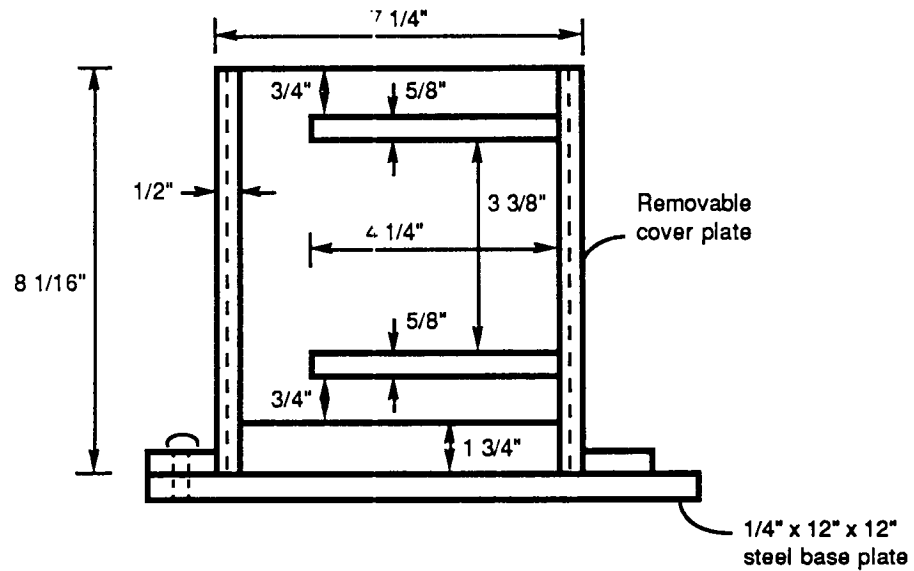


Top View

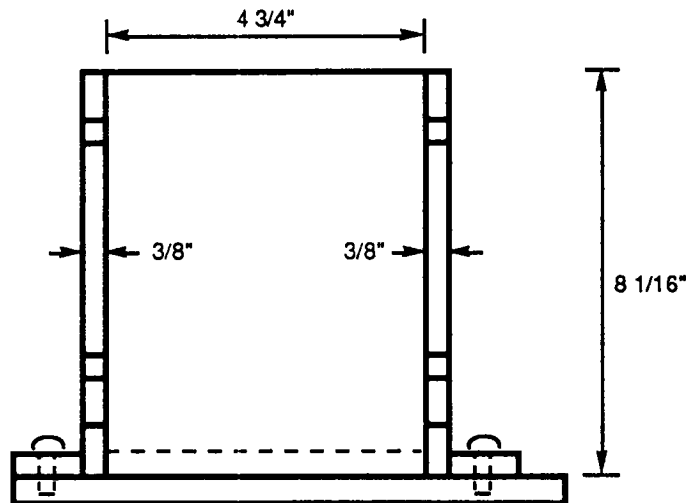


Side View

Figure A.1 Device for mounting transducers on 4 x 8-in. cylinders



Side View



Front View (without cover plate)

**Figure A.2 Steel jackets for protecting transducers during the compression testing**



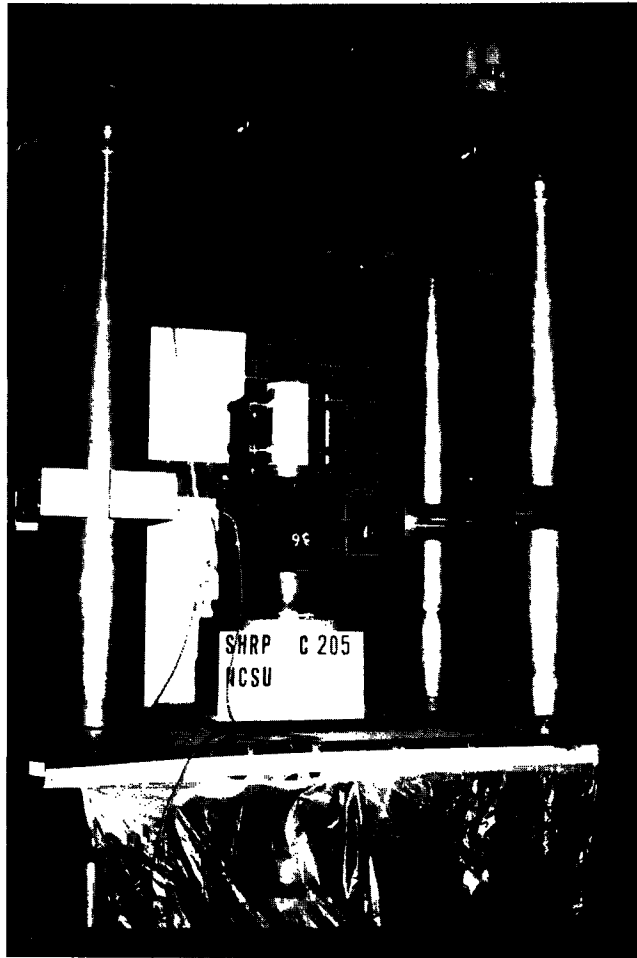
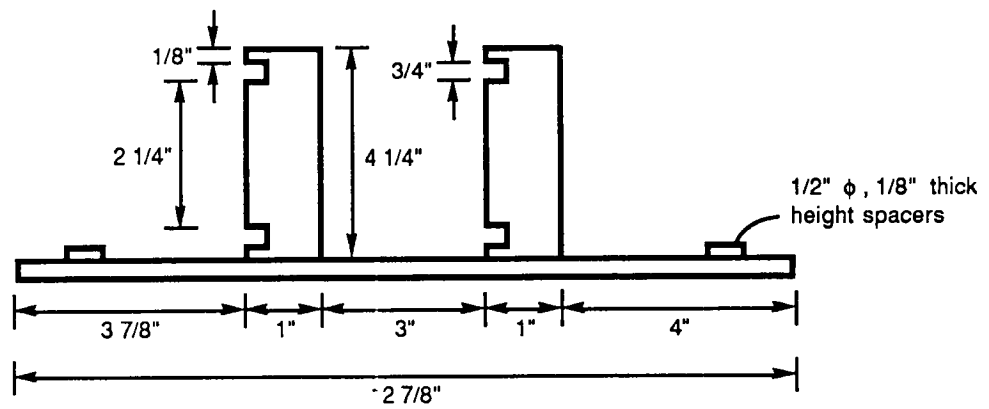
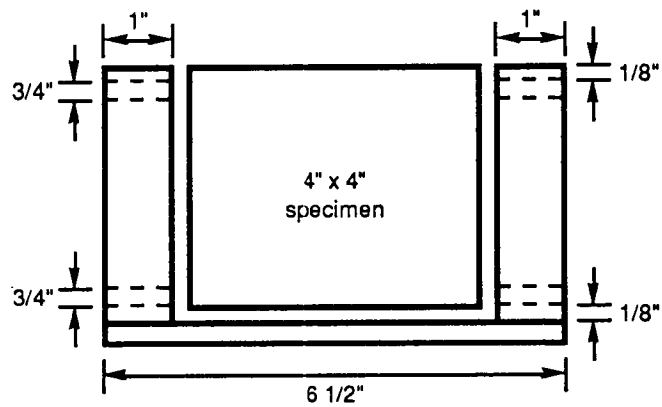


**Figure A.3** A view of the compression test setup



Front View



Side View

**Figure A.4 Mounting device of transducers for flexural testing**

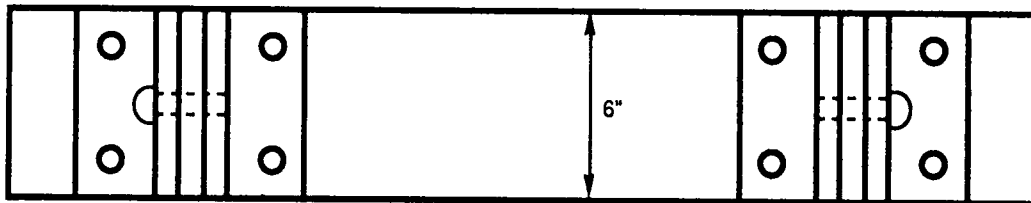
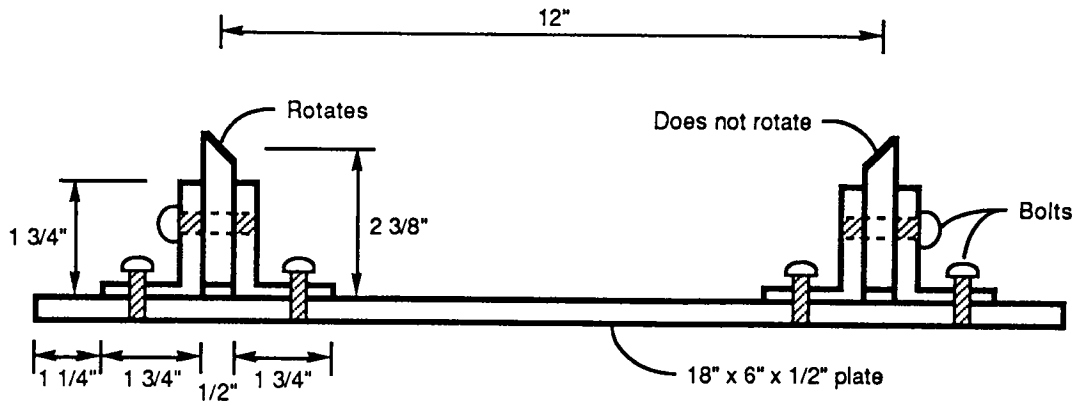
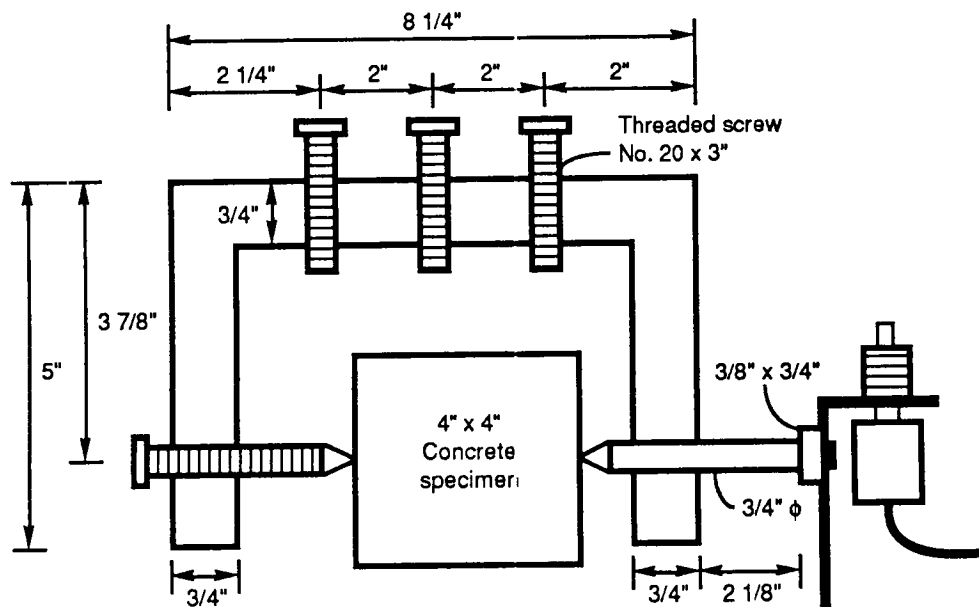
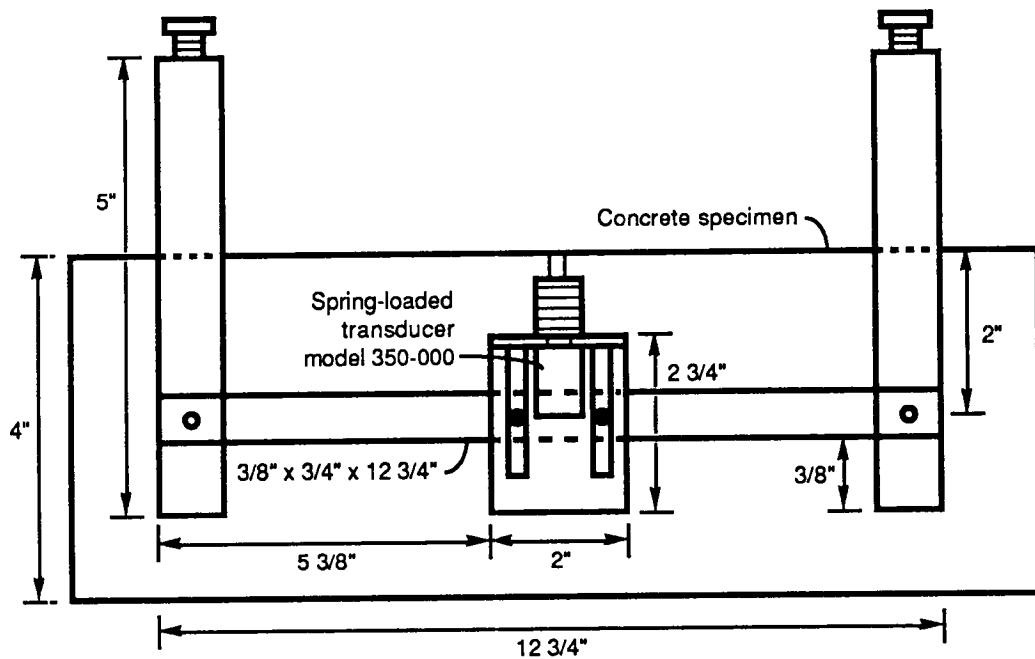


**Figure A.5 Beam support for flexural testing**

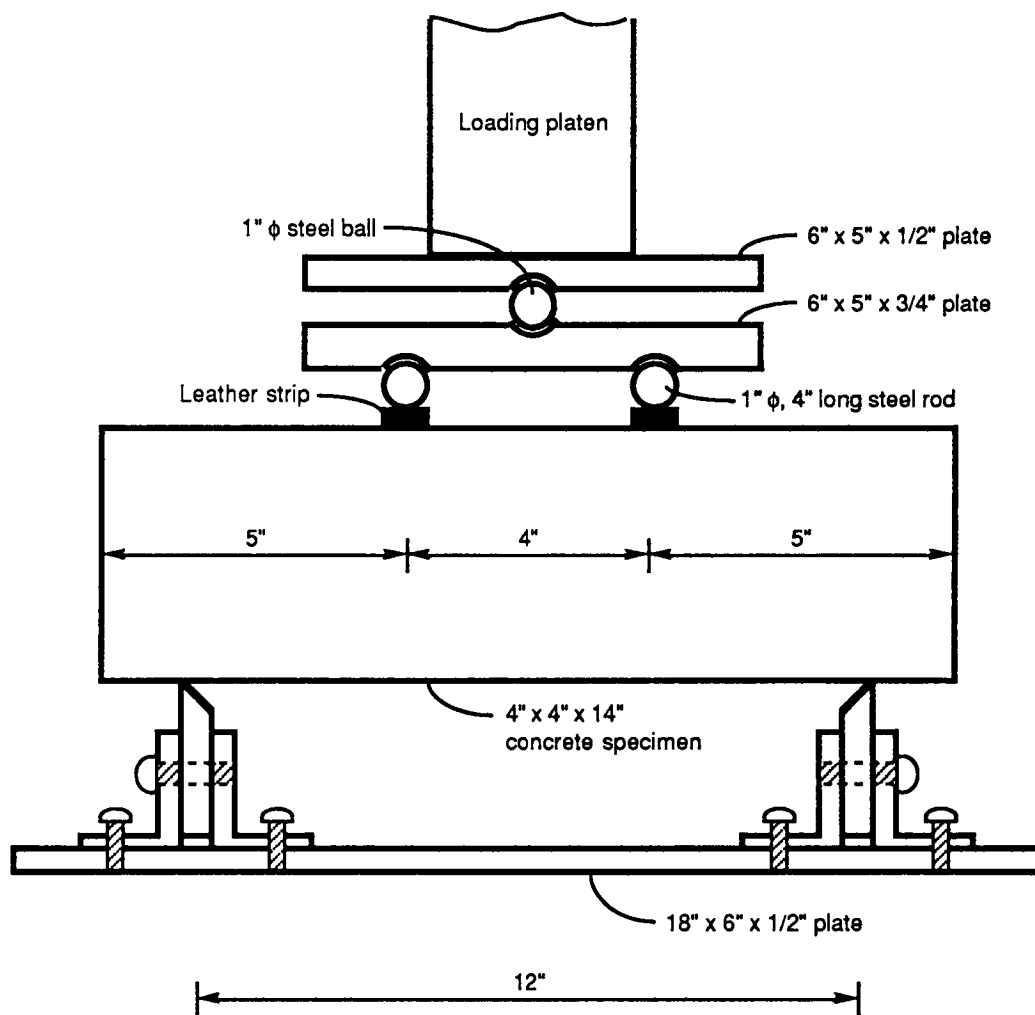


Side View



Front View

**Figure A.6** Frame mounting on the flexural test beams for recording the midspan deflection



Side View

Figure A.7 Loading arrangement for flexural test

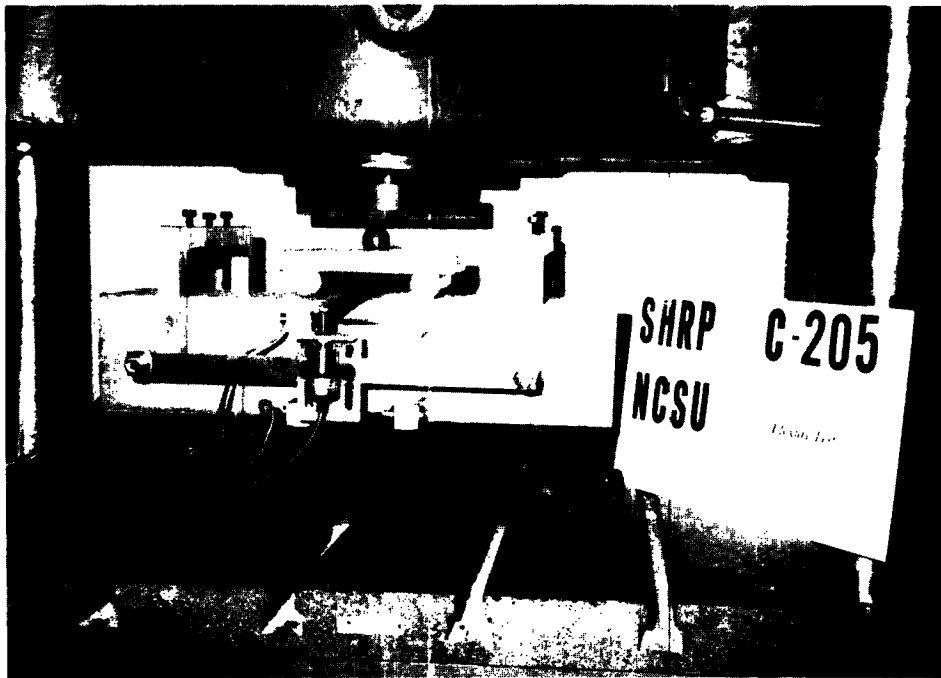


**Figure A.8** A view of the flexural test setup



**Figure A.9** Freezing-thawing chamber

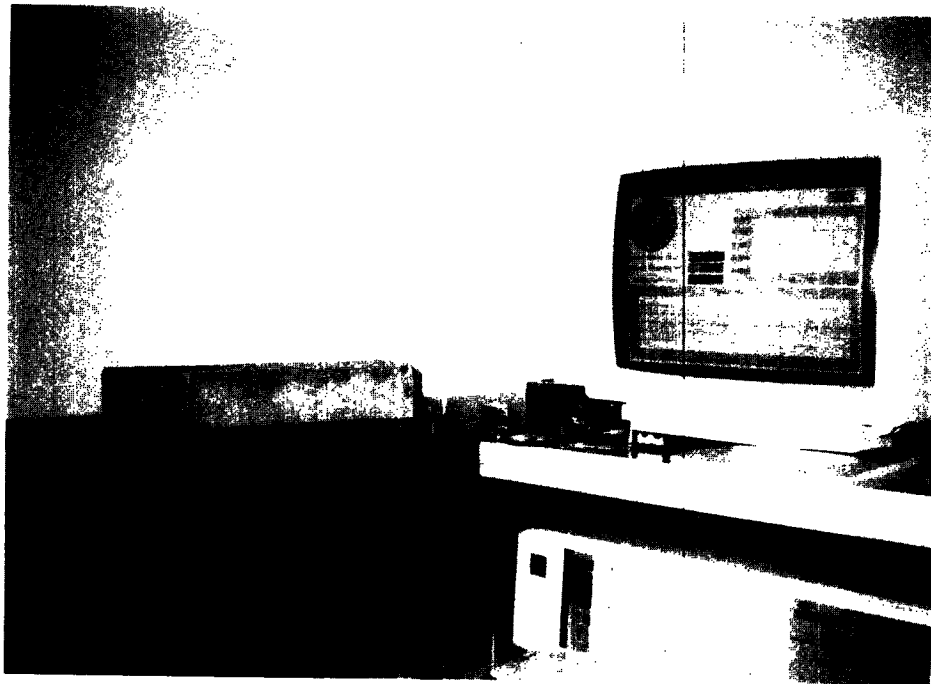


**Figure A.10** Measuring dynamic modulus of elasticity



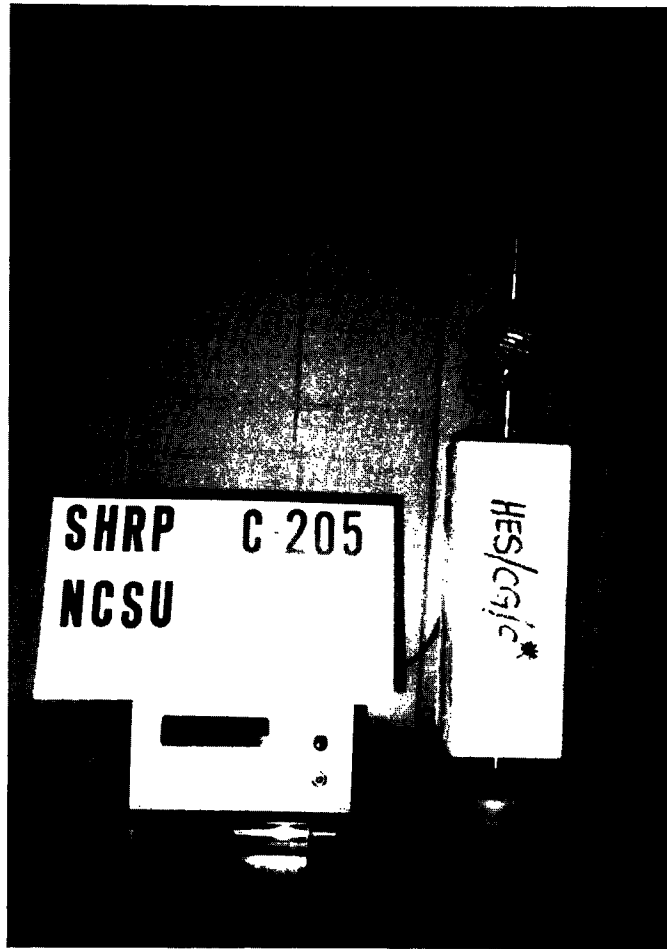


**Figure A.11** A view of the shrinkage test setup

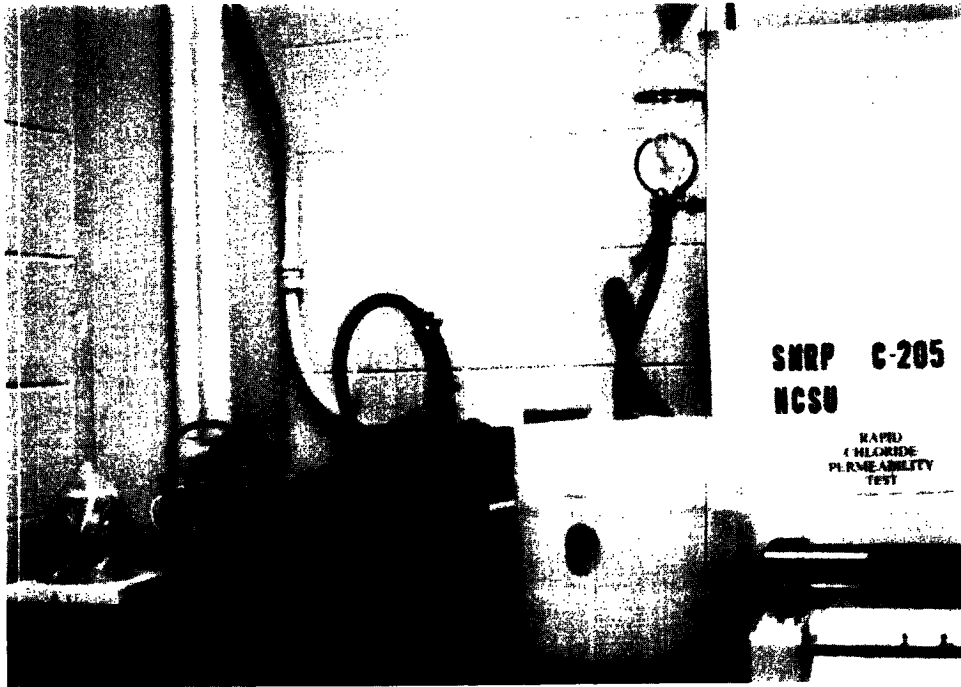


Figure A.12 RCPT vacuum saturation setup

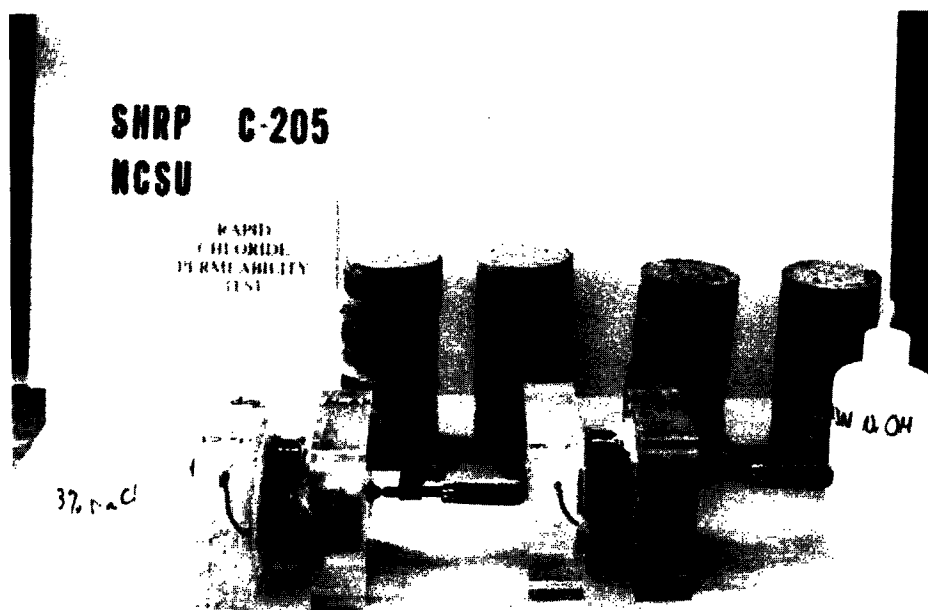
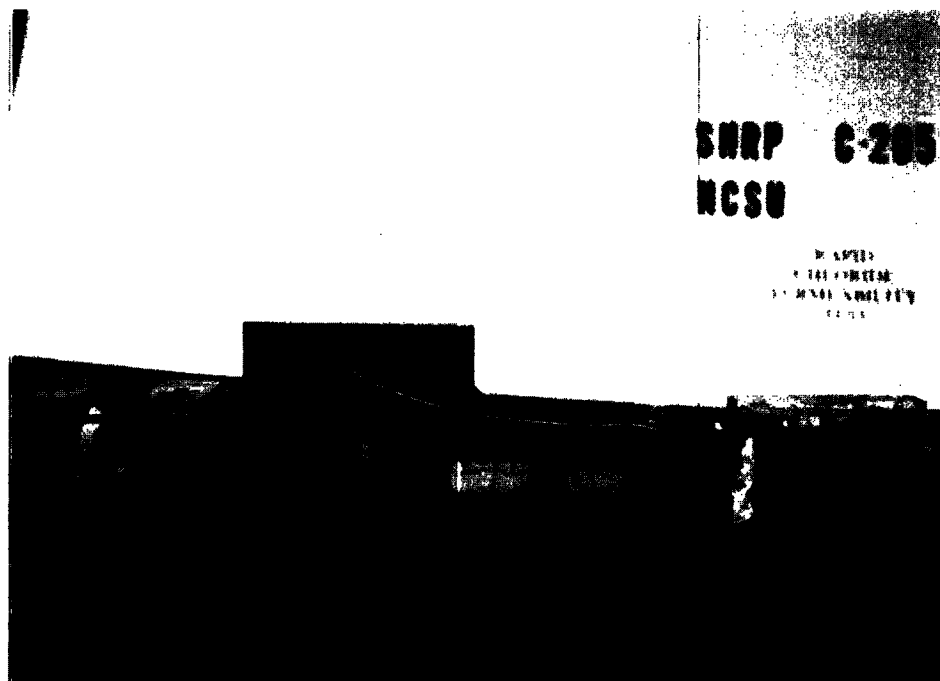
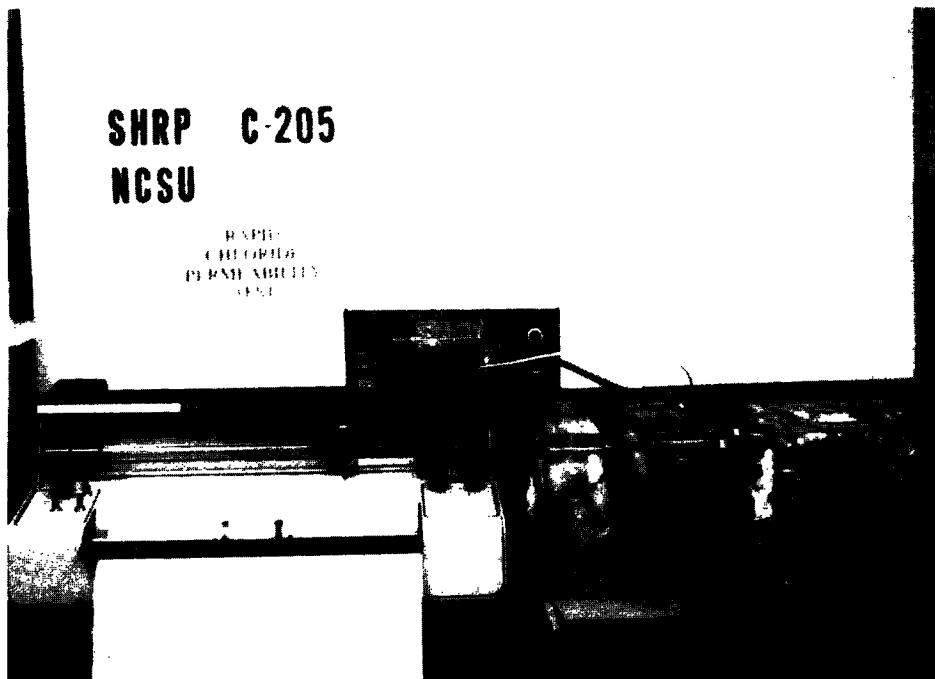


Figure A.13 RCPT specimens sealed in two test cells



**Figure A.14 RCPT test cells attached to power supply**



**Figure A.15 RCPT output being recorded**

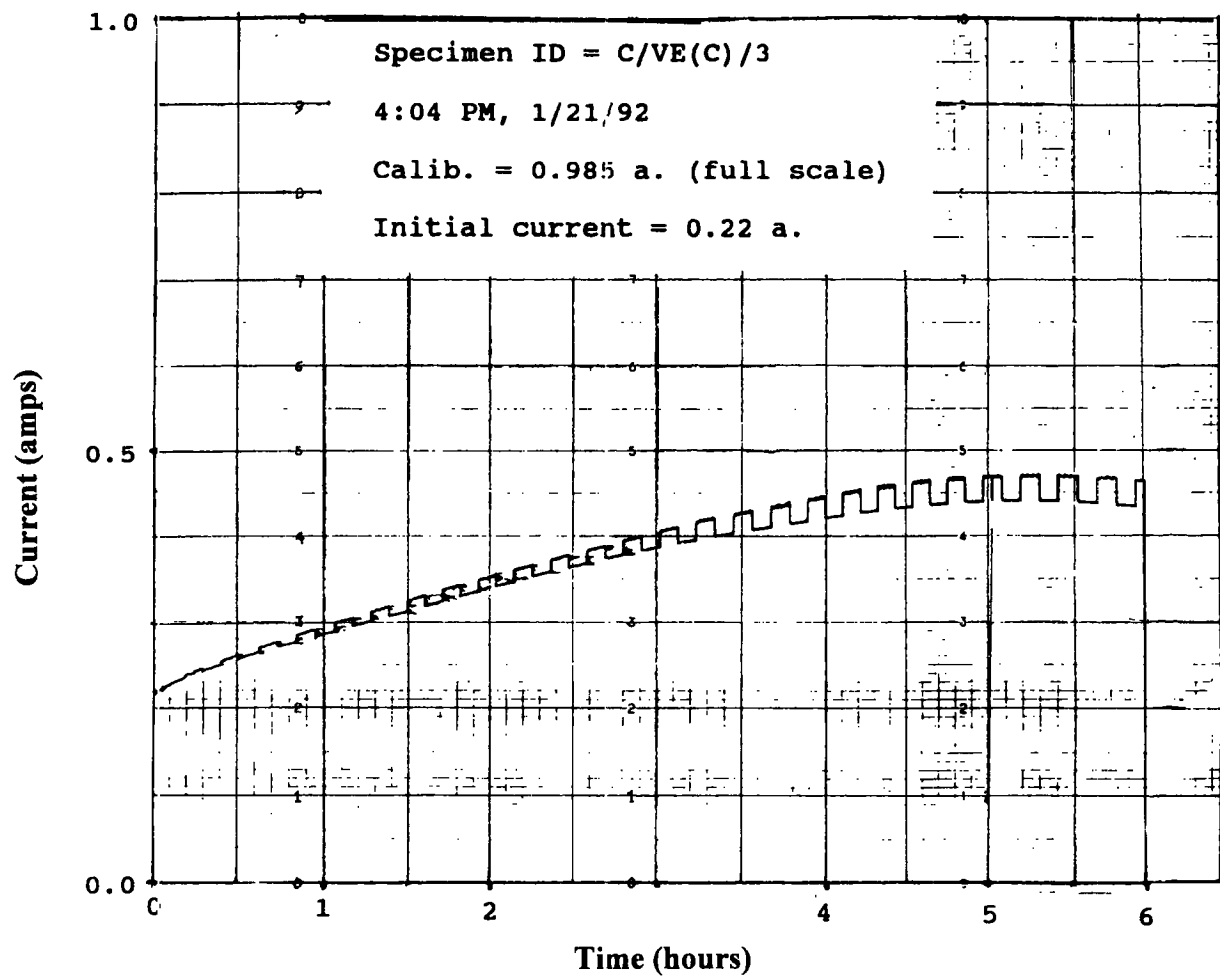
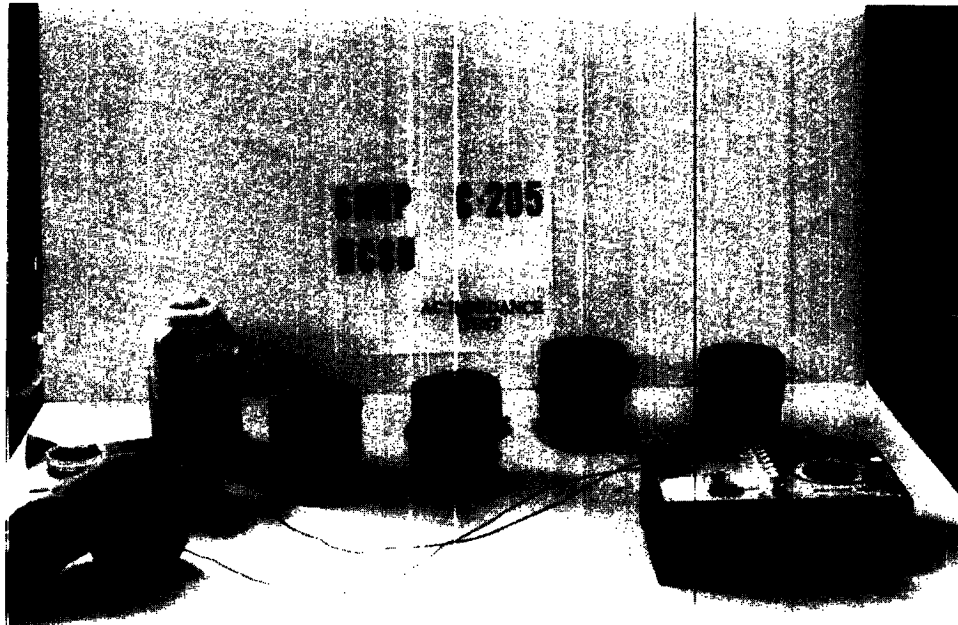


Figure A.16 RCPT output being recorded on strip chart

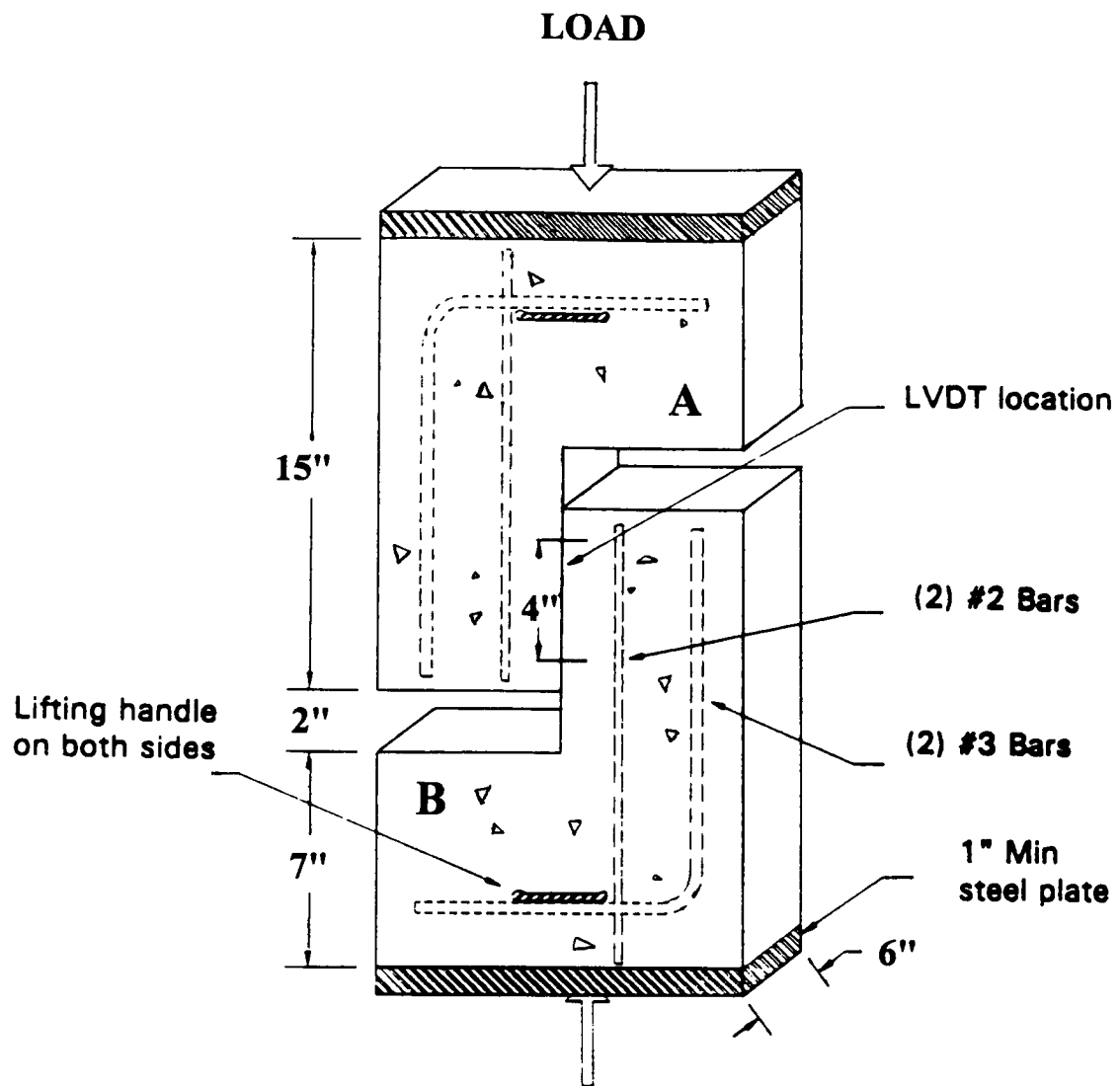


Figure A.17 AC impedance test setup



**Figure A.18 AC impedance test in progress**





**Figure A.19 Test setup for concrete-to-concrete bond**

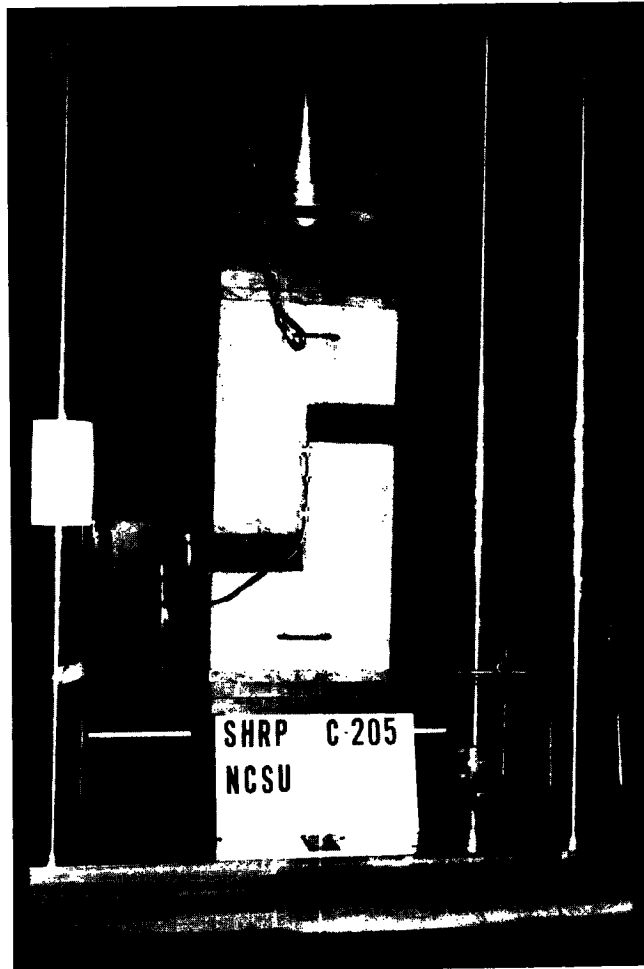


**Figure A.20** A view of the concrete-to-concrete bond test setup

## Concrete and Structures Advisory Committee

### Chairman

James J. Murphy  
*New York Department of Transportation (retired)*

### Vice Chairman

Howard H. Newlon, Jr.  
*Virginia Transportation Research Council (retired)*

### Members

Charles J. Arnold  
*Michigan Department of Transportation*

Donald E. Beuerlein  
*Koss Construction Co.*

Bernard C. Brown  
*Iowa Department of Transportation*

Richard D. Gaynor  
*National Aggregates Association/National Ready Mixed Concrete Association*

Robert J. Girard  
*Missouri Highway and Transportation Department*

David L. Gress  
*University of New Hampshire*

Gary Lee Hoffman  
*Pennsylvania Department of Transportation*

Brian B. Hope  
*Queens University*

Carl E. Locke, Jr.  
*University of Kansas*

Clellon L. Loveall  
*Tennessee Department of Transportation*

David G. Manning  
*Ontario Ministry of Transportation*

Robert G. Packard  
*Portland Cement Association*

James E. Roberts  
*California Department of Transportation*

John M. Scanlon, Jr.  
*Wiss Janney Elstner Associates*

Charles F. Scholer  
*Purdue University*

Lawrence L. Smith  
*Florida Department of Transportation*

John R. Strada  
*Washington Department of Transportation (retired)*

### Liaisons

Theodore R. Ferragut  
*Federal Highway Administration*

Crawford F. Jencks  
*Transportation Research Board*

Bryant Mather  
*USAE Waterways Experiment Station*

Thomas J. Pasko, Jr.  
*Federal Highway Administration*

John L. Rice  
*Federal Aviation Administration*

Suneel Vanikar  
*Federal Highway Administration*

11/19/92

### Expert Task Group

Stephen Forster  
*Federal Highway Administration*

Amir Hanna  
*Transportation Research Board*

Richard H. Howe  
*Pennsylvania Department of Transportation (retired)*

Susan Lane  
*Federal Highway Administration*

Rebecca S. McDaniel  
*Indiana Department of Transportation*

Howard H. Newlon, Jr.  
*Virginia Transportation Research Council (retired)*

Celik H. Ozyildirim  
*Virginia Transportation Research Council*

Jan P. Skalny  
*W.R. Grace and Company (retired)*

A. Haleem Tahir  
*American Association of State Highway and Transportation Officials*

Lillian Wakeley  
*USAE Waterways Experiment Station*

7/22/93